Optimization of Multi-Reservoir Management Rules Subject to Climate and Demand Change in the Potomac River Basin

James H. Stagge

Dissertation submitted to the Faculty of the
Virginia Polytechnic Institute and State University
in partial fulfillment of the requirements for the degree of

Doctor of Philosophy
in
Civil Engineering

Glenn E. Moglen, Chair
Thomas J. Grizzard, Jr.
Adil N. Godrej
Kostas P. Triantis

July 16, 2012
Falls Church, Virginia

Keywords: Water Resources, Optimization, Climate Change, Potomac, Hydrology

Optimization of Multi-Reservoir Management Rules Subject to Climate and Demand Change in the Potomac River Basin

James H. Stagge

ABSTRACT

Water management in the Washington Metropolitan Area (WMA) is challenging because the system relies on flow in the Potomac river, which is largely uncontrolled and augmented by the Jennings-Randolph reservoir, located 9-10 days travel time upstream. Given this lag, release decisions must be made collectively by federal, state and local stakeholders amid significant uncertainty, well in advance of accurate weather forecasts with no ability to recapture excess releases. Adding to this uncertainty are predictions of more severe and sporadic rainfall over the next century, caused by anthropogenic climate change.

This study aims to evaluate the potential impacts of demand and climate change on the WMA water supply system, identifying changes in system vulnerability over the next century and developing adaptation strategies designed to maximize efficiency in a nonstationary system. A daily stochastic streamflow generation model is presented, which succesfully replicates statistics of the historical streamflow record and can produce climate-adjusted daily time-series. Using these time series, a multi-objective evolutionary algorithm is used to optimize the system's operating rules given current and future conditions, considering several competing objectives.

This research was supported through the Via Doctoral Scholars program and by the Institute for Critical Technology and Applied Science (ICTAS).

Acknowledgments

This research project would not have been possible without the support of many people.

I am eternally grateful to Glenn Moglen for providing me with this tremendous opportunity, for his thoughtful guidance and for being my biggest supporter. I would also like to thank my dissertation committee for their helpful review of this document.

I must acknowledge the contribution of Cherie Schultz, Sarah Ahmed, and the Interstate Commission on the Potomac River Basin (ICPRB) for providing data access and continual support through this project. Your expertise with regard to the Potomac system was invaluable. I would also like to thank Megan Wiley Rivera, Steve Nebiker, Dan Sheer and Hydrologics, Inc. for OASIS support and for additional insight into the Potomac system.

I must also thank my family for their help during the dissertation process and for all the years of support leading up to it.

To Marta, my wife, who supported me and pushed me to do better each step of the way.

Contents

1 Introduction **1**

Bibliography 3

2 Manuscript 1: Markov Chain Model for Generation of Daily Climate-Adjusted Streamflows **4**

2.1 Introduction 5

2.2 Background 6

2.2.1 Stochastic Streamflow Models 6

2.2.2 Climate Change and Streamflows in the Mid-Atlantic 8

2.3 Model Definition 10

2.3.1 Model Overview 10

2.3.2 Daily Streamflow Model 10

2.3.3 Monthly Climate Model 13

2.3.4 Generating Historical and Climate-Adjusted Streamflows 14

2.4 Results 15

2.4.1 Data Preparation 15

2.4.2 Fitting the Daily Streamflow Model 16

2.4.3 Extracting Principal Components from Model Parameters 18

2.4.4 Clustering Monthly Climate States 19

2.4.5 Creating Predictors of Climate States 19

2.4.6 Simulation of Historical Streamflow 21

2.4.7 Predicted Climate Change Effects on Streamflow 27

2.5 Conclusions 30
2.6 Acknowledgments 33
Bibliography 33

3 Manuscript 2: Genetic Algorithm Optimization of a Multi-Reservoir System with Long Lag Times 39
3.1 Introduction 40
3.2 Background 42
3.2.1 Formulation of Reservoir Optimization Problems 42
3.2.2 Multobjective Evolutionary Algorithms 43
3.2.3 Water Resources Applications of Evolutionary Algorithms 44
3.3 Application 45
3.3.1 Potomac River Basin 45
3.3.2 Origins of the Potomac Basin System 47
3.4 Methods 49
3.4.1 Systems Modeling 49
3.4.2 Streamflow Time Series 49
3.4.3 Optimization Scheme 50
3.4.4 Objective Function and Constraints 51
3.5 Results 54
3.5.1 Potomac Water Supply Response 54
3.5.2 Operating Rule Optimization 57
3.6 Conclusions 66
3.7 Acknowledgments 68
Bibliography 68

4 Manuscript 3: Water Resources Adaptation to Climate and Demand Change Using Multiobjective Evolutionary Algorithms 73
4.1 Introduction 74
4.2 Methods 76

4.2.1 Washington Metropolitan Area Water Supply Model 76
4.2.2 Multiobjective optimization 77
4.2.3 Climate adjusted streamflow generation 80
4.3 Results 81
4.3.1 Projected Changes to WMA Water Supply Reliability 81
4.3.2 Adaptation Strategies 87
4.4 Conclusions 96
4.5 Acknowledgments 99
Bibliography 99

5 Conclusions **103**

List of Figures

2.1 Daily flow simulation model. 11
2.2 Streamflow analysis and model fitting procedure. 13
2.3 Streamflow generation procedure. 15
2.4 Daily streamflow model parameters. 18
2.5 Monthly mean flows for the historical scenario (1961-2000). 23
2.6 Correlogram of daily streamflow. 25
2.7 Variation in monthly mean due to climate change (CCC). 29
2.8 Flow duration curve for July subject to climate change (CCSM). 31

3.1 Potomac watershed and Washington DC water supply. 41
3.2 Objective function - Penalty weights. 52
3.3 Objective function for the historical and simulated streamflow time series. . 55
3.4 Optimized buffer equation - Historical time series. 59
3.5 Optimized load shift equation - Historical time series. 61
3.6 Demand Restriction - Pareto Front comparison. 67

4.1 Potomac watershed and Washington DC water supply. 75
4.2 Effect of demand increase and reservoir sedimentation on Storage and Recreation Season objectives. 83
4.3 Effect of climate change on system objectives. 86
4.4 Optimized buffer equation under future conditions with respect to Flowby. 90
4.5 Progression of optimal Buffer Equation with respect to the Recreation Season. 91

List of Tables

2.1 Evaluated global climate models (IPCC - AR4). 16
2.2 Climate variable discriminating power. 21
2.3 Mann-Whitney Test for historical validation of GCM Means. 26
2.4 Percent Hydrologic Alteration of 20th Century GCM flow distribution. . . . 26
2.5 Percent change in mean annual flow for climate change realizations. 27
2.6 Percent change in $7Q_{10}$ minimum flow for climate change realizations. . . . 30

3.1 WMA operational characteristics. 46
3.2 System optimization results - Historical time series. 58
3.3 Parameters of the demand restriction rule. 65

4.1 WMA operational characteristics. 77
4.2 Projected WMA population and demand change (2010-2040). 82
4.3 Projected sedimentation and storage loss (2010-2040). 84
4.4 Evaluated global climate models (IPCC - AR4). 85
4.5 Optimization results for 2040 demand/sedimentation conditions. 88
4.6 Optimization results for future conditions (CSIRO A2, 2070-2099 climate). . 89
4.7 Optimized demand restriction triggers, in % usable storage. 95
4.8 Optimized demand restriction water use reduction (%). 96

Chapter 1

Introduction

The combined effect of continued urban expansion coupled with predictions of more severe and intermittent precipitation due to climate change points to a potential increase in the frequency and severity of water shortages in the U.S. Mid-Atlantic states. The Washington DC metropolitan water supply is of particular interest because water release decisions must be made well in advance of the water's usage due to long travel times between the primary water supply reservoir and the city's water intakes. In light of this evolving water supply challenge, a quantitative evaluation of the effects of demand and climate change is necessary to identify potential vulnerabilities in the water supply system. In addition, operational rules must be reevaluated to ensure that current needs are met efficiently and to identify adaptation strategies to counteract the effect of future demand and climate change.

When implemented in 1982, the Washington DC metropolitan area (hereafter "WMA") water supply system was considered an example of combining optimization and simulation techniques to improve water resource efficiency, replacing plans for as many as 16 major reservoirs with a distant water supply reservoir (Jennings Randolph Reservoir) and one small, nearby reservoir (Little Seneca Reservoir) (Palmer 2007). While this design allows the 38,000 km^2 Potomac watershed to remain largely uncontrolled, it increases the importance of effective water management, particularly as population growth and cli-

mate change place greater stress on the system. The largest physical operational issue in the WMA system is the location of the Jennings Randolph Reservoir 300 km upstream of Washington DC, which creates a 9-10 day delay between water supply releases and their capture at water supply intakes located at Great Falls (MD) and Little Falls (Washington, DC). This situation creates a unique challenge for water supply managers because the necessary forecast lead time is beyond the scope of accurate weather forecasts.

In the addition to the physical challenges of the water supply system, the WMA faces unique management challenges due to the region's complex government and institutional landscape. The current water supply system operates under a series of eight separate agreements among agencies including the U.S. Army Corps of Engineers (USACE), the states of Maryland and Virginia, the District of Columbia, two local utilities, and the Interstate Commission on the Potomac River Basin (ICPRB). In the face of these competing interests and hydrologic uncertainty brought about by long lag times, a system is needed to quantitatively and objectively determine the optimum timing, magnitude and location of water supply releases.

These challenges are addressed in three distinct manuscripts, each focusing on a major theme:

Manuscript 1 presents a novel method for generating synthetic, climate-adjusted daily streamflow time series. This method relates General Circulation Model (GCM)-scale climate indicators to discrete climate states in a Markov chain, which in turn controls the parameters of a daily flow model. The analysis and generation procedures are described in detail, using the Potomac River as a case study. This method is capable of generating long sequences of feasible, synthetic daily flows and is used in this context to create input time series for Manuscripts 2 and 3.

Manuscript 2 examines the existing water management strategies of the WMA, given current demand and climate. A multi-objective evolutionary algorithm scheme is used to optimize the system's operating rules, maximizing system-wide bene-

fit while considering several competing objectives, which range from water supply and reservoir storage to recreation benefit and environmental flows.

Manuscript 3 evaluates the potential impacts of demand and climate change on the WMA water supply system, identifying changes in system vulnerability over the next century. Using a similar optimization framework to Manuscript 2 and climate-adjusted streamflow time series generated in Manuscript 1, strategies for adaptation are tested. These adaptation strategies include policy and operating rules designed to maximize effectiveness and to maintain current levels of service, given demand and climate change over the next century.

These studies apply novel techniques, data, and analyses to quantitatively determine water supply releases in a system with long lag times and changing demand and climate. In addition to its significance in the field of water management research, this work supports ongoing work by the ICPRB, providing a set of tools to improve the robustness and efficiency of the WMA water supply system.

Bibliography

Palmer, R. (2007). The confluence of a career: Virtual droughts, shared-vision planning, and climate change. *Journal of Water Resources Planning and Management 133*, 288.

Chapter 2

Manuscript 1: Markov Chain Model for Generation of Daily Climate-Adjusted Streamflows

Abstract

A daily stochastic streamflow generation model is presented, which successfully replicates statistics of the historical streamflow record and can produce climate-adjusted daily time-series. A monthly climate model relates General Circulation Model (GCM)-scale climate indicators to discrete climate states in a Markov chain, which in turn controls the parameters of a daily flow model. Daily flow is generated by a two-state (increasing/decreasing) Markov chain, with rising limb increments randomly sampled from a Weibull distribution and the falling limb modeled as exponential recession. When applied to the Potomac River, a 38,000 km^2 basin in the Mid-Atlantic United States, the model reproduces daily, monthly, and annual statistics of the historical streamflow record, including extreme drought flows. This method can be used across a wide range of water resources planning applications and offers the advantage of a parsimonious model, requiring only a sufficiently long historical streamflow record and large-scale climate data.

Simulation of Potomac streamflows subject to the Special Report on Emissions Scenarios (SRES) A1b, A2, and B1 emission scenarios predict a slight increase in mean annual flows over the next century, with the majority of this increase occurring during the winter and early spring. Conversely, mean summer flows are projected to decrease due to climate change, caused by a shift to shorter, more sporadic rain events. Date of the minimum annual flow is projected to shift 2-5 days earlier by the 2070-2099 period.

2.1 Introduction

Water resources planners and engineers are currently attempting to reconcile two competing concepts: first, that water management policy must adapt to address the nonstationary nature of hydrologic systems, and second, that estimates of streamflow effects due to climate change often have greater uncertainty than their climatic components, temperature precipitation and evapotranspiration (Matalas 1997). As stated by Srikanthan and McMahon (2001), one of the major gaps in the design and operation of hydrological systems is the quantification of uncertainty as a result of climatic variability.

This paper presents a novel extension of existing daily stochastic streamflow models (Sargent 1979; Aksoy and Bayazit 2000; Szilagyi et al. 2006) to generate long period climate-adjusted streamflow time-series. This is accomplished by linking parameters of a daily flow generation model to discrete climate states in a monthly Markov-chain climate model. Climate states are classified using GCM-scale climate indicators and state transition probabilities are modified to simulate non-stationarity.

The proposed method is an alternative to the often onerous and uncertain task of creating a detailed conceptual rainfall-runoff-routing model and downscaling GCM climate data to daily weather patterns at the regional and watershed scales. It benefits from avoiding daily GCM outputs, which tend to have greater uncertainty , in favor of monthly climatic trends and draws the corresponding flow response from the historical record. It can generate very long sequences of feasible, synthetic daily flows which are vital in designing adaptive water management policies. The proposed method could also be incor-

porated as a real-time forecasting tool. Finally, the method reproduces flow statistics at daily, monthly, and annual time scales, including low flows and the characteristic shape and correlation structure of daily hydrographs, while maintaining a parsimonious structure.

This paper presents the analysis and generation steps of the proposed method in detail. Performance is evaluated using the Potomac River as a case study. This 38,000 km^2 basin is located in the Mid-Atlantic United States, along the borders of Maryland, Virginia and West Virginia. The Potomac River is vital for supplying water to the Washington, DC metropolitan area, accounting for approximately 78% of the annual water demand (Ahmed et al. 2010). In light of this importance, a quantitative evaluation of the effects of climate change on the Potomac River is required to ensure that water management plans are sufficiently robust to satisfy future requirements.

2.2 Background

2.2.1 Stochastic Streamflow Models

Generation of synthetic streamflow time series is typically employed to extend the historical record and expand the set of feasible conditions a water management system may encounter, while maintaining the distribution (mean, variance, skewness, serial correlation) and seasonality of the historic streamflow record. Original stochastic streamflow methods focused on long-term water planning and tended to operate at the monthly or annual time scale, typically employing some form of the autoregressive (AR) model. One of the first autoregressive models for streamflow generation, the Thomas-Fiering model (Thomas and Fiering 1962) is, in essence, a periodic lag-one AR(1) process. Though still employed, the Thomas-Fiering model has generally been supplanted by the Box-Jenkins set of autoregressive-moving average (ARMA) functional forms (Box and Jenkins 1970). ARMA(1,1) models have generally been shown to be more effective at generating monthly streamflow timeseries (Bartolini and Salas 1993; Stedinger et al. 1985). These

models are sometimes classified as periodic autoregressive moving average (PARMA) models, referring to their periodic structure, with seasonally varying means, standard deviations, and lag coefficients.

In their most basic form, autoregressive models assume normality, which is rare in natural streams. Flows tend to be positively skewed, with a lower bound approaching zero, related to baseflow, and an unbounded upper tail, corresponding to extreme flood events. To effectively use autoregressive models, raw flow must therefore be transformed to approximate a normal distribution, using differencing, logarithm transforms, the gamma distribution (Hirsch 1979), or the Box-Cox transformation (Box and Cox 1964). Without these transformations, autoregressive models can produce anomalous results, such as negative flows.

The first attempts at daily streamflow generation also employed the AR model, typically with a lag-1 or lag-2 process (Beard 1967; Quimpo 1968; Quimpo and Yevjevich 1967; Payne et al. 1969). However, the characteristic hydrograph shape, with its intermittent, highly skewed storm pulses and gradual recession, is difficult to reproduce using autoregressive models without significant modifications (Sharma et al. 1997). Several methods have since been proposed which maintain historical distributions, while better approximating natural hydrograph shapes, including disaggregation schemes and shot noise/Markov Chain models.

Rather than modeling daily flows directly, disaggregation schemes begin with monthly or annual models, such as ARMA, and then apportion flows to create daily or weekly series. Original parametric disaggregation models used statistical parameters from the historic time series to downscale annual flows (Valencia and Schakke 1973; Stedinger and Vogel 1984; Maheepala and Perera 1996). In large systems, this type of disaggregation model can quickly become over-parameterized (Grygier and Stedinger 1988). More recent approaches to disaggregation operate on the principle of resampling. The method of fragments, originally proposed by Harms and Campbell (1967), resamples short duration fragments of the historical record (Srikanthan and McMahon 1982) or synthetically generated hydrographs (Porter and Pink 1991) and scales them to match monthly or an-

nual sums. Nonparametric techniques such as moving block bootstrapping (Vogel and Shallcross 1996) or K-Nearest Neighbor models (Lall and Sharma 1996; Prairie et al. 2006; Buishand and Brandsma 2001) have been applied more recently to identify appropriate fragments.

Shot noise (SN) models were introduced to produce a more realistic daily hydrograph by modeling the in-stream response produced by a pulse, corresponding to a storm event. In the original SN streamflow models, Weiss (1977) modeled rainfall occurrences as a Poisson process, with intensities following an exponential distribution. Watershed response is also modeled exponentially, with separate transfer functions for baseflow and direct runoff. Treiber and Plate (1975) extended this model using transition (Markov) probabilities to control pulse and recession days and a transfer function which convolved pulses to generate runoff. Sargent (1979) condensed this method, focusing on a more conceptual model of runoff generation, using a modified exponential distribution for pulse heights and an exponential decay for recession curves.

The shot noise/Markov chain model is more physically consistent with hydrologic processes, is capable of maintaining flow characteristics at the monthly and annual aggregated scale, and performs favorably when compared to other models (Chapman 1997). This general model formulation has since been used to generate synthetic daily streamflows in a wide range of hydrologic scanarios (Kottegoda 1980) including intermittent streams (Aksoy and Bayazit 2000; Aksoy 2003) and multiple sites (Szilagyi et al. 2006).

2.2.2 Climate Change and Streamflows in the Mid-Atlantic

Climate research suggests that the Earth's climate is changing due to human activities which alter the composition of the global atmosphere, increasing levels of carbon dioxide and other greenhouse gases (Meehl et al. 2007). All scenarios assessed by the Intergovernmental Panel on Climate Change (IPCC) project increases in global mean surface air temperature, with the scenarios beginning to diverge by the end of the next century (2090-2100) (Meehl et al. 2007).

Climate projections in the Mid-Atlantic region predict moderate increases in mean annual temperature, precipitation, and streamflow over the next century (Najjar et al. 2009; Pyke et al. 2008; Hayhoe et al. 2008; Meehl et al. 2007). An evaluation of the four best performing GCMs in the Chesapeake Bay watershed suggests an increase in mean annual temperature of 3.9$\pm$1.1°C and an increase in precipitation of 9$\pm$12% by the end of the century under the A2 scenario (Najjar et al. 2009). This continues the historical trend of precipitation increases throughout the northeast U.S. during the 20th century (Groisman et al. 2001, 2004). Milly et al. (2005) predict a 3.6% increase in mean annual streamflow (SRES A1B) for the 2041-2060 scenario in the Mid-Atlantic, with 55-70% of GCM models showing an increase in flow. Variability in these results follows the pattern outlined in Matalas (1997), with the greatest confidence in temperature models, followed by precipitation and ultimately streamflow, which shows the greatest uncertainty.

Despite projected increases in mean annual precipitation and flow for the Mid-Atlantic, variation in the distribution and seasonality of precipitation and runoff is potentially more important for water resources management. Storm events are projected to become both more severe and intermittent, with precipitation intensity expected to increase by one standard deviation along the east coast of the U.S. by the end of the 21st century, concurrent with a decrease in the total number of storm events (Meehl et al. 2007). The annual number of dry days in the region is projected to increase by 0.25–0.5 standard deviations by 2100 (Tebaldi et al. 2006). This increase in dry days, combined with an increase in heat waves, defined as consecutive days with temperatures at least 5°C higher than daily norms, will likely produce longer and more pronounced droughts in the region (Meehl et al. 2007).

These projections suggest a moderate increase in mean flows, but with greater likelihood of both flooding, due to storm intensity, and drought, due to prolonged dry periods. Seasonality is also expected to shift, with the greatest increase in precipitation occurring during the winter and spring (Najjar et al. 2009). Similar seasonal trends were noted in Mccabe and Ayers (1989), Moore et al. (1997) and Hayhoe et al. (2007).

2.3 Model Definition

2.3.1 Model Overview

The proposed model is designed to simulate daily streamflows under both current and potential future climate conditions. It is a combination of a monthly climate model, which generates climate based on the likelihood of discrete climate states, and a daily streamflow model, which generates hydrographs based on parameters tied to the climate state.

2.3.2 Daily Streamflow Model

The daily streamflow generation model consists of two parts: (i) determination of the river's state, i.e. increasing or decreasing streamflow, and (ii) calculation of the ascension or recession curve based on this state. A two-state Markov chain is employed to determine whether flow is increasing (wet), or decreasing (dry) on a given day. The Markov chain is assumed to be first order, depending only on whether the previous day was "wet" or "dry", and can be represented by the transition probability matrix:

$$P = \begin{bmatrix} P_{dd} & P_{dw} \\ P_{wd} & P_{ww} \end{bmatrix}$$

where P_{dd} is the probability of a dry day given the previous day was dry, P_{dw} is the probability of a wet day given the previous day was dry, P_{wd} is the probability of a wet day following a dry day, and P_{ww} is the probability of a wet day given the previous day was wet.

The ascension limb of the daily hydrograph, occurring on wet days, is simulated by randomly generating daily flow increases, ΔQ, from a Weibull distribution. The Weibull distribution was found to provide the best fit to flow increments in the Potomac data set, mirroring results in Szilagyi et al. (2006). The two-parameter gamma distribution used in Aksoy (2003) was tested, but was found to provide a poor fit to the data. Randomly

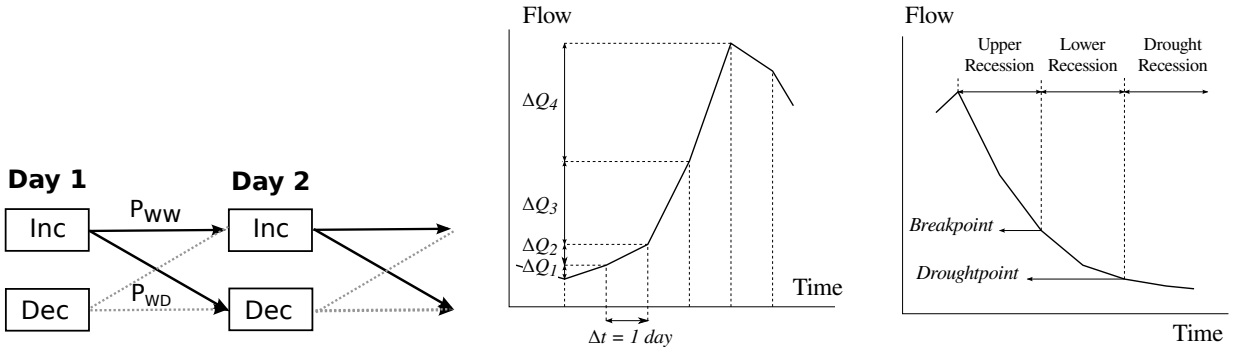

(a) *Daily Markov state transition*

(b) *Increasing limb*

(c) *Decreasing limb*

Figure 2.1: *Daily flow simulation model.*

generated increment values are then ranked in increasing order from the smallest to the largest increment, which occurs at the hydrograph peak. This preserves the correlation structure of the ascension curve and the characteristic shape of daily hydrographs (Aksoy 2003).

The recession curve, occurring on dry days, is modeled as exponential decay, which is a simple, yet generally accepted form for baseflow recession (Tallaksen 1995):

$$Q = Q_o e^{-bt} \tag{2.1}$$

Previous studies have split the recession curve into two portions (upper and lower) with unique recession coefficients (Sargent 1979; Aksoy 2003; Szilagyi et al. 2006). These recession equations take the form:

$$Q = Q_o e^{-b_{\text{upper}} t} \tag{2.2}$$

$$Q = Q^* e^{-b_{\text{lower}} (t - t^*)} \tag{2.3}$$

where b_{upper} is the upper recession coefficient, b_{lower} is the lower recession coefficient, Q_o is the preceding peak flow, Q^* is the initial flow in the lower recession, t is the number

of days after the peak, and t^* is the time from the start of the lower recession. Conceptually, the upper coefficient describes recession following a large storm event, which is primarily influenced by channel storage, while the lower coefficient models baseflow recession, which is influenced by groundwater storage. Rather than employing an arbitrary splitting criterion, like the monthly mean flow (Aksoy 2003) or the 90% ratio (Sargent 1979), breakpoints were selected iteratively to minimize the sum of squared error for the upper and lower recession curves.

Because the purpose of this model is to generate daily streamflow scenarios for use in water resources planning and drought management, greater attention was paid to low flow modeling. With this in mind, a third recession coefficient was added to model extreme low flow recession:

$$Q = Q_{\text{drought}} e^{-b_{\text{drought}}(t - t_{\text{drought}})} \tag{2.4}$$

where $b_{drought}$ is the drought recession coefficient, $Q_{drought}$ is the initial flow in the drought recession, and $t_{drought}$ is the time from the start of the drought recession. This addition considerably improved low flow accuracy, preventing flows from approaching zero during extreme low flow events. Inclusion of an additional term is reasonable in the Potomac River application given that previous uses focused on intermittent streams, where zero flow is expected (Aksoy 2003). The extreme low flow criteria point was set at the 5% low flow exceedance level by maximizing goodness-of-fit and confirmed visually using flow-duration curves. The drought recession coefficient is assumed to be equal for all climate states, as it depends only on baseflow and river stage. The low flow drought condition is experienced very rarely, with only 56% of years in the historical record (1931-2007) falling below this level at any point, and typically only for 1-5 days.

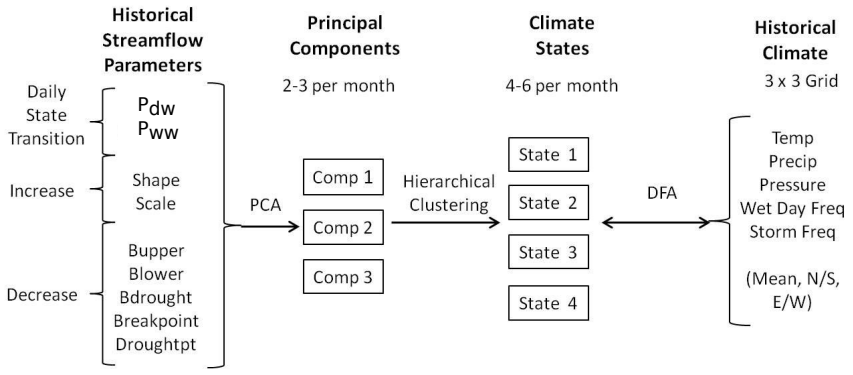

Figure 2.2: *Streamflow analysis and model fitting procedure.*

2.3.3 Monthly Climate Model

Simulation of monthly climate states is governed by a first-order Markov chain, with transition probabilities derived from the historical record. Monthly climate states may be tied to temperature, precipitation, humidity, atmospheric pressure, or any number of climate indices. Classifying monthly climate into discrete states is common in synoptic atmospheric research and has been used to correlate global climate indicators with local weather cycles (Kalkstein et al. 1987; Yarnal and Draves 1993; Michelangeli et al. 1995; Huth 1999). Several climate generation models use Markov chains to describe climatic patterns, either explicitly using circulation typing or implicitly using hidden Markov models (Hughes and Guttorp 1994; Bellone et al. 2000; Thyer and Kuczera 2003; Sansom and Thomson 2007). Climate change is simulated by adjusting the Markov transition probabilities based on GCM scenarios, mirroring shifts in weather patterns.

During the analysis process (Figure 2.2), principal component analysis (PCA) Hotelling (1933) is used (i) to investigate patterns in variation within the daily streamflow model parameters and (ii) to condense these parameters into a smaller set of components that are mutually orthogonal. Use of PCA in this fashion is a common method designed to simplify and normalize multivariate climate data prior to clustering (Corte-Real et al. 1999; Kidson 2000).

The resulting normalized and orthogonal components are grouped using a hierarchical Ward (1963) clustering algorithm in JMP statistical software (SAS Institute Inc. 2007). Ward's method minimizes the within-cluster sum of squares at each cluster step, while merging clusters based on the squared distance between the new centroid and the two original centroids, weighted by the number of observations (Ward 1963).

Clustered streamflow parameters are then tied to large-scale climate indices using historical GCM data. This analysis is performed using discriminant function analysis (DFA), a statistical method used to determine the set of continuous variables that best assign observations to pre-determined groups. In this instance, DFA is used to identify the combination of 15 potential climate measures that best classifies membership to the monthly climate states determined through clustering.

2.3.4 Generating Historical and Climate-Adjusted Streamflows

To generate historical or climate adjusted daily streamflows based on GCM simulations, the analysis process is essentially reversed: (i) discriminant functions are used to classify future GCM realizations into monthly climate states, (ii) new climate state transition probabilities are calculated, and (iii) the daily flow model is executed using the newly adjusted climate transition probabilities and historical flow parameters associated with each climate state.

Accuracy of this process may be validated by analyzing the historical record. In this case, the discriminant functions are used to re-classify historical months into climate states, allowing for some misclassification due to errors in the discriminant functions. Transition probabilities are then obtained, daily streamflows generated, and results compared with the actual historical time series at daily, monthly, and annual scales. This step provides for both validation of the model and a baseline model, against which the climate-adjusted results can be compared (Figure 2.3).

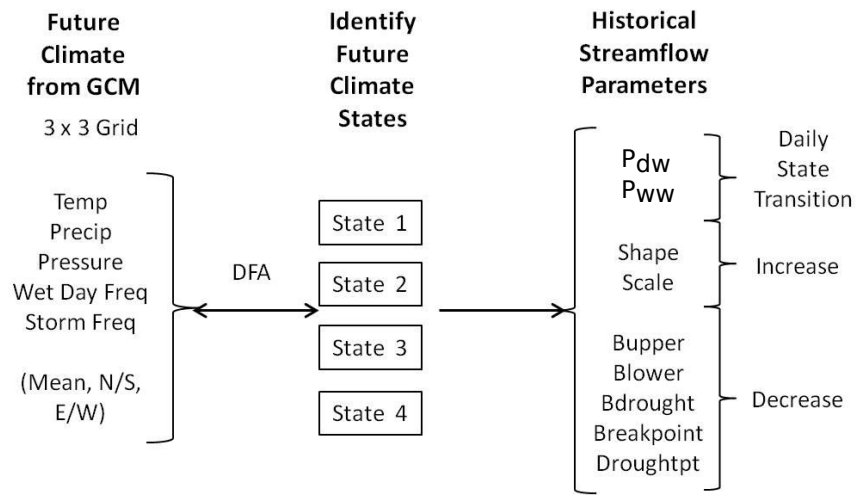

Figure 2.3: *Streamflow generation procedure. Mean refers to the area-weighted mean, N/S refers to the North/South trend and E/W refers to the East/West trend.*

2.4 Results

2.4.1 Data Preparation

The Potomac River was used as a case study to demonstrate the capabilities of the proposed method. Flows were analyzed and simulated for USGS stream gauge 01646500, located on the Potomac River near the Little Falls pumping station in Washington, DC. A daily record of streamflows between 10/01/1929 and 11/30/2007 was obtained from the Interstate Commission on the Potomac River Basin (ICPRB). This data set was adjusted by the ICPRB to reflect historic flows in the Potomac River without the effects of human interaction, calculated by adding daily river withdrawals and subtracting reservoir releases from the historical record (Ahmed et al. 2010). This adjustment compensates for the effects of increasing population and development, allowing for more accurate comparisons across a long time series.

Both monthly and daily historical climate data were obtained from the NOAA-CIRES 20th Century Reanalysis (V2) dataset, made available by NOAA and the U.S. Department of Energy (Compo et al. 2011). Grid dimensions (2.0° latitude x 2.0° longitude) are compa-

Table 2.1: *Evaluated global climate models (IPCC - AR4).*

Model	Institution	Location	Reference
CCSM3	National Center for Atmospheric Research (NCAR)	USA	Collins et al. (2006)
CGM_3.1	Canadian Centre for Climate Modeling and Analysis	Canada	Flato (2005)
CSIRO_MK3	CSIRO Atmospheric Research	Australia	Gordon et al. (2002)
MIROC_3.2	Center for Climate System Research	Japan	Watanabe et al. (2011)
PCM1	National Center for Atmospheric Research (NCAR)	USA	Washington et al. (2000)

rable to available climate-adjusted GCM data sets, which reduces the likelihood of scaling effects.

Five GCMs (Table 4.4) were used to simulate climate adjusted streamflows. Each GCM is based on the IPCC's AR 4 round of climate models and was accessed via the WCRP CMIP3 Multi-Model data portal (Meehl et al. 2007). For all GCMs, climate variables identical to the historical climate dataset were used, with historical climate represented by the Climate of the 20th Century (20C3M) scenario and potential future climate simulated by the SRES A1b, A2, and B1 emission scenarios. Current conditions were simulated based on the 1961-2000 time period, while future climate scenarios were separated into three segments of equal duration: 2010-2039, 2040-2069, and 2070-2099.

2.4.2 Fitting the Daily Streamflow Model

Parameters of the daily streamflow model were fit to each month in the historical record individually, each day classified as being either in an increasing "wet" state or a decreasing "dry" state. State transition probabilities were calculated as:

$$P_{ij} = \frac{n_{ij}}{\sum_j n_{ij}}, \qquad i, j = w, d \tag{2.5}$$

where n_{ij} is the number of observed transitions from state i to j. Wet day increments for each month were fit to the Weibull distribution using the "fitdistrplus" package in R

(version 2.12.0) (Delignette-Muller et al. 2010). Goodness of fit was summarized using the Bayesian information criterion (BIC). Dry day recession coefficients were calculated using nonlinear least-squares estimation (R-"nls" package). Flows were then ranked and all potential breakpoints tested iteratively to determine the optimal splitting criterion between the upper and lower recession curves.

The two transition probabilities of the daily flow model operate in tandem to describe the frequency and duration of the increasing limb, with P_{dw} analogous to storm frequency and P_{ww} analogous to storm duration. As would be expected for the region, the winter and early spring is characterized by low frequency, long duration events (low P_{dw}, high P_{ww}) while the summer and early fall months are characterized by high frequency and short duration events (high P_{dw}, low P_{ww}) (Figure 2.4a).

Fitted recession coefficients control the recession rate for three distinct flow zones, with b_{upper} related to recession following large storm events, b_{lower} related to baseflow recession, and $b_{drought}$ related to recession during extreme low flows. As expected, the recession coefficients affiliated with groundwater storage show considerably less variability than b_{upper} (Figure 2.4b). Recession coefficients decrease during the spring recharge period as more groundwater is available for baseflow, slowing recession rates. Alternatively, the large peak in b_{upper} during the fall coincides with the lowest annual groundwater levels. Following a large storm event in the fall, recession is rapid and quickly returns to baseflow levels.

The scale and shape parameters of the increasing limb Weibull distribution control the magnitude and flashiness of the increasing limb, respectively. Low shape parameter values correspond to a more flashy flow distribution, with both more extreme high flow increments and more increments near zero. As would be expected, these low shape values occur during the summer and early fall months, when rain events tend to be convective and severe in nature (Figure 2.4c). In contrast, the late winter and spring are characterized by high shape parameters, corresponding to more frontal storm events. The scale parameter is related to the magnitude of storm events and, as such, mirrors the general

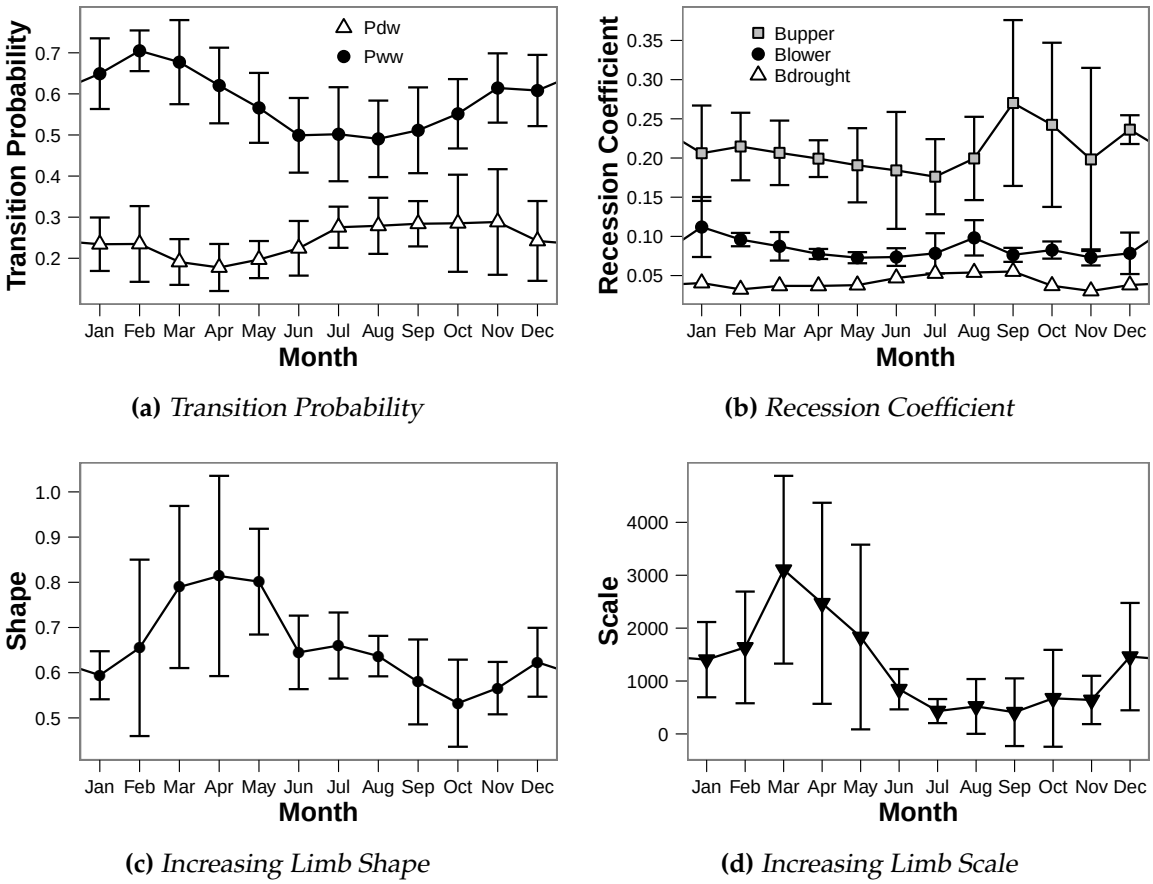

(a) *Transition Probability*

(b) *Recession Coefficient*

(c) *Increasing Limb Shape*

(d) *Increasing Limb Scale*

Figure 2.4: *Daily streamflow model parameters. Line represents mean parameter, while errors bars signify standard deviation.*

shape of monthly flows in the Potomac River, with peaks in March and April and lowest flows in September and October (Figure 2.4d).

2.4.3 Extracting Principal Components from Model Parameters

Because of scaling issues and the potential for correlation among the streamflow parameters (P_{dw}, P_{ww}, shape, scale, b_{lower}, b_{upper}, and breakpoint), PCA was used to calculate a smaller set of normalized, orthogonal summary statistics. The scale parameter and the breakpoint between upper and lower recession curves were adjusted using a logarithmic transform prior to being normalized because of their highly skewed nature.

Three stopping criteria were used in the PCA work: the Kaiser-Guttman criteria (eigenvalues $\lambda > 1$) (Guttman 1954; Kaiser 1960), the Scree plot (Cattell 1966), and Parallel Analysis (Horn 1965). Agreement among these tests was common and typically resulted in 2-3 components being retained for each month. Approximately 60-81% of the standardized variance was explained by these components. Across most months, the first eigenvector explained 38-50% of the variance, with predominant loadings from the recession coefficients, breakpoint and scale parameters, each in the same direction. The second component generally explained 17-31% of the variance and typically took loadings from the state transition probabilities, P_{dw} and P_{ww}, in opposing directions. Where present, the third component explained 15-17% of the overall variance, with loading solely from either P_{ww} or the shape factor. There was no discernible temporal pattern in loading or in variance explained.

2.4.4 Clustering Monthly Climate States

Following PCA, the resulting normalized, orthogonal components were grouped using a hierarchical Ward (1963) clustering algorithm in JMP statistical software (SAS Institute Inc. 2007). Clustering showed a slight temporal trend, with the winter and spring months tending towards more (5-6) distinct clusters and the summer tending towards fewer (4) clusters. Greater variability in flow regimes during the winter and spring months may be caused by a wider variety of complicating climate factors, including snowmelt and long-term groundwater storage.

2.4.5 Creating Predictors of Climate States

Clusters of historical streamflow regimes were then related to historical climate using discriminant function analysis. Potential climate variables used in this study include: mean surface temperature (K), mean surface pressure (Pa), mean precipitation rate (kg m^{-2} s^{-1}), wet day frequency (%), and individual storm frequency (%). Wet day frequency is the ratio of days with measurable (> 0.25 cm) rainfall to total days in a month, while

individual storm frequency is the ratio of unique rainfall events to total days in a month. These two measures describe the frequency and duration of rainfall in a given month. To avoid issues at monthly boundaries, ongoing storm events that began prior to the first day of a month are considered a unique storm event.

For each of these 5 climate variables, 3 measures were used to summarize climate across the 3x3 spatial grid: watershed area-weighted mean, North to South (N-S) variation, and East to West (E-W) variation. This simplification resulted in 15 potential discriminating variables. When extending this method to other applications and geographical locations, any number of climate indicators could be employed, including other gridded GCM climate variables or summary variables, such as measures of quasi-periodic global climate patterns such as the El Niño-Southern Oscillation (ENSO) and the Atlantic Multidecadal Oscillation.

All climate variables followed a normal distribution, satisfying one of the primary assumptions of DFA, although violations of this normality assumption do not tend to affect results significantly (Tabachnick and Fidell 2007). Climate predictor variables were transformed to prevent dissimilar variances and selected in a stepwise fashion, evaluating the entire model at each step against Wilks' lambda (Λ) (F-Test) and the relative percent misclassified. Percent misclassified ranged from 14% to 42%, with the best fit occurring during the summer months and the worst fit in the winter and spring. This trend suggests that streamflow in the winter and spring months is partially related to variables other than the immediate climate, such as snowmelt or groundwater recharge. Flow regime during the summer is less dependent on these extraneous variables and is more readily explained by the current climate.

Other trends are apparent in the discriminating power of the climate variables (Table 2.2). Mean monthly precipitation rate is significant for nearly all months and typically explains the most variability within each monthly discriminant function. The area-weighted mean is important during winter and spring, when most precipitation occurs in large, frontal events; however, the directional components (N-S, E-W) become significant in late summer and early fall as storm events become more spatially fragmented.

Table 2.2: *Climate variable discriminating power. Numbers refer to the rank order in which the variables enter the discriminating equation.*

		Jan	**Feb**	**Mar**	**Apr**	**May**	**Jun**	**Jul**	**Aug**	**Sep**	**Oct**	**Nov**	**Dec**
% Misclassified		33.8	31.0	32.4	39.4	42.3	33.8	14.1	26.8	19.7	19.4	22.2	31.9
# Variables		5	5	5	5	5	5	5	6	7	7	6	5
STemp	Mean							3			4	2	
	N-S								3		7		
	E-W					5	5				6		
SPress	Mean			2	5				5				
	N-S		4	4				2		4	3		4
	E-W	1	2			4	1						
PRate	Mean	2	1	1	1	1		1	1	1	1	1	1
	N-S							5		5			3
	E-W	4			3				6	6	2	3	5
WetDay	Mean	3	3	3		3	3			2			
	N-S				2		2	4	4	3		6	2
	E-W		5	5								4	
StormFrq	Mean	5			4	2	4						
	N-S									7	5		
	E-W								2			5	

Number of days with measurable rainfall (WetDay) is the second most consistent climate indicator, present in the majority of discriminant functions and following the same pattern as total precipitation, with the area-weighted mean dominating winter and spring and directional components dominating during summer. Atmospheric pressure is a significant climate indicator both during the mid-winter and summer months. Atmospheric pressure in the summer likely functions as an indicator of convective storm events. Temperature and unique storm events (StormFrq) tend to have the least discriminating power; however, regional mean temperatures become significant during the summer months.

2.4.6 Simulation of Historical Streamflow

Historical flow sequences were generated using the Climate of the 20th Century (20C3m) scenarios for each GCM and compared to the observed historical record in order to vali-

date the streamflow generation method and to identify any bias introduced by the climate models. Stochastic simulation of flow reproduced the observed historical record closely at the daily, monthly and annual time steps. The MIROC, CSIRO and NCAR CCSM models were consistently the best performers across all metrics, while the NCAR PCM1 and CCC models generally produced poorer statistical agreement. As a general rule, agreement was best during months with a consistent climate, whereas months at the transition between seasons produced greater error.

Seasonal Trends

All GCMs adequately modeled the seasonality among monthly aggregated flows on the Potomac River (Figure 2.5). Across all months, the model with the most consistent agreement is the MIROC model. The CSIRO and NCAR CCSM models were also capable of reproducing the central tendency and distribution of monthly means (Table 2.3). The PCM1 and CCC models perform adequately for the majority of months, with some deviation occurring due to an underestimate of the median and higher flows. Variance among months with low flows was the most successfully modeled monthly parameter, which is likely related to the emphasis on drought modeling in the model's creation.

Monthly agreement is best for mid-seasonal months across all GCM models, with greater error at the seasonal transitions. Agreement during the summer and early fall (Jun - Oct) is best, with Mann-Whitney p-values between 0.168 and 0.990, suggesting no statistical difference (Table 2.3). All GCMs underestimate the median for February ($p = 0.039$-0.384), but match the distribution well (Kolmogorov-Smirnov $p = 0.042$-0.343). Likewise, the distribution of monthly flows in May agree well with the historical record, but tend to underestimate the median. November and December have good agreement with regards to the median and low flows, with some underestimates of the upper limb of the distribution (Figure 2.5).

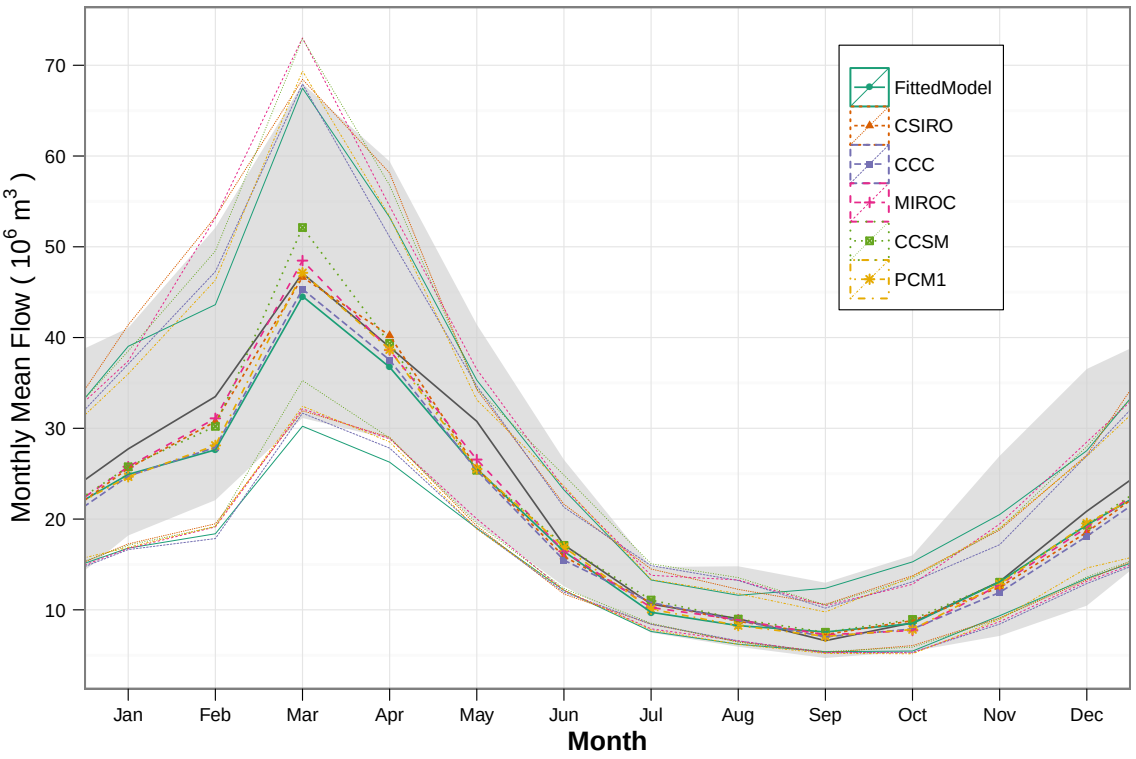

Figure 2.5: *Monthly mean flows for the historical scenario (1961-2000). Median values are displayed as central lines, with black representing the historical record and colored lines representing the various models. The 25th and 75 th percentiles are represented by the shaded area for the historical record and thin lines for model simulations.*

Annual Statistics

At the annual time step, several statistics are reproduced successfully, including the annual mean, coefficient of variation (CV), date of minimum flow and date of maximum flow. No statistical difference exists for the MIROC, CSIRO, and CCSM models (p = 0.151-0.301) between the GCM generated distribution of annual mean flows and the observed, while the CCC and PCM1 models show a slight statistical difference (p = 0.023-0.039) attributed to a slight underprediction (Table 2.3). The distribution of Annual CV is also well-captured for all GCMs ($p > 0.05$), except for the CCC model (p = 0.024) (Table 2.3).

The occurrence of the annual minimum and maximum, with medians of Sep 28 and Mar 7 respectively, are modeled successfully by all GCMs. Dates were adjusted based on water year (Oct 1 - Sep 30) for maximum flow and low flow year (Apr 1 - Mar 31) to

prevent discontinuities. Date of the minimum flow has significantly less variation than the date of the maximum flow.

While the fitted models produce a slight bias in the distribution of annual minimum flow for the wettest years, all models reproduce the extreme low flows (recurrence interval < 3 years) very well. While this limitation should be considered when using the model, it is important to note that years with greater than average low flows are of less consequence for low flow modeling and the $7Q_{10}$ is a much more useful measure for simulating drought operations. All GCMs have similar performance with respect to extreme low flows, except for the PCM1 model, which tends to predict more severe low flows than the historical record.

Daily Flow Distribution

Daily flow behavior tends to be more difficult to replicate than the aggregated monthly or annual statistics because of the numerous climatic factors affecting daily flows and the rapid changes in flow brought about by storm events. The proposed model captures much of this daily variability, successfully simulates the distribution of daily flows, and replicates the autocorrelation structure. As with monthly aggregated flows, the best agreement occurs in months with relatively stable climate, rather than during transitional seasons. The distribution of daily flows is most consistent for January and the summer months (June, July and August).

The MIROC and CSIRO GCMs produce the most consistent agreement for the daily flow distribution (Table 2.4). The remaining models perform well for most months, with some isolated months exhibit a slight bias. The CCSM model agreement is good in all aspects, except for predicting high flow events occurring in September and October (Hydraulic Alteration $> 10\%$) . The PCM1 and CCC GCMs both successfully reproduce the daily flow distribution for all months, except for the winter, where they underpredict median storm events (50-75% exceedance probability). Across all months, the CCSM model tends to be the "wettest" model, producing consistently higher flow distributions, while

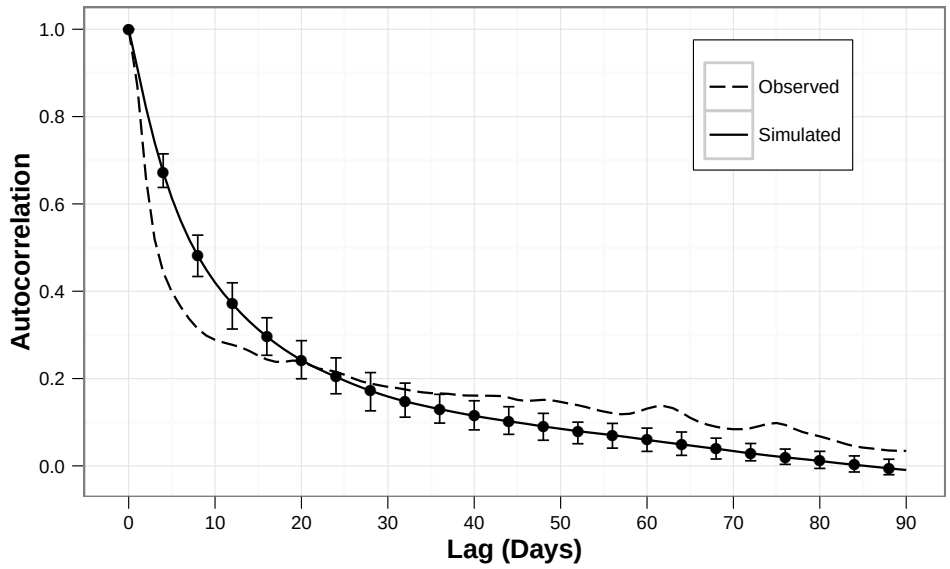

Figure 2.6: *Correlogram of daily streamflow.*

the PCM1 model tends to be the "driest" model, producing the lowest daily flow distributions.

Some seasonal trends exist within the daily flow distributions. Daily flows during the winter months are reproduced well across the entire flow distribution, while the model tends to overpredict low flows during the spring (March and April). Summer flows are captured well, though all GCMs exhibit a tendency to underpredict the highest 15% of flows during the fall months (Sep, Oct and Nov), with the remainder of the distribution reproduced very well. Fall storm events may prove difficult to model because they occur in a time period when precipitation events are transitioning from convective to frontal behavior and when hurricanes or tropical storms may impact the region.

The underlying structure of the Markov model adequately reproduces the autocorrelation structure of the daily streamflows (Figure 2.6). This result matches findings from other similar studies of Markov chain-based streamflow generation models (Xu et al. 2001).

Table 2.3: *Mann-Whitney Test for historical validation of GCM Means. Test statistic is the Mann-Whitney p-value, with underlined values indicating a statistically significant difference from the historical.*

	Annual		*Monthly*										
	Mean	CV	Jan	Feb	Mar	Apr	May	Jun	Jul	Aug	Sep	Oct	Nov	Dec
Fit Model	0.103	0.078	0.370	0.039	0.090	0.201	0.112	0.398	0.463	0.715	0.253	0.920	0.721	0.114
CCC	0.023	0.024	0.228	0.069	0.152	0.272	0.097	0.168	0.573	0.253	0.963	0.535	0.199	0.054
CSIRO	0.151	0.053	0.524	0.308	0.185	0.941	0.066	0.171	0.674	0.430	0.626	0.696	0.434	0.057
MIROC	0.197	0.122	0.346	0.384	0.434	0.500	0.247	0.406	0.869	0.285	0.653	0.537	0.498	0.084
CCSM	0.301	0.052	0.379	0.260	0.802	0.670	0.086	0.757	0.473	0.203	0.587	0.715	0.523	0.103
PCM1	0.039	0.060	0.190	0.091	0.270	0.423	0.059	0.519	0.604	0.696	0.990	0.574	0.451	0.093

Table 2.4: *Percent Hydrologic Alteration of 20th Century GCM flow distribution. Alteration calculated based on 5 percentile flow bins.*

Model	Annual	Jan	Feb	Mar	Apr	May	Jun	Jul	Aug	Sep	Oct	Nov	Dec	Mean
FitModel	1.0	2.6	7.3	10.4	9.9	6.6	3.4	3.5	4.7	3.5	7.4	10.7	9.8	6.6
CCC	1.7	3.9	6.5	8.4	8.9	8.3	2.9	3.9	5.0	10.8	8.3	12.9	10.3	7.5
CSIRO	1.5	3.6	5.4	8.8	9.7	7.7	4.6	4.4	5.4	5.4	9.3	12.2	9.9	7.2
MIROC	0.8	4.1	7.6	8.1	8.4	6.5	4.8	2.7	3.6	6.4	7.2	9.5	7.3	6.3
CCSM	1.1	4.8	6.5	6.7	8.3	6.6	5.4	2.4	4.9	10.6	10.0	9.8	6.4	6.9
PCM1	1.1	4.1	7.4	9.2	9.6	7.9	3.1	2.1	4.3	9.2	7.7	12.3	10.7	7.3
Mean	1.2	3.9	6.8	8.6	9.1	7.3	4.0	3.2	4.7	7.7	8.3	11.2	9.1	

Table 2.5: *Percent change in mean annual flow for climate change realizations.*

Model	2010-2039	2040-2069	2070-2099
CCC	3.73 *(2.62 – 4.37)*	3.34 *(-0.11 – 5.98)*	5.04 *(3.20 – 7.47)*
CCSM	0.50 *(-2.29 – 2.50)*	3.54 *(1.86 – 5.08)*	3.89 *(0.70 – 6.49)*
CSIRO	0.19 *(-3.09 – 6.47)*	2.35 *(1.15 – 4.03)*	0.68 *(-4.88 – 9.64)*
MIROC		2.23 *(1.37 – 3.25)*	3.10 *(-1.13 – 6.88)*
PCM1	6.23 *(5.66 – 6.79)*	8.58 *(7.42 – 9.59)*	8.60 *(7.78 – 9.27)*

2.4.7 Predicted Climate Change Effects on Streamflow

The effect of climate change on streamflow in the Potomac River was evaluated by generating daily streamflow time series subject to three climate change emission scenarios (SRES A1b, A2, and B1) for three discrete time periods (2010-2039, 2040-2069, 2070-2099).

Annual Flows

Simulation of climate adjusted streamflows under the three emission scenarios suggests an increase in mean annual flow between 1 and 7% by 2070-2099 (Table 2.5). A consistent increase of 2-4% in the 2040-2069 time period matches closely with Milly's (2005) prediction of a 3.6% increase in mean annual flow. The greatest increase in mean annual flow occurs in the CCC and PCM1 models, while the remaining GCMs show greater variability and only a moderate increase in mean annual flow. In addition to this slight increase in mean annual flow, the coefficient of variation (CV) among annual flows is predicted to increase significantly, suggesting a wider distribution of flows. As expected, these trends continue throughout the century and are most evident for the A2 scenario and less detectable for the B1 scenario.

There is little projected change in the date of the annual maximum flow; however, the date of the minimum annual flow is predicted to occur 2-5 days earlier by the 2070-2099 time period, on average. This shift is consistent across all GCM models and scenarios.

Seasonal Trends

Nearly all GCM simulations show an increase in mean monthly flows for the Potomac River in the months between December and April, with this shift increasing throughout the next century (Figure 2.7). As expected, this increase is greatest for the highest emission scenario, A2. In addition to an increase in the central tendency of winter flows, the distribution of monthly flow is projected to increase in variability, particularly increasing for high flows. This trend of increased flow during the winter and early spring corresponds well with studies by Najjar et al. (2009), Mccabe and Ayers (1989), Hayhoe et al. (2007), which project similar seasonal shifts.

In contrast, the model realizations predict a decrease in summer flows, particularly for the months of July and August (Figure 2.7). This seasonal trend is evident for all GCMs except for PCM1.

The months of October and November show the greatest uncertainty in predictions for monthly flows over the next century. This is not a surprising result, given their difficulty in validation. The NCAR models (CCSM and PCM1) and CSIRO all predict a significant increase in flow during these months in the future, which may be attributable to tropical storm events or other long duration, high precipitation events. However, a similar trend is not apparent in the other GCM realizations.

Extreme Low Flows

Estimates of the change in extreme low flows predict a slight decrease in the $7Q_{10}$ minimum flow given the modeled emission scenarios. A notable decrease was detected for all GCMs, except for the NCAR CCSM model, which produces mixed results and the PCM1 model, which produced a consistent increase. For those models with an apparent decrease in extreme low flows, the $7Q_{10}$ minimum flow is predicted to decrease by 0-10.1%, with the greatest decrease attributable to the A2 emission scenario (Table 2.6). This trend suggests that droughts will increase in severity over the modeled time period.

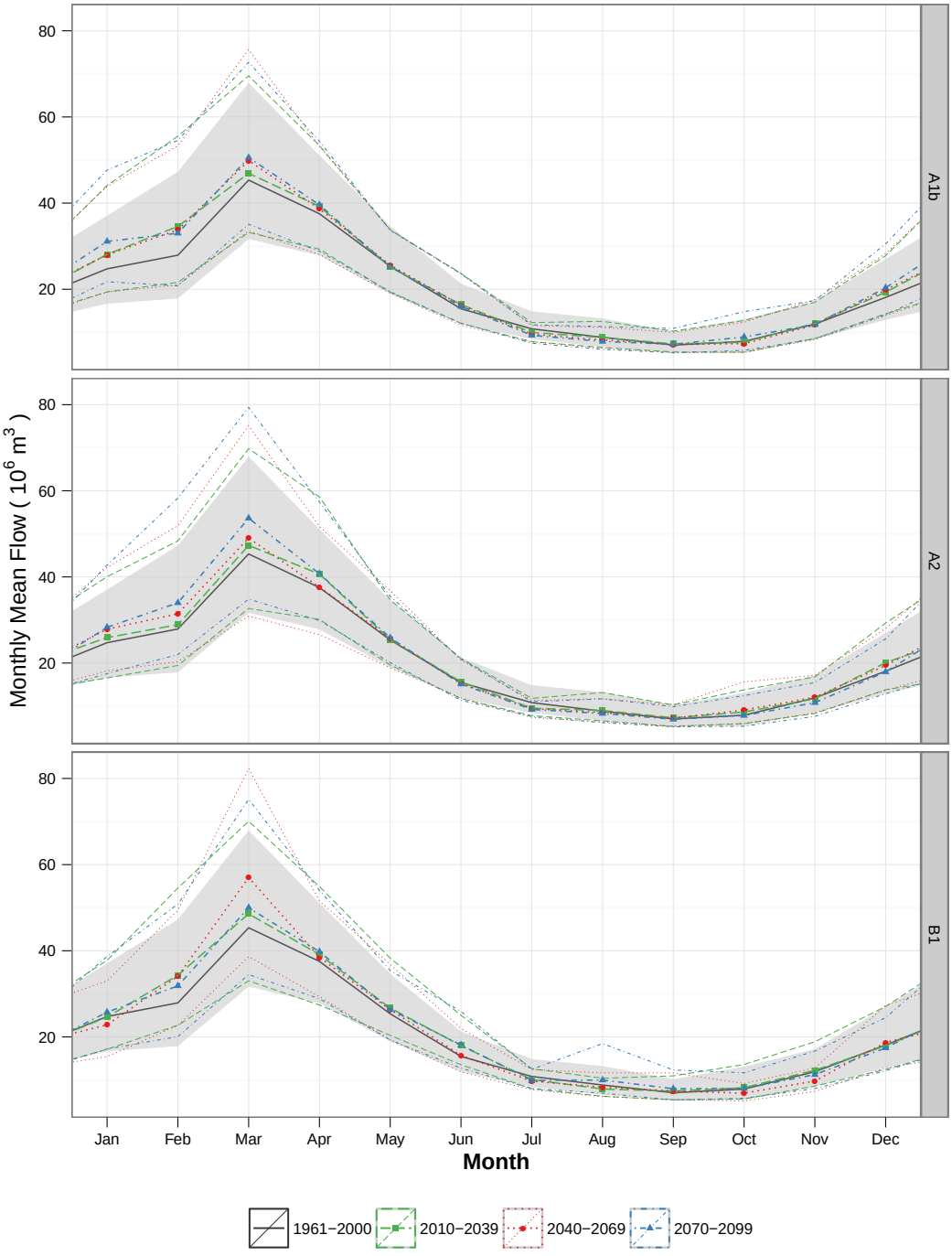

Figure 2.7: *Variation in monthly mean due to climate change (CCC). Median values are displayed as central lines, with black representing the historical record and colored lines representing climate change time steps. The 25th and 75 th percentiles are represented by the shaded area for the historical record and thin lines for climate change simulations.*

Table 2.6: *Percent change in $7Q_{10}$ minimum flow for climate change realizations.*

Model	2010-2039	2040-2069	2070-2099
CCC	-1.82 *(-5.98 – 1.62)*	-0.83 *(-2.73 – 0.66)*	-0.09 *(-3.25 – 4.69)*
CCSM	2.21 *(1.00 – 4.57)*	-0.03 *(-2.07 – 3.09)*	2.60 *(-1.66 – 5.84)*
CSIRO	-5.74 *(-7.87 – -2.09)*	-3.11 *(-5.63 – -1.34)*	-5.57 *(-10.06 – -3.32)*
MIROC		-1.17 *(-2.69 – 0.43)*	-4.31 *(-5.91 – -1.68)*
PCM1	2.99 *(2.93 – 3.05)*	3.23 *(2.28 – 4.10)*	9.07 *(6.94 – 10.87)*

Daily Flows

The apparent increase in winter flows is attributable to an increase across the entire range of streamflows, rather than an increase in a particular part of the flow distribution. This trend continues until the transitional months of March and April, where the increase occurs primarily in the low and middle flows (60-90% exceedance), with no change in either extreme low flows or high flows.

The decrease in July and August flow is explained by a consistent decrease in flows during these months across all levels of flow, except for the extreme low flows (90-99% exceedance) which remain consistent with the historical record.

As in the case of monthly means, the fall months exhibit mixed trends across the projected future climatic conditions. The CCSM, CSIRO and PCM1 models, which project a significant increase in mean flow during the months of September and October, attribute this to an increase in high streamflow events (exceedance $< 40\%$), which further points to an increase in large, sustained rainfall events, potentially related to tropical storm events.

2.5 Conclusions

A stochastic streamflow method was developed that links a monthly climate model with a daily streamflow generation model. Using discriminant functions, GCM-scale climate data may be directly related to discrete streamflow states, which in turn control the generation of daily streamflow time series. With engineers and planners increasingly focused

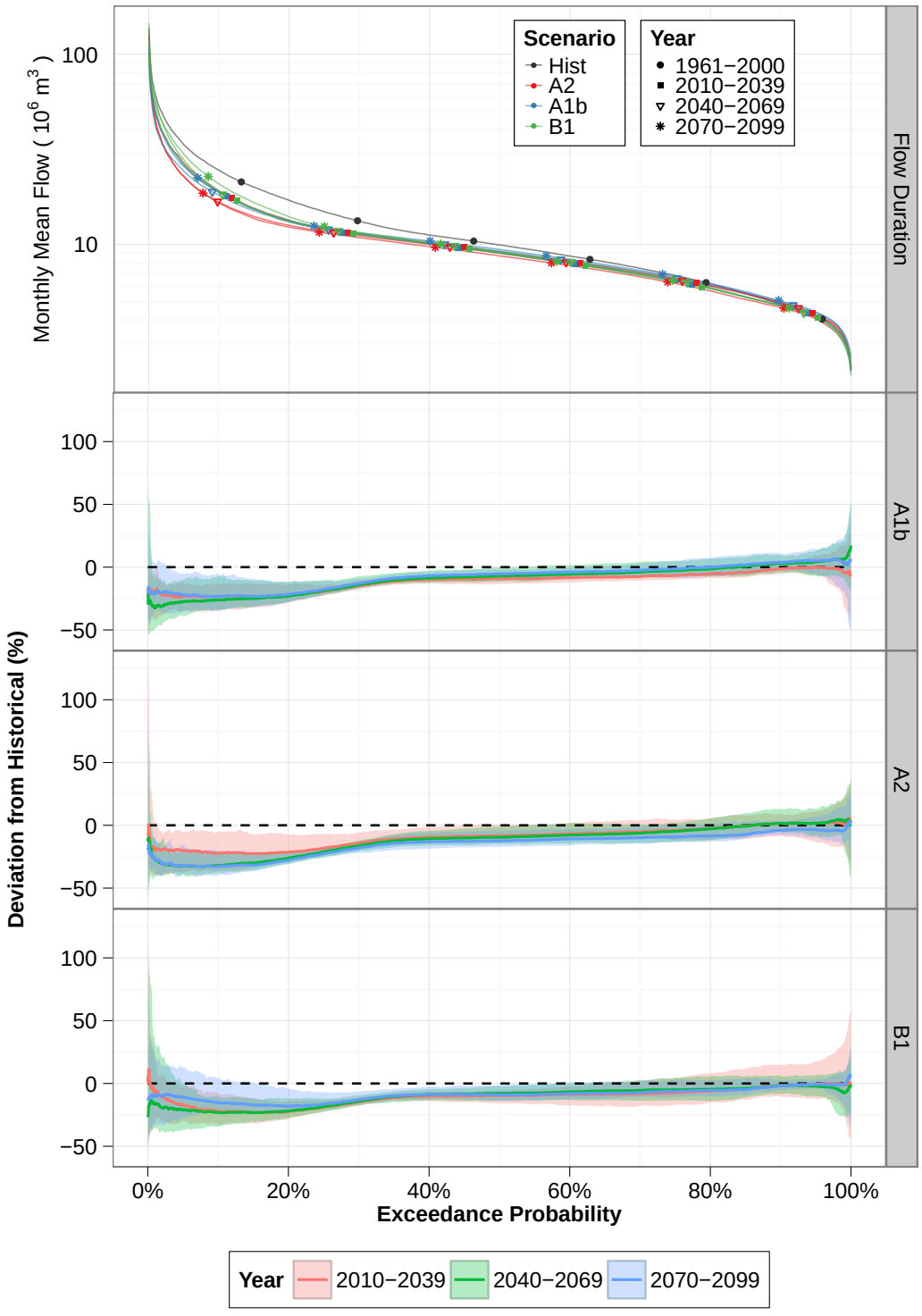

Figure 2.8: *Flow duration curve for July subject to climate change (CCSM). The upper figure shows the entire distribution of July flows, while the lower figures present the percent change relative to the historical.*

on the potential effects of climate change on water resources, this model allows the generation of long daily streamflow time series which can be used for simulation or adaptation studies.

A case study was presented using the Potomac River to evaluate the method. Historical streamflow statistics are reproduced successfully at the daily, monthly and annual time steps. In addition, the autocorrelation structure of daily streamflow is maintained. Bias correction was not utilized in this study to allow for direct analysis of the model without significant transformation, however, future iterations could evaluate the benefits of bias correction in this context.

Extending this model to evaluate the effect of climate change on streamflow in the Potomac produced results in keeping with other streamflow projections for the Mid-Atlantic. Mean annual streamflow is projected to increase by 1-7% by 2100, with the majority of this increase occurring during the winter and early spring. This increase occurs across all levels of streamflow. Conversely, summer flows are projected to decrease, particularly during July and August, caused by a decrease in large, sustained storm flows. This change in summer flow is projected to increase the severity of extreme low flows slightly and to shift the date of the annual minimum flow, which historically occurs in mid-September, 2-5 days earlier by the 2070-2099 time period. The models diverge in their predictions of the fall months, suggesting a need for further research and potentially additional climate indicators. Some GCMs predict a large increase in mean flow during September and October, which may point to an increase in tropical storm events.

The included case study presents the streamflow analysis and simulation process as applied to an individual streamflow station; however, this model may be expanded to simulate climate-adjusted streamflow at multiple locations within a watershed using spatial disaggregation techniques such as the method of fragments (Porter and Pink 1991) or by simulating at each location simultaneously using a covariate term.

As presented, the method is an extensible framework, which can be modified to include additional climate indicators or more complex streamflow models, providing significant opportunities for future exploration. For instance, there is potential for better

simulation of tropical events or for including periodic global climate patterns such as the El Niño-Southern Oscillation (ENSO) as these simulation models improve.

2.6 Acknowledgments

James Stagge is a Via Doctoral Fellow and gratefully acknowledges support from the Via program and the Institute for Critical Technology and Applied Science (ICTAS). The authors would also like to thank the Interstate Commission on the Potomac River Basin (ICPRB) and Hydrologics, Inc. for providing data access and research support.

Bibliography

Ahmed, S. N., K. R. Bencala, and C. L. Schultz (2010). 2010 Washington Metropolitan Area water supply reliability study; part 1: Demand and resource availability forecast for the year 2040. Technical Report ICPRB 10-01, Interstate Commission on the Potomac River Basin.

Aksoy, H. (2003). Markov chain-based modeling techniques for stochastic generation of daily intermittent streamflows. *Advances in Water Resources 26*(6), 663–671.

Aksoy, H. and M. Bayazit (2000). A model for daily flows of intermittent streams. *Hydrological Processes 14*(10), 614–633.

Bartolini, P. and J. D. Salas (1993). Modeling of streamflow processes at different time scales. *Water Resources Research 29*(8), 2573–2587.

Beard, L. R. (1967). Simulation of daily streamflows. In *Proc International Hydrology Symposium*, Fort Collins, Colorado, pp. 624–632.

Bellone, E., J. P. Hughes, and G. P (2000). A hidden Markov model for downscaling synoptic atmospheric patterns to precipitation amounts. *Climate Research 15*(1).

Box, G. and G. M. Jenkins (Eds.) (1970). *Time Series Analysis, Forecasting and Control*. San Francisco: Holden Day.

Box, G. E. P. and D. R. Cox (1964). An analysis of transformations. *Journal of the Royal Statistical Society, Series B 2*, 211–252.

Buishand, T. A. and T. Brandsma (2001). Multisite simulation of daily precipitation and temperature in the Rhine basin by nearest-neighbor resampling. *Water Resour. Res. 37*, 2761–2776.

Cattell, R. B. (1966). The scree test for the number of factors. *Multivariate Behavioral Research 1*(2), 245–276.

Chapman, T. (1997). Stochastic modelling of daily rainfall in the Western Pacific. *Math. Comput. Simulat. 43*, 351–358.

Collins, W. D., C. M. Bitz, M. L. Blackmon, G. B. Bonan, C. S. Bretherton, J. A. Carton, P. Chang, S. C. Doney, J. J. Hack, T. B. Henderson, J. T. Kiehl, W. G. Large, D. S. McKenna, B. D. Santer, and R. D. Smith (2006). The Community Climate System Model Version 3 (CCSM3). *Journal of Climate 19*, 2122–2143.

Compo, G. P., J. S. Whitaker, P. D. Sardeshmukh, N. Matsui, R. J. Allan, X. Yin, B. E. Gleason, R. S. Vose, G. Rutledge, and P. Bessemoulin (2011). The Twentieth Century Reanalysis Project. *Quarterly Journal of the Royal Meteorological Society 137*(654), 1–28.

Corte-Real, J., B. Quian, and H. Xu (1999). Circulation patterns, daily precipitation in Portugal and implications for climate change simulated by the second Hadley Centre GCM. *Climate Dynamics 15*, 921–935.

Delignette-Muller, M. L., R. Pouillot, J.-B. Denis, and C. Dutang (2010). *fitdistrplus: help to fit of a parametric distribution to non-censored or censored data*. R package version 0.1-3.

Flato, G. (2005). The Third Generation Coupled Global Climate Model (CGCM3).

Gordon, H. B., L. D. Rotstayn, J. L. McGregor, M. R. Dix, E. A. Kowalczyk, S. P. O'Farrell, L. J. Waterman, A. C. Hirst, S. G. Wilson, M. A. Collier, I. G. Watterson, and T. I. Elliott (2002). The CSIRO Mk3 climate system model. Technical Report 60, CSIRO Atmospheric Research Technical Paper.

Groisman, P. Y., R. W. Knight, and T. R. Karl (2001). Heavy precipitation and high streamflow in the contiguous United States: Trends in the twentieth century. *Bulletin of the American Meteorological Society 82*(2), 219–246.

Groisman, P. Y., R. W. Knight, T. R. Karl, D. R. Easterling, B. Sun, and J. H. Lawrimore (2004). Contemporary changes of the hydrological cycle over the contiguous United States: Trends derived from in situ observations. *Journal of Hydrometeorology 5*(1), 64–85.

Grygier, J. C. and J. R. Stedinger (1988). Condensed disaggregation procedures and conservation corrections for stochastic hydrology. *Water Resources Research 24*(10), 1574–1584.

Guttman, L. (1954). Some necessary conditions for factor analysis. *Psychometrika 19*, 149–161.

Harms, A. G. and T. H. Campbell (1967). An extension to the Thomas-Fiering model for the sequential generation of streamflow. *Water Resources Research 3*(3), 653–661.

Hayhoe, K., C. Wake, B. Anderson, X.-Z. Liang, E. Maurer, J. Zhu, J. Bradbury, A. DeGaetano, A. Stoner, and D. Wuebbles (2008). Regional climate change projections for the Northeast USA. *Mitigation and Adaptation Strategies for Global Change 13*, 425–436.

Hayhoe, K., C. Wake, B. Anderson, X.-Z. Liang, E. Maurer, J. Zhu, J. Bradbury, A. DeGaetano, A. M. Stoner, and D. Wuebbles (2007). Regional climate change projections for the Northeast USA. *Mitigation and Adaptation Strategies for Global Change 13*(5-6), 425–436.

Hirsch, R. (1979). Synthetic hydrology and water supply reliability. *Water Resources Research 15*(4), 1603–1615.

Horn, J. L. (1965). A rationale and test for the number of factors in factor analysis. *Psychometrika 30*(2), 179–185.

Hotelling, H. (1933). Analysis of a complex of statistical variables into principal components. *Journal of Educational Psychology 24*(6), 417–441.

Hughes, J. P. and P. Guttorp (1994). A class of stochastic models for relating synoptic atmospheric patterns to regional hydrologic phenomena. *Water Resources Research 30*, 1535–1546.

Huth, R. (1999). Statistical downscaling in central Europe: evaluation of methods and potential predictors. *Climate Research 13*, 91–101.

Kaiser, H. F. (1960). The application of electronic computers to factor analysis. *Educational and Psychological Measurement 20*(1), 141–151.

Kalkstein, L. S., G. Tan, and J. A. Skindlov (1987, Jun). An evaluation of three clustering procedures for use in synoptic climatological classification. *Journal of Applied Meteorology 26*, 717–730.

Kidson, J. W. (2000). An analysis of New Zealand synoptic types and their use in defining weather regimes. *International Journal of Climatology 20*(3), 299–316.

Kottegoda, N. T. (1980). *Stochastic water resources technology*. New York: John Wiley & Sons.

Lall, U. and A. Sharma (1996). A nearest neighbor bootstrap for resampling hydrologic time series. *Water Resources Research 32*(3), 679–693.

Maheepala, S. and B. J. C. Perera (1996). Monthly hydrologic data generation by disaggregation. *Journal of Hydrology 178*(1-4), 277–291.

Matalas, N. C. (1997). Stochastic hydrology in the context of climate change. *Climatic Change 37*, 89–101.

Mccabe, Jr., G. J. and M. A. Ayers (1989). Hydrologic effects of climate change in the Delaware River basin. *Water Resources Bulletin 25*(6).

Meehl, G. A., C. Covey, T. Delworth, M. Latif, B. McAvaney, J. F. B. Mitchell, R. J. Stouffer, and K. E. Taylor (2007). The WCRP CMIP3 multi-model dataset: A new era in climate change research. *Bulletin of the American Meteorological Society 88*, 1383–1394.

Meehl, G. A., T. F. Stocker, W. D. Collins, P. Friedlingstein, A. T. Gaye, J. M. Gregory, A. Kitoh, R. Knutti, J. M. Murphy, A. Noda, and et al. (2007). Global climate projections: Climate Change 2007: The physical science basis (Chapter 10) (the fourth assessment report). *Cambridge University Press New York*, 747–845.

Michelangeli, P. A., R. Vautard, and B. Legras (1995, Apr). Weather regimes: Recurrence and quasi stationarity. *Journal of Atmospheric Sciences 52*, 1237–1256.

Milly, P. C. D., K. A. Dunne, and A. V. Vecchia (2005). Global pattern of trends in streamflow and water availability in a changing climate. *Nature 438*(7066), 347–350.

Moore, M. V., M. L. Pace, J. R. Mather, P. S. Murdoch, R. W. Howarth, C. L. Folt, C. Y. Chen, H. F. Hemond, P. A. Flebbe, and C. T. Driscoll (1997). Potential effects of climate change on freshwater ecosystems of the New England/Mid-Atlantic region. *Hydrological Processes 11*(8), 925–947.

Najjar, R., L. Patterson, and S. Graham (2009). Climate simulations of major estuarine watersheds in the Mid-Atlantic region of the US. *Climatic Change 95*, 139–168.

Payne, K., W. R. Neumann, and K. D. Kerri (1969). Daily streamflow simulation. *J. Hydraul. Div., Proc. Amer. Soc. Civ. Engrs 95*, 1163.

Porter, J. W. and B. J. Pink (1991). A method of synthetic fragments for disaggregation in stochastic data generation. In *Hydrology and Water Resources Symposium*, Institution of Engineers, Australia, pp. 187–191.

Prairie, J. R., B. Rajagopalan, T. J. Fulp, and E. A. Zagona (2006). Modified K-NN model for stochastic streamflow simulation. *Journal of Hydrologic Engineering 11*(4), 371–378.

Pyke, C. R., R. G. Najjar, M. B. Adams, D. Breitburg, M. Kemp, C. Hershner, R. Howarth, M. Mulholland, M. Paolisso, D. Secor, and et al. (2008). Climate change and the Chesapeake Bay: State-of-the-science review and recommendations. *Order: A Journal On The Theory Of Ordered Sets And Its Applications 7415*(9), 1–6.

Quimpo, R. G. (1968). Stochastic analysis of daily river flows. *J. Hydraul. Div., Proc. Amer. Soc. Civ. Engrs 94*, 43–57.

Quimpo, R. G. and V. Yevjevich (1967). Stochastic description of daily river flows. In *Proceedings of the Internatinal Hydrology Symposium*, Fort Collins, Colorado, pp. 291–297.

Sansom, J. and P. Thomson (2007, Aug). On rainfall seasonality using a hidden semi-Markov model. *Journal of Geophysical Research (Atmospheres) 112*(D15).

Sargent, D. M. (1979). A simplified model for the generation of daily streamflows. *Hydrological Sciences Journal 24*(4), 509–527.

SAS Institute Inc. (2007). Jmp, version 7.

Sharma, A., D. G. Tarboton, and U. Lall (1997). Streamflow simulation: A nonparametric approach. *Water Resources Research 33*(2), 291–308.

Srikanthan, R. and T. McMahon (2001). Stochastic generation of annual, monthly and daily climate data: A review. *Hydrology and Earth System Sciences 5*(4), 653–670.

Srikanthan, R. and T. A. McMahon (1982). Stochastic generation of monthly streamflows. *Journal of the Hydraulics Division-ASCE 108*(3), 419–441.

Stedinger, J. R., D. P. Lettenmaier, and R. M. Vogel (1985). Multisite ARMA (1, 1) and disaggregation models for annual streamflow generation. *Water Resources Research 21*(4), 497–509.

Stedinger, J. R. and R. M. Vogel (1984). Disaggregation procedures for generating serially correlated flow vectors. *Water Resources Research 20*(1), 47–56.

Szilagyi, J., G. Balint, and A. Csik (2006). Hybrid, Markov chain-based model for daily streamflow generation at multiple catchment sites. *Journal of Hydrologic Engineering 11*(3), 245.

Tabachnick, B. G. and L. S. Fidell (2007). *Using Multivariate Statistics* (Fifth ed.). Boston: Allyn & Bacon.

Tallaksen, L. (1995). A review of baseflow recession analysis. *Journal of Hydrology 165*(3), 349–370.

Tebaldi, C., K. Hayhoe, J. M. Arblaster, and G. A. Meehl (2006). Going to the extremes. *Climatic Change 79*(3-4), 185–211.

Thomas, H. A. and M. B. Fiering (1962). Mathematical synthesis of stream flow sequences for the analysis of river basins by simulation. In *Design of Water Resources*. Harvard University Press.

Thyer, M. and G. Kuczera (2003). A hidden Markov model for modelling long-term persistence in multi-site rainfall time series 1: model calibration using a Bayesian approach. *275*, 12–26.

Treiber, B. and E. J. Plate (1975). A stochastic model for the simulation of daily flows. In *Internation Symp. and Workshops on the Application of Mathematical Models in Hydrology and Water Resource Systems*, Bratislava.

Valencia, R. D. and J. C. Schakke, Jr. (1973). Disaggregation processes in stochastic hydrology. *Water Resources Research 9*, 580–585.

Vogel, R. M. and A. L. Shallcross (1996). The moving blocks bootstrap versus parametric time series models. *Water Resources Research 32*(6), 1875–1882.

Ward, J. H. (1963). Hierarchical grouping to optimize an objective function. *Journal of the American Statistical Association 58*(301), 236–244.

Washington, W. M., J. W. Weatherly, G. A. Meehl, A. J. J. Semtner, T. W. Bettge, A. P. Craig, W. G. J. Strand, J. Arblaster, V. B. Wayland, R. James, and Y. Zhang (2000). Parallel climate model (PCM) control and transient simulations. *Climate Dynamics 16*, 755–774.

Watanabe, S., T. Hajima, K. Sudo, T. Nagashima, T. Takemura, H. Okajima, T. Nozawa, H. Kawase, M. Abe, T. Yokohata, T. Ise, H. Sato, E. Kato, K. Takata, S. Emori, and M. Kawamiya (2011). MIROC-ESM: model description and basic results of CMIP5-20c3m experiments. *Geoscientic Model Development Discussions 4*, 1063–1128.

Weiss, G. (1977). Shot noise models for the generation of synthetic streamflow data. *Water Resources Research 13*(1), 101–108.

Xu, Z. X., A. Schumann, and C. Brass (2001). Markov autocorrelation pulse model for two sites daily streamflow. *Journal of Hydrologic Engineering 6*, 189–195.

Yarnal, B. and J. D. Draves (1993). A synoptic climatology of stream flow and acidity. *Climate Research 2*, 193–202.

Chapter 3

Manuscript 2: Genetic Algorithm Optimization of a Multi-Reservoir System with Long Lag Times

Abstract

A scenario of particular importance in water resources management occurs when reservoir release decisions must be made well in advance of accurate hydrologic forecasts due to long travel times between reservoir releases and demand. This typical situation is evaluated using the Washington Metropolitan Area (WMA) water supply as a case study. Several classes of operating rules are evaluated using a state-of-the-art multiobjective evolutionary algorithm linked to a hydrologic simulation/decision model. Operating rules were evaluated based on the historical period of record (1929-2007) and synthetically generated time series. The proposed optimization framework is effective for a wide range of water resources vulnerability studies and was successful in improving the efficiency of the WMA system with respect to competing objectives ranging from reservoir storage to recreation and environmental flow requirements.

3.1 Introduction

Optimization of water resources decision-making focuses on maximizing a system's benefit while considering competing objectives and the uncertainty inherent in natural systems. A scenario of particular importance for many water supply systems with long travel times occurs when release decisions must be made well in advance of the water's usage and subsequent benefit. This form of uncertainty is a unique water management challenge and must be handled carefully in optimization schemes to adequately simulate the impact of imperfect foresight. This paper demonstrates an optimization scheme using a state-of-the-art multiobjective evolutionary algorithm, capable of quantitatively and objectively determining the timing, magnitude and location of water supply releases in a system with long lag times.

The Potomac River (Figure 4.1) is the primary source of water for the Washington DC metropolitan area (hereafter WMA). When it was implemented in 1982, the WMA water supply system was considered a model for combining optimization and simulation to improve water supply efficiency (Sheer and Flynn 1983), replacing plans for as many as 16 major reservoirs with a single, distant reservoir (Jennings Randolph Reservoir) and a small, nearby reservoir (Little Seneca Reservoir). While this design allows the 38,000 km^2 Potomac watershed to remain largely uncontrolled, it increases the importance of effective water management decisions. The location of the Jennings Randolph Reservoir 300 km upstream of the Washington DC water supply intakes creates a 9 to10 day lag between reservoir releases and their subsequent capture. This delay remains beyond the forecast horizon of accurate weather predictions, requiring release decisions to be made amid significant uncertainty, with no ability to recapture excess releases.

The use of evolutionary, or genetic, algorithm solvers in water resources optimization has proven successful because of their robustness and flexibility (Oliveira and Loucks 1997; Chen 2003; Wardlaw and Sharif 1999; Momtahen and Dariane 2007). Evolutionary algorithms are capable of searching large and complex decision spaces and evaluating nonlinear and nonconvex objective functions. In addition, for multi-objective problems,

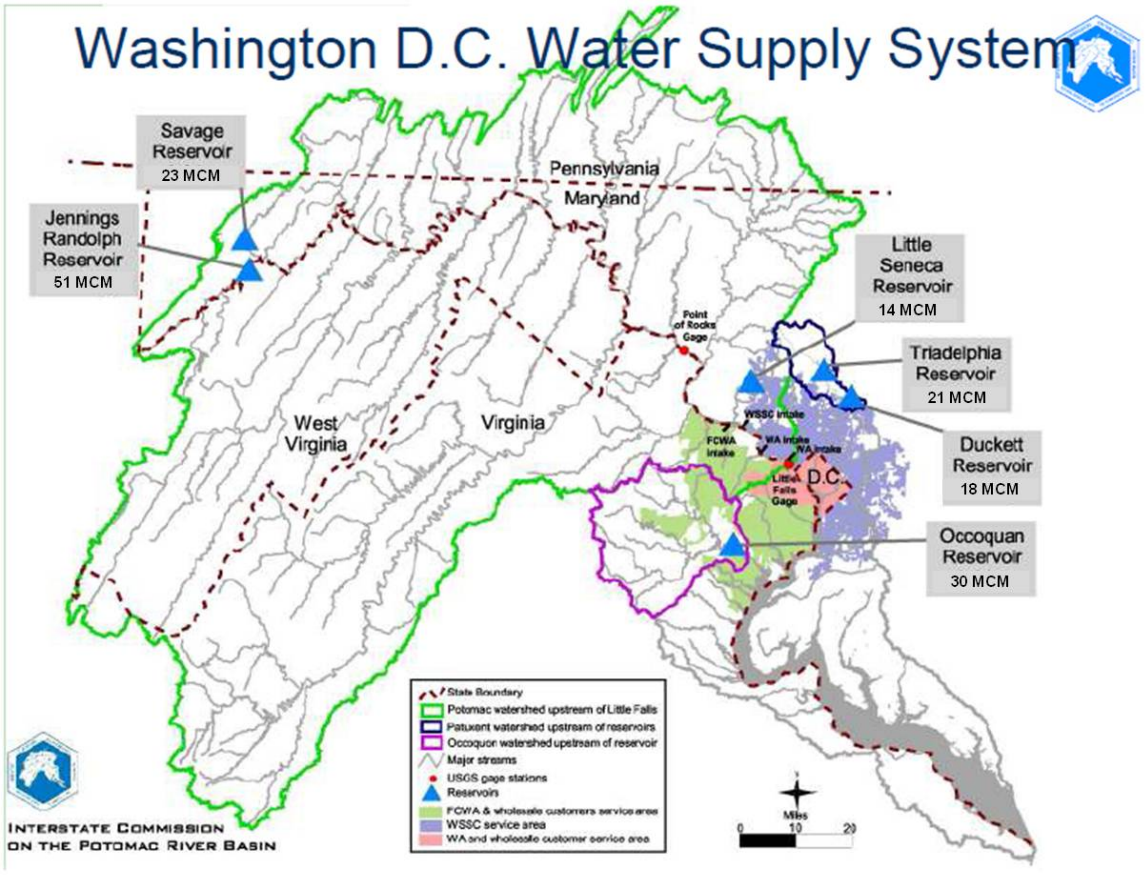

Figure 3.1: *Potomac watershed and Washington DC water supply. Volumes are shown as 10^6 m^3, or MCM. Figure generated by the Interstate Commission on the Potomac River Basin (ICPRB).*

they are considered *a posteriori* decision tools, which produce a set of optimal solutions, from which decision makers can weigh the relative importance of conflicting objectives following optimization.

By using an evolutionary algorithm solver overlaid onto a daily simulation and decision model, operating rule parameters were optimized for the WMA water supply system, a watershed with significant lag time. Operating rules were evaluated first using the historical time series (1929-2007), which includes the drought of record (1930-1931), and then using long duration synthetic time series, which allow for a wider range of feasible hydrologic scenarios, each following the distribution and temporal relationship of the

historical record. Use of synthetic time series tests the robustness of optimized rules and prevents over-fitting to the relatively small set of historical drought events.

3.2 Background

3.2.1 Formulation of Reservoir Optimization Problems

Optimization of reservoir operations depends on an accurate representation of the physical system. At its most basic, this requires continuity constraints such as a mass balance for each reservoir:

$$\frac{dS_{\mathrm{r}}}{dt} = I_{\mathrm{r}}(t) - R_{\mathrm{r}}(t) - L_{\mathrm{r}}(t) \qquad t = 1, \ldots T \tag{3.1}$$

where T is the total operation period, $S_r(t)$ is the water volume in storage in reservoir r, $I_r(t)$ is the inflow rate from the upstream system, $R_r(t)$ represents the release rate, and $L_r(t)$ is a summation of losses including evaporation, direct rainfall, and seepage. These terms are typically constrained in the model, with upper and lower bounds on reservoir storage capacity and release constraints based on the reservoir outfall. Conservation of mass between reservoirs is handled by state-space equations that describe routing, travel time, and losses.

Apart from hydraulic models used to simulate the system, it is necessary to mathematically describe operating rules, or release policies, for the system in such a way that the coefficients, and occasionally the form, of the rules can be modified to produce optimal system behavior. These rules represent the closest approximation of operational decision-making, which may also be affected by a human element in practice. A common modification to reservoir operating rules is the inclusion of a hedging term, which allows for minor demand shortages in the hopes of preventing severe shortages in the future. In systems with significant travel times, hedging can be used as a buffer, releasing

water in excess of demand to prevent shortages caused by future streamflow uncertainty (Schwartz 2000).

More complex reservoir systems typically include additional modifications, such as discrete storage zones and storage target rule curves. In zone based operations, reservoirs are divided into virtual storage zones and decisions are contingent on the volume of water contained in the reservoir. Typical zones include flood control (typically kept empty), general use, permanent storage, and dead storage, which includes water that cannot be physically discharged. In the WMA system, the Occoquan Reservoir employs a discrete zone-based system to determine hedging ratios (Hirsch 1979). The Jennings Randolph and Savage Reservoirs operating policies incorporate storage-based rule curves, which adjust storage zones seasonally (Ahmed et al. 2010).

3.2.2 Multobjective Evolutionary Algorithms

Genetic or evolutionary algorithms (EA) are a relatively recent class of numeric optimizers, first envisioned by John Holland in 1975 and developed in usable form by Goldberg (1989). They are general-purpose solvers based on the biological principles of evolution and have proven capable of calculating near optimal solutions across a wide range of complex and non-linear models. EA solvers operate by coding candidate solutions of all decision variables (genes) into strings, analogous to chromosomes. A population is created by randomly generating sets of feasible "chromosomal" solutions. Applying the objective function to each individual, the fitness is evaluated and used to preferentially select parents with the greatest fitness for the subsequent generation. Genes of the children are determined by two generalized reproductive mechanisms: crossover and mutation. Crossover involves dividing the two parent solution strings and merging them to create new solutions. Mutation involves randomly modifying an individual gene within a solution string, which introduces perturbation and aides in preventing the selection of local optima (Momtahen and Dariane 2007).

The advantage of EA methods is that they do not impose many of the limitations of traditional optimization, making them adaptable, suitable for nonlinearities, and capable of being directly linked with hydrologic simulation models without the need for simplifying assumptions (Labadie 2004). Because each realization contains full knowledge of the decision variables, complicated objective functions such as those based on drought risk indices are simple to calculate (Hashimoto et al. 1982). However, EA solvers are considered an approximative heuristic algorithm and cannot guarantee a globally optimal solution or know when an optimal solution has been found (Ferreira and Ludermir 2009).

In the majority of water allocation problems, optimization is used to balance several competing objectives. Historically, these multi-objective problems were solved by weighting the various objectives and summing the result to create a single objective problem that could be solved using traditional optimization schemes (Deb 2001). The drawback of this procedure is that weighting schemes must be determined *a priori* and the resulting solution represents only a single tradeoff value. In light of conflicting objectives, a more rigorous approach is needed to address the system as a true multi-objective problem. Multiobjective optimization solves for a set of compromise solutions, termed the Pareto optimal front, that represent optimal solutions which cannot be improved without affecting the other objectives. By using this approach, decision makers are able to see the entire objective space before decisions must be made regarding preferences and tradeoffs. Therefore, the goal of multi-objective evolutionary algorithms (MOEAs) is to use evolutionary algorithm principles of crossover and mutation to produce successively better populations that converge on the Pareto optimal front, while maintaining sufficient diversity to adequately cover the entire objective space.

3.2.3 Water Resources Applications of Evolutionary Algorithms

Evolutionary algorithms have been used successfully to optimize operating parameters in deterministic reservoir optimization (Oliveira and Loucks 1997; Chen 2003; Wardlaw and Sharif 1999). Momtahen and Dariane (2007) optimized several parameterized reservoir

release rule forms using a direct coded genetic algorithm solver and concluded that EA methods are efficient relative to traditional optimization. Despite this, Momtahen and Dariane (2007) cautions against large numbers of policy parameters which tend to cause overfitting and reduce computational efficiency.

In sensitivity tests on a 4-reservoir system, Wardlaw and Sharif (1999) found an optimal crossover probability of 0.7, meaning that parents will exchange genetic material 70% of the time with 30% of the parents copying their genes directly to the next generation without modification. Optimum results were achieved with approximately one mutation per chromosome (Wardlaw and Sharif 1999).

3.3 Application

3.3.1 Potomac River Basin

This study uses the Potomac River Basin and the WMA as a case study to apply an evolutionary algorithm optimization scheme to a system with long lag times. The WMA, currently the country's 7th largest metropolitan area, houses more than 5 million residents over its 40,000 square kilometers, and spans 15 counties and the District of Columbia. Municipal water needs of the WMA are managed by three major suppliers:

Washington Suburban Sanitary Commission (WSSC), which serves the Maryland suburbs,

Fairfax Water, which serves Fairfax County and other northern Virginia suburbs, and

Washington Aqueduct, which provides water to the District of Columbia

Additionally, the city of Rockville, MD maintains a separate water supply system, drawing from the Potomac River. The Potomac River accounts for approximately 78% of the water treated by the WMA water suppliers in a typical year, with the remainder of

demand met by reservoirs located outside the non-tidal Potomac watershed on the Occoquan (Fairfax Water) and Patuxent (WSSC) rivers (Figure 4.1). For much of the year, withdrawals from the Potomac remain a small fraction of the total flow, with average summer demands reaching 2×10^6 m^3/day and annual Potomac flows averaging 26×10^6 m^3/day (Ahmed et al. 2010). During periods of low flow, which typically occur in summer and early fall, the natural flow of the Potomac may be augmented with releases from the Jennings Randolph and Little Seneca reservoirs to satisfy withdrawal requirements. Reservoir characteristics are summarized in Table 4.1.

The Jennings Randolph Reservoir has significantly greater storage capacity available for water supply (51×10^6 m^3) than the Little Seneca (14×10^6 m^3), but is located approximately 9 days of hydrologic travel time upstream of the WMA intakes, while the Little Seneca is only 1 day upstream of the WMA intakes. The two reservoirs are therefore operated in concert, with the Jennings Randolph making primary releases and the Little Seneca being used to "fine tune" flows upstream of the intakes.

The remaining capacity in the Jennings Randolph Reservoir is allocated for flood control (42×10^6 m^3, 28% of total storage) and water quality releases (58×10^6 m^3, 38%). The Corps of Engineers manages these portions, leaving flood storage empty for emergencies and making water quality releases in conjunction with the Savage Reservoir to meet a low flow requirement in the North Branch of the Potomac measured at Luke, Maryland.

The Savage Reservoir, located 8 km from the Jennings Randolph Reservoir, is owned by the Upper Potomac River Commission (UPRC) and operated with guidance from the

Table 3.1: *WMA operational characteristics.*

Reservoir	Manager	Total Storage 10^6 m^3	Available Storage 10^6 m^3	Watershed Area km^2	Upstream Distance km	Travel Time days
Jennings Randolph	CO-OP,USACE	109	51	681	320	9
Little Seneca	CO-OP	16	14	54	25	1
Savage	UPRC	24	23	272	320	9
Patuxent	WSSC	51	39	342	-	-
Occoquan	Fairfax	31	30	1,533	-	-

U.S. Army Corps of Engineers, Baltimore District to satisfy the North Branch low flow requirement. Additionally, water supply releases are made from the Savage Reservoir concurrently with releases from Jennings Randolph per a matching agreement.

In addition to the Potomac water supply system, three WMA reservoirs are located outside the Potomac watershed and used as off-line water supply storage. The Occoquan Reservoir, managed by Fairfax Water, is located on the Occoquan River on the border of Fairfax and Prince William counties. The WSSC operates two reservoirs in series, the Triadelphia and T.H. Duckett Reservoirs, on the Patuxent River along the border of Montgomery and Howard counties in Maryland. Current operating rules specify that WSSC and Fairfax Water rely more heavily on the Potomac River during winter and spring months to preserve storage in the off-line reservoirs for use during the summer low-flow season. In 2008, 31% of WSSC's production came from the Patuxent reservoirs and 42% of Fairfax Water's production came from the Occoquan Reservoir.

3.3.2 Origins of the Potomac Basin System

While the physical organization of the Potomac Basin System is not uncommon, the circumstances surrounding its creation are unique, created, in part, by the confluence of two state governments, the federal government and multiple water suppliers. The existing water supply system began taking shape during the drought of 1966, when Washington DC was forced to declare its first "water emergency" in more than a century (Dyne 2007). At this time, predictions of future demand concluded that demand would soon exceed natural flows in the Potomac River, prompting the U.S. Army Corps of Engineers to identify 16 potential dam sites on the river (U.S. Army Corps of Engineers 1963). Because of public opposition, only one of the proposed reservoirs, the Jennings Randolph, was built, with construction beginning in 1975 and ending in 1981. During this time, water allocation studies (Sheer 1996; Palmer et al. 1979, 1982) concluded that demand could be met through coordinated operation of the existing Patuxent and Occoquan reservoirs and the Jennings Randolph, allowing flow in the Potomac to remain largely unimpeded. Even greater protection was offered by constructing the smaller Little Seneca Reservoir in 1985

to act as a buffer against uncertainty in releases from the upstream Jennings Randolph Reservoir.

Because of the unique jurisdictional issues associated with shared water across water suppliers, state governments, and the federal government, several agreements were signed to ensure equitable access to water during a drought event (Low Flow Allocation Agreement, 1978) and to facilitate shared decision-making (U.S. Army Corps of Engineers 1982). As part of the Water Supply Coordination Agreement, the water suppliers share the operating and capital costs of the reservoirs and must jointly agree on the timing and magnitude of water supply releases from the Jennings Randolph and Little Seneca reservoirs during periods of drought.

Water supply releases have been made on three occasions since completion of the current WMA water supply system. During the first release, in the summer of 1999, water was released from the Jennings Randolph Reservoir over a period of 26 days and from the Little Seneca Reservoir one day, totaling 11×10^6 m^3 (Dyne 2007). The 1999 drought highlighted the need for coordinated water conservation measures, with Maryland, Virginia and Washington DC each imposing different water restrictions. To address this issue, the Metropolitan Washington Council of Governments (MWCOG) adopted a Water Supply and Drought Plan in 2000 (Metropolitan Washington Council of Governments 2000) which contains specific triggers for water restrictions. Consistent water restrictions were not a problem in 2002, when 26×10^6 m^3 were released in 3 pulses between mid-July and late September. Water supply releases made in 2010 were taken solely from the Jennings Randolph Reservoir between September 10 and September 21 and again on September 23 (Ahmed et al. 2010). In each instance, cooperative operations between the Interstate Commission on the Potomac River Basin (ICPRB), the multistate organization that acts as coordinator within the river basin, and the WMA water suppliers ran smoothly and the augmented flow of the Potomac provided adequate water to meet demand.

3.4 Methods

3.4.1 Systems Modeling

Hydraulic routing and reservoir operations were simulated using OASIS (Version 3.09.033), developed by Hydrologics, Inc. OASIS is a water management simulation and decision model, which uses a node-arc architecture to model reservoirs, reaches, inputs and withdrawals. Operating rules are expressed as goals or constraints and solved via linear programming using a daily time step, mimicking the imperfect foresight of daily operational decision-making.

The OASIS model was developed in conjunction with the ICPRB and water suppliers to ensure that all data, operating rules, and assumptions were accurate. Reservoir details, including stage-storage curves, sedimentation rates, and existing operational rule curves, were provided by the ICPRB. Current Potomac channel routing and travel time estimates were also provided to the authors. Daily demand among the three major WMA water suppliers was simulated using a set of multivariate regression equations, incorporating an autoregressive-moving average (ARMA) error term, provided in Ahmed et al. (2010).

3.4.2 Streamflow Time Series

Two streamflow time series were evaluated: the historical time series (1929-2007) and a group of stochastically generated streamflow time series. The historical record was adjusted by the ICPRB to remove the effect of reservoir releases and upstream consumptive use, creating a time series of historical streamflows unaffected by demand change and human interaction (Hagen and Steiner 1998; Hagen et al. 1998b,a; Hagen and Steiner 1999).

To expand the set of feasible conditions beyond the historical streamflow time series, synthetic daily time series were generated using the stochastic method described in Stagge (2012). This method uses a coupled monthly Markov climate model and daily Markov streamflow model to accurately reproduce the distribution (mean, variance, skew-

ness) and seasonality of the historical streamflow record. Parameters are successfully modeled at the annual, monthly and daily time scales (Stagge 2012). Flows were then spatially disaggregated based on the commonly used "Method of Fragments" (Srikanthan and McMahon 1982; Porter and Pink 1991) and bias corrected using quantile-quantile mapping (Panofsky and Brier 2007).

3.4.3 Optimization Scheme

Optimization of system operating rules was carried out using $\mathcal{S}$-metric Evolutionary MultiObjective Algorithm (SMS-EMOA) (Emmerich et al. 2005; Beume et al. 2007), an Indicator-based multiobjective evolutionary algorithm (MOEA), wrapped around the OASIS simulation model. SMS-EMOA is a steady-state (μ + 1) MOEA designed to maximize the multi-dimensional hypervolume ($\mathcal{S}$-metric) dominated by a finite number of points. The use of hypervolume as a quality metric was originally proposed by Zitzler and Thiele (1998) and was proven by Fleischer (2003) to converge to the Pareto set, given a finite search space and reference point. Hypervolume measures assign greater weight to regions with unique points or high curvature, which tends to produce more detailed estimates of the Pareto front than crowding distance, used as selection criterion in NSGA-II (Deb et al. 2002), which seeks to distribute solutions uniformly. Use of dominated hypervolume is also invariant to linear scaling of the objective functions.

The version of SMS-EMOA used in this study is based on the EMOA package (Mersmann 2011) in R and uses simulated binary crossover (SBX) and polynomial mutation (Deb 2001). In benchmark studies, this version of SMS-EMOA was shown to outperform several other multiobjective evolutionary algorithms in solution convergence, while maintaining a well-distributed solution set (Beume et al. 2007). In an extensive assessment of state-of-the-art MOEAs (Reed et al. 2012), a model using the hypervolume indicator, Indicator-Based Evolutionary Algorithm (IBEA) (Zitzler and Künzli 2004), performed very well, scoring among the best for hydrologic model calibration and groundwater calculation problems.

3.4.4 Objective Function and Constraints

The WMA water management optimization problem is formulated as a multi-objective optimization system, with objectives designed to cover the range of potential benefits within the Potomac River system in a quantifiable manner. To the greatest extent possible, the operational constraints and objectives in this model were developed through close consultation with the water suppliers and the ICPRB. Target volumes and flows were often based on legal agreements, such as the Low Flow Allocation Agreement. Because the functional limit of current MOEAs has been shown to be approximately 10 objectives (Reed et al. 2012), this optimization model uses six objectives, which include:

1. **Shortage**, which minimizes delivery shortages to the water suppliers (volume)
2. **Storage**, which minimizes low storage volumes in any of the reservoirs (volume)
3. **Flowby**, which minimizes days when flow in the Potomac does not exceed low flow requirements (days of violation)
4. **Rec. Season**, which minimizes days during the recreation season that Jennings Randolph levels fall below recreation facilities (days of violation)
5. **Whitewater**, which minimizes days when whitewater releases cannot be made due to low storage volume (days of violation)
6. **Env. Flows**, which minimizes days when flow in the Potomac falls below recommended environmental levels for three consecutive days (days of violation)

These objectives are presented as a constrained multi-objective optimization problem:

$$\text{Minimize} \quad Z = [Z_{\text{Short}}, Z_{\text{Stor}}, Z_{\text{Flowby}}, Z_{\text{Rec Season}}, Z_{\text{WW}}, Z_{\text{Env Flows}}] \tag{3.2}$$

where each of the Z terms represent individual objective functions.

The first objective, Z_{Short} (Equation 3.3), sums the percent water delivery shortage at all supply points, including WSSC, Fairfax Water, the USACE, the city of Westernport,

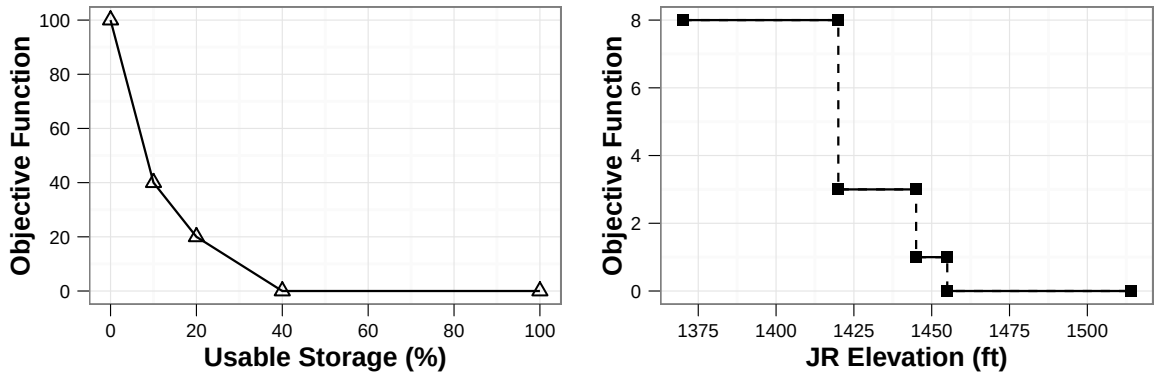

(a) *Storage Penalty* **(b)** *Recreation Penalty*

Figure 3.2: *Objective function - Penalty weights.*

MD, and the city of Rockville, MD. In Equation 3.3, Dem_i refers to daily demand, Del_i refers to daily delivery, T represents the total number of days in the time series, and i represents the 5 water suppliers.

$$Z_{\text{Short}} = \sum_i \sum_{t=0}^{T} \begin{cases} \frac{\text{Dem}_i(t) - \text{Del}_i(t)}{\text{Dem}_i(t)} & \text{if } \text{Dem}_i(t) > \text{Del}_i(t) \\ 0 & \text{otherwise} \end{cases} \tag{3.3}$$

The second objective, Z_{Stor} (Equation 3.4), calculates a penalty when reservoir usable storage falls below 40%. In Equation 3.4, S_j represents usable storage (%) in reservoir j, which corresponds to the 6 reservoir storage accounts: (1) Jennings Randolph Water Quality, (2) Jennings Randolph Water Supply, (3) Savage, (4) Patuxent, (5) Occoquan, and (6) Little Seneca. The storage penalty is a piecewise function (Figure 3.2a), which applies increasingly larger penalties as reservoir usable storage approaches zero.

$$Z_{\text{Stor}} = \sum_j \sum_{t=0}^{T} \begin{cases} 100 - 6 \times S_j(t) & \text{if } 0 \leq S_j(t) < 10\% \\ 60 - 2 \times S_j(t) & \text{if } 10 \leq S_j(t) < 20\% \\ 40 - S_j(t) & \text{if } 20 \leq S_j(t) < 40\% \\ 0 & \text{if } S_j(t) \geq 40\% \end{cases} \tag{3.4}$$

Equation 3.5 describes the flowby penalty, Z_{Flowby}, which sums all days when the legally prescribed flowby, Q_{Flowby} is not satisfied by flow, Q_k, at each of the k locations. The pertinent flowbys are 60 MGD at Luke, MD, 300 MGD at Great Falls, MD and 100 MGD at Little Falls, MD.

$$Z_{\text{Flowby}} = \sum_{k} \sum_{t=0}^{T} \left(\frac{Q_k(t) < Q_{\text{Flowby}}}{T} \right) \tag{3.5}$$

The fourth objective function, $Z_{\text{Rec Season}}$ (Equation 3.6), refers to the summer Recreation Season, which occurs each year between May 1 and August 31, represented in the function by $T_{\text{Rec Season}}$. During this period, water managers strive to maintain water levels in the Jennings Randolph Reservoir, represented as Elev_{JR}, above three recreation access points. These points, termed E_{Beach}, E_{WV}, and E_{MD}, are 443.5 m, 440.4 m, and 432.8 m above sea level, respectively. The penalty function increases as each access point becomes inaccessible (Figure 3.2b).

$$Z_{\text{Rec Season}} = \sum_{t=0}^{T_{\text{Rec Season}}} \left(\left(\frac{E_{\text{JR}}(t) > E_{\text{Beach}}}{T_{\text{Rec Season}}} \right) + 2 \times \left(\frac{E_{\text{JR}}(t) > E_{\text{WV}}}{T_{\text{Rec Season}}} \right) + 5 \times \left(\frac{E_{\text{JR}}(t) > E_{\text{MD}}}{T_{\text{Rec Season}}} \right) \right) \tag{3.6}$$

Z_{WW} (Equation 3.7) calculates the ratio of days when whitewater releases cannot be made due to low storage volume. Whitewater releases are set to occur on the 15th and 30th of April and May, whose set is represented as T_{WW}. Whitewater releases are represented by Q_{WW}.

$$Z_{\text{WW}} = \sum_{t=0}^{n_{\text{WW}}} \left(\frac{Q_{\text{WW}}(t) = 0}{T_{\text{WW}}} \right) \tag{3.7}$$

The final objective function, $Z_{\text{Env Flows}}$ (Equation 3.8), uses a measure to summarize water supply activity's effect on the ecological health of the Potomac River. While the

legal flowby requirement below Little Falls, MD is set at 200 MGD, the Potomac Basin Large River Environmental Flow Needs study stated that there "is strong concern that a continuous, multi-day period of flows at or very close to 100 MGD would be injurious to the biota" (Cummins et al. 2010). This function sums the number of occurrences when flow below Little Falls, MD, Q_{LF}, remains below 200 MGD for 3 or more consecutive days.

$$Z_{\text{Env Flows}} = \sum_{t=0}^{n} \left(\frac{(Q_{\text{LF}}(t) \text{ and } Q_{\text{LF}}(t-1) \text{ and } Q_{\text{LF}}(t-2)) < 200 \text{ MGD}}{n} \right) \tag{3.8}$$

3.5 Results

For both historical time series and synthetic time series, performance of the system under existing reservoir release rules was compared to rule optimized using multiobjective evolutionary algorithms.

3.5.1 Potomac Water Supply Response

Simulation of the WMA water supply system response to historical and synthetic time series provides an insight into how the the system reacts under drought conditions and can identify areas of particular vulnerability. Water supply response was simulated using the 79 year (1929-2007) historical record and 10 synthetic streamflow time series of equal length. Stochastically generated streamflows generated in Stagge (2012) closely match the daily, monthly and annual distribution of historical streamflows, while maintaining autocorrelation.

As expected, the WMA water supply system response under these time series is similar to the simulated response using the true historical flows, with respect to the 6 objective functions. Because a 6-dimensional surface cannot be presented visually, Figure 3.3 displays each pair of objective functions individually. This figure compares 10 simulations, represented by black•'s, with the historical record, represented by a red ▼ for the full time

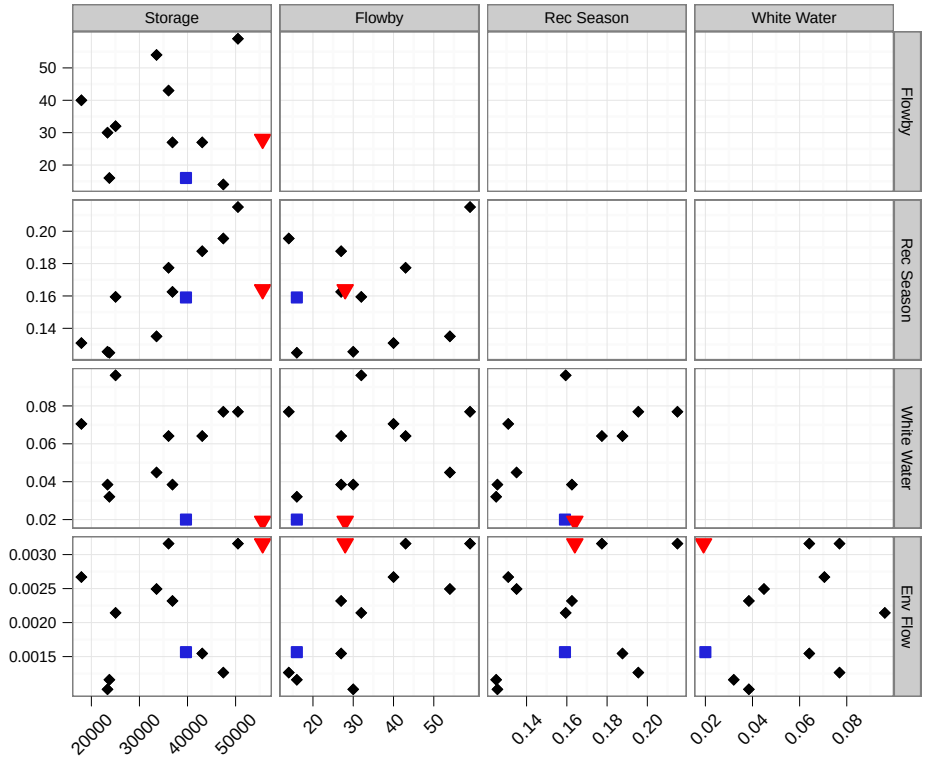

Figure 3.3: *Objective function for the historical and simulated streamflow time series. Actual historical simulation is represented by red ▼, the historical record with the Dust Bowl years removed is represented by blue ■, and simulated streamflows are represented by ●.*

series and a blue red ■ for the historical time series with the Dust Bowl era removed. Axes in Figure 3.3 are unitless and scale-invariant, as they represent the various objective functions.

According to Figure 3.3, the 10 synthetic streamflow realizations produce fewer failures than the historical record (shown in red), with respect to storage and environmental flows but produce more whitewater failures. It is important to note that a large portion of storage failures in the historical record occurred during the extreme drought between 1930 and 1932. If these years are removed from the record, shown in Figure 3.3 by a blue ■, the frequency and magnitude of the various penalties show much greater similarities.

As is the case for many climate models (Schubert et al. 2004; Seager et al. 2008), the stochastic streamflow generation model cannot reproduce the most extreme drought con-

ditions of the "Dust Bowl" era. These conditions are unlike any other drought during the modern era (Cook et al. 2008) and caused highly irregular weather across much of the United States, including the multi-year drought in the Potomac watershed lasting from the summer of 1930 through the winter of 1931, with historically low recharge occurring during the intervening winter. This anomaly is difficult to explain using only climatic factors (Schubert et al. 2004) and is more thoroughly explained by a combination of climate and land surface feedback, whereby high dust loads caused by lack of vegetation suppressed precipitation (Schubert et al. 2004; Miller et al. 2004; Rosenfeld et al. 2001). Extraneous interaction factors are not captured in the streamflow generation model (Stagge 2012), which relies on transition probabilities between discrete monthly climate states. All other climate-driven droughts are simulated successfully (Figure 3.3).

While comparing multiple realizations, patterns begin to emerge among the objective functions. The storage, Z_{Stor}, and recreation objectives, $Z_{\text{Rec Season}}$, are closely related, as both are volumetric measures albeit for different reservoirs and time frames. Operating rules that minimize these objectives can be classified as "storage-conservative", favoring storage in the reservoirs at the expense of downstream flows. The whitewater objective, Z_{WW}, is most closely related to recreation storage, though not strongly tied to the storage objective. This is logical, as whitewater releases and the recreation season objective depend on maintaining adequate storage in the Jennings Randolph Reservoir during an overlapping season in the late spring (April 1-May 30). By comparison, Z_{Stor} tends to focus on extreme low flows, which occur in late summer long after whitewater releases.

The flowby, Z_{Flowby}, and environmental, $Z_{\text{Env Flows}}$, objectives are closely related, as they are both flow measurements and promote a less conservative water management scheme. Operational rules that minimize these objectives tend to make larger and more frequent reservoir releases to ensure that downstream goals are met, at the expense of reservoir storage. In the case of a system with long lag times, optimizing these objective functions can be viewed as increasing the flow buffer.

No shortage failures occur in simulations of current climate and demand, based on rules provided by the WMA water suppliers. These existing operating rules prioritize

daily demand as their primary goal. This remains a reasonable model, as suppliers were reticent to allow service outages if demand could otherwise be met. Therefore priority was given to operating rules that met this objective.

3.5.2 Operating Rule Optimization

Five distinct rule modifications were considered in this study: the buffer equation, load shifting, demand restrictions, and reservoir rule curves for the Jennings Randolph and Patuxent reservoirs. Optimal rule modifications were calculated based on historical flows and one of the more challenging synthetic streamflow realizations which remained within the typical range from the historical record.

An overview of optimization results is presented in Table 3.2. This table shows the maximum percent improvement, relative to simulation using existing operating rules, for each rule modification. Each of the optimized rules tend to improve system performance, though there is no single modification which is dominant across all objectives (Table 3.2). This is in part because each modification has a distinct purpose. For instance, the majority of storage failures in the historical record occur in the Patuxent reservoir system. Because of this, the Patuxent rule curve is most effective at preventing this type of failure, followed by the Load Shifting rule, which shifts demand to the Patuxent and Occoquan reservoirs, with a preference for the reservoir with more usable storage capacity. Likewise, the objectives that deal with the main stem of the Potomac, Z_{Flowby} and $Z_{\text{Env Flows}}$, are most effectively minimized by the Buffer Equation and Demand Restrictions, which both adjust flows in the Potomac. Finally, the Jennings Randolph rule curve modification is most effective at minimizing $Z_{\text{Rec Season}}$ and Z_{WW}, as these objectives deal directly with storage in the Jennings Randolph Reservoir. While the Jennings Randolph rule modification improved $Z_{\text{Rec Season}}$, this objective showed the smallest improvement (Table 3.2) because recreation season releases are handled by a separate set of stepped rules that were not included for evaluation in this study.

Table 3.2: *System optimization results - Historical time series. All values represent the maximum % improvement over the existing operation rules.*

Rule Modification	Z_{Stor}	Z_{Flowby}	$Z_{\text{Rec Season}}$	Z_{WW}	$Z_{\text{Env Flows}}$
Buffer Eq	0.5	21.4	0.51	0	17.8
JR Rule Curve	0.01	10.7	0.5	66.67	15.5
Patux Rule Curve	8.6	0	0.3	0	1.1
Load Shifting	2.4	7.1	0.1	0	4.4
Demand Res	0.8	14.3	0.1	0	18.9

The historical time series proved to be more challenging for the system, producing higher penalties, but also allowing greater improvements through modifications of the operational rules. Because the synthetic time series was less challenging for the WMA system, the improvements due to rule modification in this case were meager.

Buffer Equation

Within the WMA water supply operating rules, the buffer equation is designed to balance storage levels along the main stem of the Potomac River, namely between the upstream Jennings Randolph and downstream Little Seneca Reservoirs. Reservoir releases from the Jennings Randolph are calculated based on estimated demand using a 9-day lookahead; however, the buffer equation adjusts these releases based on the imbalance, in percent usable storage, between the Jennings Randolph Water Supply volume and Little Seneca storage. If the Water Supply volume in the Jennings Randolph is lower than storage in the Little Seneca Reservoir, the buffer is negative, reducing releases from the upstream Jennings Randolph under the assumption that the deficit will be satisfied through additional releases from the downstream Little Seneca Reservoir. Conversely, if levels in the Little Seneca Reservoir are lower than the Jennings Randolph Water Supply account, the buffer is positive, producing a release from the Jennings Randolph Reservoir that is larger than necessary, based on the assumption that Little Seneca releases will be curtailed to allow the reservoir to refill. Under the current policy, the slope of the Buffer Equation (Figure 3.4) is identical for both of these situations, adding or subtracting a maximum of 568×10^3 m^3/d.

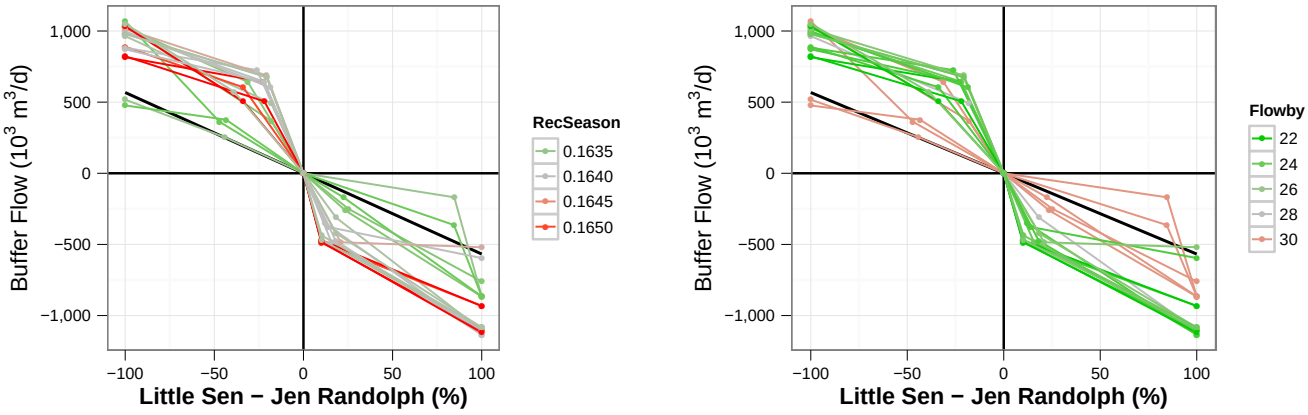

(a) *Recreation Season* **(b)** *Flowby*

Figure 3.4: *Optimized buffer equation - Historical time series. Current operating rules are shown by the bold, black line between 568×10^6 m^3/d and - 568×10^6 m^3/d. For each non-dominated solution, the color scale shows the improvement (green) or decrease (red) in objective function relative to current policy.*

The Buffer Equation directly controls releases from the Jennings Randolph Water Supply storage, though it also indirectly affects releases from the Little Seneca Reservoir. In this way, it incorporates the uncertainty caused by travel time.

An alternative formulation for the Buffer Equation is proposed, which deviates from existing policy by 1) allowing unique slopes for positive and negative storage imbalances, 2) adding a breakpoint to each equation to allow different slopes for high imbalances and low imbalances, and 3) handling the case of storage imbalances where reservoir volume remains greater than 90% separately from all other cases. Each of these rule adjustments were designed to increase flexibility for specific instances, rather than applying a single rule for all circumstances. The results of multiobjective optimization suggest that a 21.43% improvement in Z_{Flowby} and a 17.78% improvement in $Z_{\text{Env Flow}}$ can be achieved by increasing the slope of the Buffer Equation (Figure 3.4). This improvement comes at the cost of recreational season storage, due to increased releases from the Jennings Randolph Reservoir (Figure 3.4). Conversely, Recreational Season storage can be improved by maintaining the existing Buffer Equation, but greatly decreasing the Buffer Equation for situations when usable storage is greater than 90%. In the case of positive imbalances, i.e. Jennings Randolph storage (%) is less than Little Seneca, the buffer flow approaches

zero. This additional rule prevents unnecessary attempts to balance storage between the Little Seneca and Jennings Randolph when storage is nearly full. By balancing increases in slope for the main Buffer Equation and a significant decrease in Buffer flows for cases where the reservoirs are nearly full, all objectives may be improved.

Load Shifting

While the Buffer Equation deals only with balancing releases between the Jennings Randolph and Little Seneca, Load Shifting controls how daily demand is allocated to the offline reservoirs, the Patuxent and Occoquan. Because of the strategic importance of the Little Seneca Reservoir in fine-tuning Potomac flow, demand is shifted to the offline reservoirs prior to requiring releases from the Little Seneca Reservoir. When predicted flow in the Potomac River is not sufficient to satisfy predicted demand, production at the Patuxent and Occoquan water treatment plants is temporarily increased above standard production levels. Following the load shifting event, production at the offline reservoirs is curtailed an equivalent amount, to replenish storage. Load shifting occurs only when storage in the Jennings Randolph, Little Seneca, Occoquan and Patuxent remains above trigger points, called Load Shift Storage Indices.

The modified Load Shifting rules adjust the Load Shift Storage Indices as well as the ratio between the Patuxent and Occoquan Reservoirs. In the existing operating procedure, unmet demand is apportioned equally between the Patuxent and Occoquan Reservoirs. Rather then maintain a balance between these two reservoirs during a load shift event, the proposed rules allow the ratio to be other than 50% and allow this ratio to adjust dynamically based on the ratio of available storage between the reservoirs. This Load Shift equation, shown in 3.4a, is defined by three points, with the midpoint representing the standard percent of the load allocated to the Patuxent Reservoir. When usable storage is higher in the Patuxent Reservoir, a higher percent of the load is allocated to this reservoir and vice versa. The final parameter evaluated in this scheme is the threshold that determines when a load shift event ends and demand can be returned to the Potomac River. In the existing model, Potomac flows must be $1{,}136 \times 10^6$ m^3/d in excess of

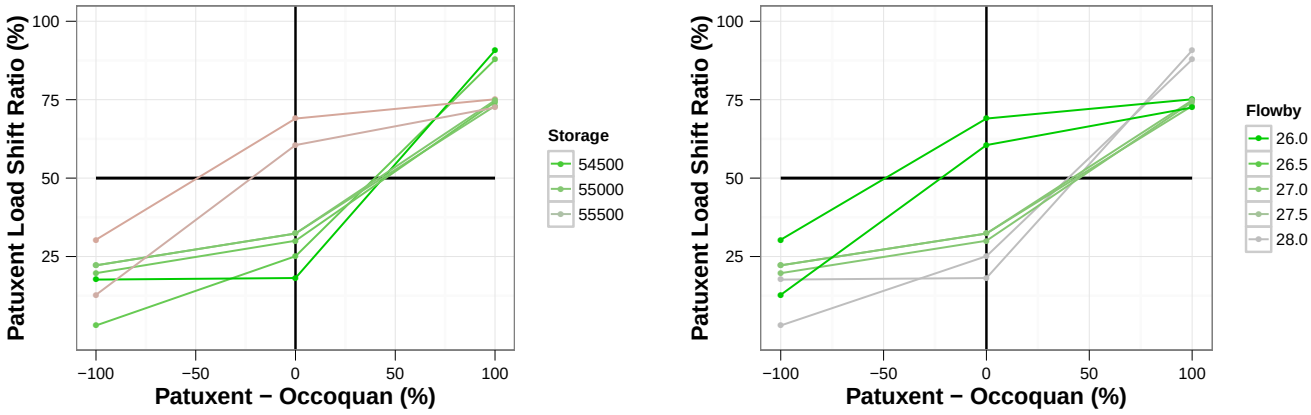

(a) *Storage* **(b)** *Flowby*

Figure 3.5: *Optimized load shift equation - Historical time series. Current operating policy is a constant 50% allocation between the Patuxent and Occoquan Reservoirs, shown as a bold, black line. For each non-dominated solution, the color scale shows the improvement (green) or decrease (red) in objective function relative to current policy.*

demand and flowby level before a load shifting event may end. This "Load Shift Buffer" works to prevent oscillating between load shifting and regular operation.

Consistent improvement is realized by increasing the Load Shift Storage Indices and decreasing the Load Shift Buffer flow. Increasing the Load Shift Storage Index reduces load shifting to the Patuxent and Occoquan as storage in the system becomes extremely low. The greatest increases in Load Shift Storage Index, relative to total storage are in the Jennings Randolph (1,000 - 1,500$\times 10^6$ m^3), Patuxent (700-1,000$\times 10^6$ m^3), and Little Seneca (350-800$\times 10^6$ m^3). The increase in Occoquan Storage Index is relatively small (0-200 $\times 10^6$ m^3), suggesting that the Occoquan is capable of handling greater load than the Patuxent. This is due to its relatively high watershed area, which promotes recharge. By increasing this threshold point, more support is required from the Little Seneca Reservoir, which tends to be underutilized in the existing rules. Reducing the Load Shift Buffer allows a Load Shift event to end sooner, reducing pressure on the offline reservoirs once Potomac flows become adequate to support demand. In both cases, improvement is mostly attributed to decreasing load on the Patuxent Reservoir, which is stressed in the current system based on Z_{Stor} failures.

Additional improvements are possible by lowering the Load Shift equation, further decreasing the load on the Patuxent Reservoir. Decreasing the standard Patuxent load from 50% to 33% and including the balancing equation strikes an effective compromise between the Z_{Stor} objective and the flow objectives, Z_{Flowby} and $Z_{\text{Env Flow}}$ (Figure 3.5). This policy reduces Patuxent storage failures by 3.17 % and Occoquan storage failures by 2.66%, while causing no change in Flowby failures and actually improving environmental flows slightly (Figure 3.5). Raising the Load Shift equation improves Z_{Flowby} at the expense of Z_{Stor}, while the opposite is true for decreases in the Load Shift equation.

Monthly Rule Curves

The Jennings Randolph and Patuxent reservoirs were selected to undergo rule curve optimization, based on Patuxent Reservoir's high number of simulated storage failures and the Jennings Randolph's importance for water supply, recreation and whitewater releases. All reservoirs in the WMA water supply system operate according to zone-based rule curves in some form, except for Little Seneca which maintains a full storage volume throughout the year.

Jennings Randolph storage is managed by the Baltimore District Corps of Engineers and uses 3 zone-based rule curves (high, medium, and low) to guide releases during the non-Recreation Season months (September through April). These releases are designed to approximate the natural contribution of the Potomac River's impounded North Branch, while refilling the reservoir prior to the summer recreation season. Recreation releases are handled by a separate set of stepped rules, designed to maintain recreational storage targets, conditional on current storage.

Multiobjective optimization was used to adjust the the low and middle rule curves, ignoring the high rule curve, which is set near the Corps of Engineers' upper storage limit to provide adequate flood storage. As expected, adjustments to the Jennings Randolph rule curves produced the greatest impact on objectives directly related to Jennings Randolph storage, reducing $Z_{\text{Rec Season}}$ by 0.51% and Z_{WW} by 66.67%. Z_{Stor} was not greatly impacted

by optimization because the majority of storage failures occur in other reservoirs. Among the optimized rules, the greatest improvements were realized by modifying the minimum curve, which controls releases when storage in the Jennings Randolph is very low. Very little improvement was attributed to changes in the middle rule curve.

Whitewater releases and recreation season storage were improved by increasing the middle and low rule curves between March and May, immediately prior to the recreation season, which forces the Jennings Randolph Reservoir to operate more conservatively, decreasing the daily release from 734×10^3 to 294×10^3 m^3/d at a higher cutoff point. This modification allows for an additional 4 whitewater releases over the course of the historical record and improves recreation season storage modestly (0.51 %), but increases the environmental flow penalty. This tradeoff occurs because conservative operation of the Jennings Randolph forces downstream reservoirs to satisfy water deficits, either by shifting load to the Patuxent and Occoquan or by making Little Seneca releases. In both cases, releases can be made with more precision because they depend on current conditions, rather than the 9-day forecast.

Immediately following the recreation season, in September, performance was consistently improved by increasing the minimum curve elevation, causing the Jennings Randolph water quality account to operate more conservatively when storage is extremely low. After September, the optimized rule curves deviate, based on the preferred objective. Z_{Flowby} and $Z_{\text{Env Flows}}$ can be improved by 10.71 and 15.54%, respectively, by lowering the low rule curve, allowing for larger releases at the expense of Jennings Randolph storage. This modification is effective if aquatic life along the entire length of the Potomac River would benefit from intermittent flow pulses. However, using Jennings Randolph storage to decrease the number of consecutive low flow days can be inefficient because of upstream losses and the potential for natural storm events to occur during the 9-day travel time. If the only point of environmental concern is downstream of Little Falls, small pulse releases could be made from the Little Seneca Reservoir to eliminate consecutive days with flow close to the minimum flowby.

Modification of the Patuxent rule curve is almost entirely designed to maintain storage in the highly stressed Patuxent Reservoir, thereby improving system storage, Z_{Stor}. The Patuxent Reservoir is typically the first reservoir in the WMA system to fall below 40% usable storage in any of the historical or simulated drought years. Thus, the optimized rule curves greatly improve Z_{Stor} with little impact on the other objectives because of the Patuxent's location outside of the Potomac watershed.

The Patuxent operates based on 2 rule curves and an emergency storage trigger, which control daily water treatment withdrawals based on usable storage. Adjusting the upper and lower rule curves using multiobjective optimization produced an 8.64% improvement in system storage. This improvement is produced by raising the Lower curve consistently throughout the entire year, causing the Patuxent to function more conservatively during periods of extreme low flows. Modifications to the Upper curve occur primarily in the summer and early fall, when droughts are likely to occur. During the drought period, the optimized rules increase the Upper rule curve, forcing a reduction of Patuxent withdrawals and thereby decreasing the frequency and severity of storage failures. During the recharge period, beginning in December and continuing through May, the optimized Upper rule curve remains nearly identical to current operations. These results suggest that the Patuxent Reservoir can be operated more conservatively without causing significant detriment to the remainder of the WMA system.

Demand Restrictions

Following inconsistent implementation of water restrictions during the drought of 1999, the Metropolitan Washington Council of Governments standardized the use of water demand restrictions by setting three trigger levels: voluntary, mandatory and emergency (Metropolitan Washington Council of Governments 2000). As part of this agreement, regional governments agreed to declare water restrictions simultaneously based on the pre-determined triggers. Voluntary restrictions are triggered when combined storage in the Jennings Randolph and Little Seneca reservoirs falls below 60%. Trigger points for mandatory and emergency restrictions are set at 25 and 5% of either Jennings Randolph or

Table 3.3: *Parameters of the demand restriction rule. Current MWCOG demand restriction policy is presented as a single value, labeled "MWCOG", while optimized results, "Optim", are presented as a range. Optimized values for Mandatory and Emergency restrictions are not presented, as these restrictions are not imposed.*

	Jen Randolph WS Index		Little Seneca Index		Demand Reduction (%) June-Sep		Demand Reduction (%) Remainder of Year	
	MWCOG	Optim	MWCOG	Optim	MWCOG	Optim	MWCOG	Optim
Voluntary	60	75-85	60	74-85	5	1.2-4.7	3	4.1-7.3
Mandatory	25		25		9.2		5	
Emergency	5		5		15		15	

Little Seneca storage, respectively. The mandatory and emergency rules are close approximations of the actual MWCOG demand triggers, simplified to improve computational time. The potential demand reduction values, shown in Table 3.2, are based on water use reductions during the drought of 1999 and other historical restrictions throughout the region. Reduction in water use is typically achieved by banning of lawn watering, filling of swimming pools, operation of ornamental fountains, and other similar activities.

Under current levels of demand and both the historical and synthetic streamflow record, the combined storage of the Jennings Randolph water supply account and Little Seneca remains greater than 75.80% at all times, suggesting that voluntary restrictions would never be implemented using the current scheme. Because this is not likely the intended goal of the MWCOG rules, the demand restriction triggers were evaluated using the multiobjective optimization framework. To allow for greater flexibility in the model, the voluntary trigger which previously considered Jennings Randolph water supply and Little Seneca storage together was separated, allowing each reservoir to be evaluated based on a specific trigger point, similar to rules for Mandatory and Voluntary restrictions. In addition, percent reduction for each restriction level was evaluated within very tight bounds to determine if there was any notable benefit of maximizing percent reduction.

Evaluation of the model suggests that operations could be improved by increasing the trigger for voluntary demand restriction. By raising the voluntary demand restriction setpoints to the range of 74-84 %, demand restrictions are called in 2-3 years over the

historical record. Mandatory and Emergency restrictions are never imposed. This policy is more consistent with the MWCOG's expectation of requiring demand restrictions only during the most severe droughts. Because water use restrictions are called so infrequently, even in the optimized rules, the percent restrictions appear to have less impact than the trigger point.

Figure 3.6 presents the Pareto front of optimized demand restriction rules. The Pareto front is defined as the set of solutions in which each objective function cannot be improved without negatively affecting another objective. In other words, the Pareto front represents optimal solutions for all possible objective weighting schemes. In order to present this 6-dimensional surface, pairwise combinations of the objective functions are presented in grid form. For each 2-dimension pair, the blue surface represents the set of solutions which minimize the pair of objectives. Other non-dominated points, shown in black, do not minimize the particular pair of objectives but provide an optimal solution elsewhere in the objective space. Using this figure, tradeoffs among the objectives can be easily considered.

Figure 3.6 illustrates that increases in the demand restriction trigger improves all objectives, except for Z_{WW}. The extent of this improvement is balanced between improving Z_{Stor} and the flow-based objectives ($Z_{\text{Rec Season}}$ and $Z_{\text{Env Flows}}$). The location of the current policy point, far from the Pareto front, suggests that improvements can be realized for all objectives.

3.6 Conclusions

Efficient water management policies are critical in water supply systems with significant lag between reservoir releases and their subsequent use to meet demand. The Washington DC Metropolitan Area water supply system, which is characterized by a 9-day lag, was used as a case study to evaluate a rule optimization scheme, using a multiobjective evolutionary algorithm linked to a hydrologic/decision simulation model. Evolutionary

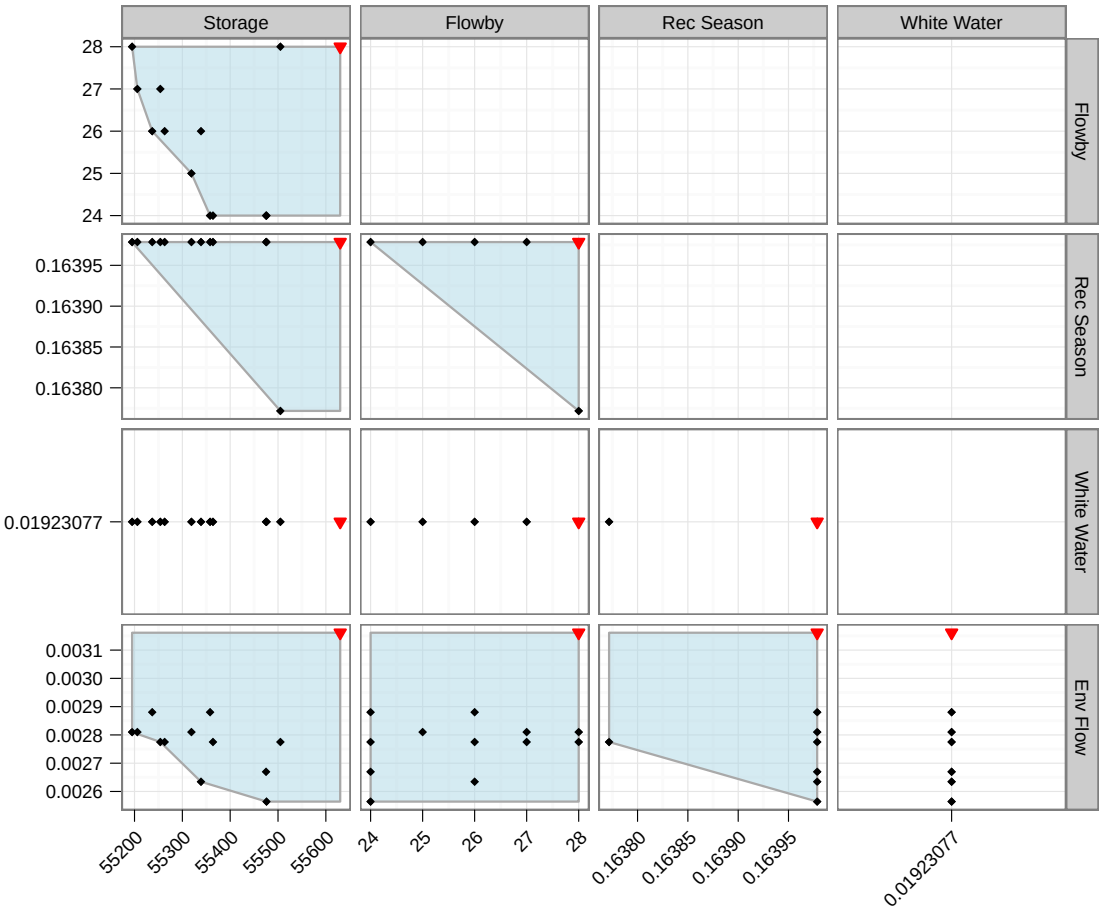

Figure 3.6: *Demand Restriction - Pareto Front comparison. Comparison of current operating procedures, shown by a red ▼, and the set of optimized demand restriction rules. The blue surface represent the Pareto front for each pair of objective functions.*

algorithms are capable of searching large and complex decision spaces and are robust to nonlinear functions and constraints.

Optimization of the water management rules proved effective at improving system performance and provided insight into reducing uncertainty caused by the physical layout of the system. In total, 6 objective functions were considered, which measured demand shortage, reservoir storage, minimum river flowby, recreation days, whitewater releases, and environmental benefit.

While no single rule modification was dominant across all objectives, certain changes provided consistent improvements. Modifying the Load Shift Index, which prevents load being shifted to the Patuxent and Occoquan reservoirs during times of low storage, reduced storage penalties by 2.4 % and flowby penalties by 7.1%. Additionally, the existing trigger points for water use restrictions were found to be set too low, never engaging, even during the historical drought of record. Increasing these triggers allowed for occasional water use restrictions to be placed on the region's consumers, improving flowby and environmental flows by 14.3 and 18.9%, respectively.

Other modifications involve a tradeoff between objectives. Modification of the Buffer Equation, which balances storage between the upstream Jennings Randolph Reservoir and the downstream Little Seneca Reservoir was able to improve both storage in the Jennings Randolph and downstream flow metrics. However, if Jennings Randolph storage was maximized via excessively conservative release policies, downstream flows were negatively impacted.

The methods outlined in this study have great potential for continued study within the WMA and application to other, similarly complex water supply systems that could benefit from more efficient water resources decision-making.

3.7 Acknowledgments

James Stagge is a Via Doctoral Fellow and gratefully acknowledges support from the Via program and the Institute for Critical Technology and Applied Science (ICTAS). The authors would also like to thank the Interstate Commission on the Potomac River Basin (ICPRB) and Hydrologics, Inc. for providing data access and research support.

Bibliography

Ahmed, S. N., K. R. Bencala, and C. L. Schultz (2010). 2010 Washington Metropolitan Area water supply reliability study; part 1: Demand and resource availability forecast for the

year 2040. Technical Report ICPRB 10-01, Interstate Commission on the Potomac River Basin.

Beume, N., B. Naujoks, and M. Emmerich (2007). SMS-EMOA: Multiobjective selection based on dominated hypervolume. *European Journal of Operational Research 181*, 1653–1669.

Chen, L. (2003). Real coded genetic algorithm optimization of long term reservoir operation. *J. Amer. Water Res. Assoc 39*(5).

Cook, B. I., R. L. Miller, and R. Seager (2008). Dust and sea surface temperature forcing of the 1930's 'Dust Bowl' drought. *Geophysical Research Letters 35*.

Cummins, J., C. Buchanan, C. Haywood, H. Moltz, A. Griggs, R. C. Jones, R. Kraus, N. Hitt, and R. V. Bumgardner (2010). Potomac basin large river environmental flow needs. Technical report, Interstate Commission on the Potomac River Basin.

Deb, K. (2001). *Multi-Objective Optimization using Evolutionary Algorithms*. Chichester, UK: John Wiley & Sons.

Deb, K., A. Pratap, S. Agarwal, and T. Meyarivan (2002). A fast elitist multi-objective genetic algorithm: NSGA-II. *IEEE Transactions on Evolutionary Computation 6*, 182–197.

Dyne, V. (2007). Water, water .

Emmerich, M., N. Beume, and B. Naujoks (2005). An EMO algorithm using the hypervolume measure as selection criterion. Volume 3410 of *Lecture Notes in Computer Science*, pp. 62–76. Springer.

Ferreira, A. A. and T. B. Ludermir (2009). Genetic algorithm for reservoir computing optimization. *Proc. Int. Joint Conf. Neural Networks*.

Fleischer, M. (2003). The measure of Pareto Optima: Applications to multi-objective metaheuristics. In *Evolutionary Multi-Criterion Optimization. Second International Conference, EMO 2003*, pp. 519–533. Springer.

Goldberg, D. E. (1989). *Genetic algorithms in search, optimization and machine learning*. Reading, MA: Addison-Wesley Publishing Company.

Hagen, E. R. and R. C. Steiner (1998). Occoquan Reservoir watershed: ”natural” daily inflow development. Technical Report 98-3, Interstate Commission on the Potomac River Basin.

Hagen, E. R. and R. C. Steiner (1999). Little Seneca Reservoir ”natural” daily inflow development. Technical Report 99-3, Interstate Commission on the Potomac River Basin.

Hagen, E. R., R. C. Steiner, and J. L. Ducnuigeen (1998a). Jennings Randolph Reservoir watershed: "natural" daily inflow development. Technical Report 98-5, Interstate Commission on the Potomac River Basin.

Hagen, E. R., R. C. Steiner, and J. L. Ducnuigeen (1998b). Patuxent Reservoirs: "natural" daily inflow development. Technical Report 98-4a, Interstate Commission on the Potomac River Basin.

Hashimoto, T., J. R. Stedinger, and D. P. Loucks (1982). Reliability, resilience, and vulnerability criteria for water resource system performance evaluation. *Water Resour. Res. 18*(1).

Hirsch, R. (1979). Synthetic hydrology and water supply reliability. *Water Resources Research 15*(4), 1603–1615.

Labadie, J. W. (2004). Optimal operation of multireservoir systems: State-of-the-art review. *J. Water Resour. Plann. Manage 130*(2).

Mersmann, M. (2011). *emoa: Evolutionary Multiobjective Optimization Algorithms*. R package version 0.4-8.

Metropolitan Washington Council of Governments (2000). Metropolitan Washington water supply and drought awareness response plan: Potomac River system. Technical Report 20703, Washington DC.

Miller, R. L., I. Tegen, and J. Perlwitz (2004). Surface radiative forcing by dust aerosols and the hydrologic cycle. *J. Geophys. Res. 109*.

Momtahen, S. and A. B. Dariane (2007). Direct search approaches using genetic algorithms for optimization of water reservoir operating policies. *J. Water Resour. Plann. Manage 133*(3).

Oliveira, R. and D. P. Loucks (1997). Operating rules for multireservoir systems. *Water Resources Research 33*(4).

Palmer, R. N., J. A. Smith, J. L. Cohon, and C. ReVelle (1982). Reservoir management in the Potomac River basin. *J. Water Resour. Plann. Manage 108*(1), 47–66.

Palmer, R. N., J. R. Wright, J. A. Smith, J. L. Cohon, and C. S. ReVelle (1979). Policy analysis of reservoir operations in the Potomac River Basin, volume i. executive summary. Technical Report 59, University of Maryland, Water Resources Series.

Panofsky, H. W. and G. W. Brier (2007). Some applications of statistics to meteorology. *Journal of Water Resources Planning and Managemnt 133*, 288.

Porter, J. W. and B. J. Pink (1991). A method of synthetic fragments for disaggregation in stochastic data generation. In *Hydrology and Water Resources Symposium*, Institution of Engineers, Australia, pp. 187–191.

Reed, P. M., J. D. Herman, J. R. Kasprzyk, and J. B. Kollat (2012). Evolutionary multiobjective optimization in water resources: The past, present, and future. *Advances in Water Resources*.

Rosenfeld, D., Y. Rudich, and R. Lahav (2001). Desert dust suppressing precipitation: A possible desertification feedback loop. In *Proc. Natl. Acad. Sci. USA*, Volume 98, pp. 59755980.

Schubert, S. D., M. J. Suarez, P. J. Region, R. D. Koster, and J. T. Bacmeister (2004). On the cause of the 1930s Dust Bowl. *Science 303*, 18551859.

Schwartz, S. S. (2000). Multiobjective management of Potomac River consumptive use. *J. Water Resour. Plann. Manage 126*(5).

Seager, R., Y. Kushnir, M. F. Ting, M. Cane, N. Naik, and J. Velez (2008). Would advance knowledge of 1930s SSTs have allowed prediction of the Dust Bowl drought? *Journal of Climate 21*, 3261–3281.

Sheer, D. P. (1996). A perspective on the Washington Metropolitan Area water supply problem. Technical Report ICPRB M-6, Interstate Commission on the Potomac River Basin.

Sheer, D. P. and K. Flynn (1983). Water supply. *Civil Engineering, ASCE*, 50–53.

Srikanthan, R. and T. A. McMahon (1982). Stochastic generation of monthly streamflows. *Journal of the Hydraulics Division-ASCE 108*(3), 419–441.

Stagge, J. H. (2012). Markov chain model for generation of daily climate-adjusted streamflows. In *Optimization of Multi-Reservoir Management Rules Subject to Climate and Demand Change in the Potomac River Basin, Ph.D. Dissertation, Chapter 2*. Blacksburg, VA: Virginia Tech.

U.S. Army Corps of Engineers (1963). Potomac River Basin report. Technical report, Dept. of the Army, U.S. Army Engineer Division, North Atlantic, Baltimore Basin Studies Branch.

U.S. Army Corps of Engineers (1982). Water supply coordination agreement. Technical report.

Wardlaw, R. and M. Sharif (1999). Evaluation of genetic algorithms for optimal reservoir system operation. *J. Water Resour. Plann. Manage 125*(1).

Zitzler, E. and L. Thiele (1998). Multiobjective optimization using evolutionary algorithms - a comparative case study. In *Conference on Parallel Problem Solving from Nature (PPSN V)*, Amsterdam, pp. 292–301.

Zitzler, M. and S. Künzli (2004). Indicator-based selection in multiobjective search. In *Conference on Parallel Problem Solving from Nature (PPSN VIII)*, pp. 832–842. Springer.

Chapter 4

Manuscript 3: Water Resources Adaptation to Climate and Demand Change Using Multiobjective Evolutionary Algorithms

Abstract

The effects of climate change are increasingly being considered in conjunction with population/demand change and reservoir sedimentation in forecasts of water supply vulnerability. A case study is presented, based on the Washington DC Metropolitan Area water supply, where the relative effects of these factors are evaluated first by simulation and then addressed using a multiobjective evolutionary algorithm to develop adaptation strategies. Optimized reservoir management policies were compared *a posteriori* using 6 distinct objectives, ranging from reservoir storage to environmental and recreational benefit. Simulation of future conditions show the system becoming more stressed with time. Reservoir sedimentation is projected to increase the severity of reservoir storage failures (volume $< 40\%$), by 114%. Demand increases and climate change are projected to further

stress the system, causing longer periods of low flow in downstream water bodies and a loss of recreational use due to low reservoir storage. Optimized rules are capable of mitigating some of these effects, most notably returning simulations of 2070-2099 climate to historical levels.

4.1 Introduction

Climate research suggests that the Earth's climate is changing in response to changes in the global atmospheric composition, brought about by human activities (Meehl et al. 2007). As atmospheric research improves the reliability of global climate predictions, water resources planners and engineering must consider climatic changes as potentially important factors in predicting and addressing water vulnerability.

As with other non-stationary factors typically considered in water supply planning, such as demand change and reservoir sedimentation, the risks posed by a changing climate must be identified and evaluated. Once vulnerabilities are identified, adaptation strategies can be developed to mitigate these effects.

This process is applied to the Potomac River and the Washington DC Metropolitan Area (WMA) water supply system (Figure 4.1) . The relative and combined effects of demand change, reservoir sedimentation, and climate change are evaluated for the WMA over the next century. System operating rules are then optimized based on several conflicting objectives using a state-of-the-art multiobjective evolutionary algorithm, SMS-EMOA. Results of this optimization provide insight into potential adaptation strategies that could be employed to improve efficiency and maintain the current level of service in the WMA in the future without the need for physical modifications to the system.

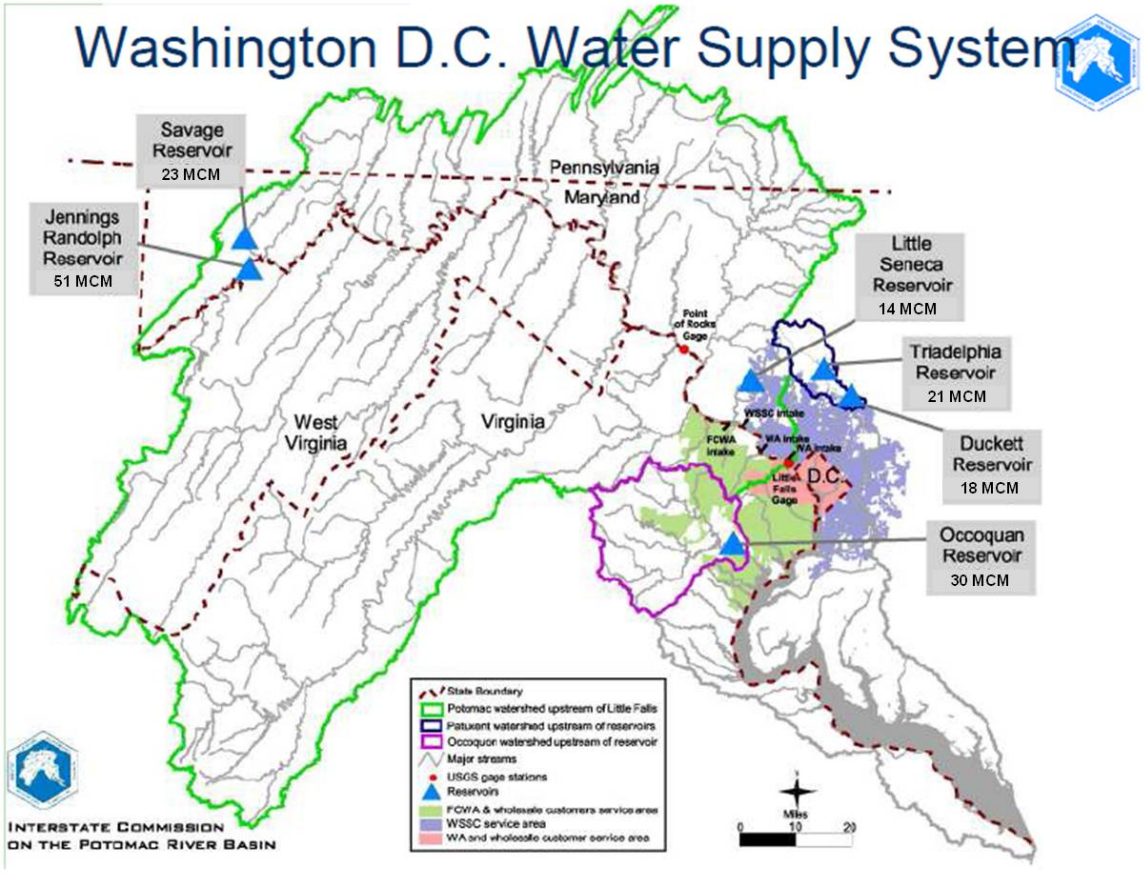

Figure 4.1: *Potomac watershed and Washington DC water supply. Volumes are shown as 10^6 m^3, or MCM. Figure generated by the Interstate Commission on the Potomac River Basin (ICPRB).*

4.2 Methods

4.2.1 Washington Metropolitan Area Water Supply Model

As in Stagge (2012b), the WMA is used as a case study to evaluate the effects of demand and climate change on water resources operations. The WMA houses more than 5 million residents across 40,000 square kilometers in Maryland, Virginia and Washington DC. Municipal water needs of the WMA are managed by three major suppliers:

Washington Suburban Sanitary Commission (WSSC), which serves the Maryland suburbs,

Fairfax Water, which serves Fairfax County and other northern Virginia suburbs, and

Washington Aqueduct, which provides water to the District of Columbia.

The current water supply system is the result of several design iterations and collaboration among the numerous levels of government, water suppliers and citizen groups. Details of the system are provided in Stagge (2012a) and Ahmed et al. (2010). This system relies predominantly ($\approx$ 78% annually) on flow from the Potomac River to satisfy water demands, with the remainder of water provided by two off-line reservoirs: the Patuxent Reservoir system operated by WSSC and the Occoquan Reservoir operated by Fairfax Water (Table 4.1). Flow in the Potomac is augmented by two reservoirs. The Jennings Randolph Reservoir is the larger of the two (109×10^6 m^3), but is located approximately 9 days hydrologic travel time upstream of the WMA intakes (Table 4.1). The Little Seneca Reservoir is located only a day upstream of the MWA intakes, but has significantly smaller usable storage and a smaller watershed area. These two reservoirs are therefore operated in concert, with the Jennings Randolph providing primary releases and the Little Seneca used to "fine tune" flows immediately upstream of the intakes. While allowing the main stem of the Potomac River to remain relatively uncontrolled, this layout adds uncertainty to the system, as release decisions must be made in advance of accurate weather forecasts.

Hydraulic routing and reservoir operations were simulated using OASIS (Version 3.09.033), developed by Hydrologics, Inc. OASIS is a water management simulation and decision model, which uses a node-arc architecture to model reservoirs, reaches, inputs and withdrawals. Operating rules are expressed as goals or constraints and solved via linear programming using a daily time step, mimicking the imperfect foresight of daily operational decision-making.

The OASIS model was developed in conjunction with the ICPRB and water suppliers to ensure that all data, operating rules, and assumptions were accurate. Reservoir details, including stage-storage curves, sedimentation rates, and existing operational rule curves, were provided by the ICPRB, as well as the current Potomac channel routing and travel time estimates. Daily demand among the three major WMA water suppliers was simulated using a set of multivariate regression equations, incorporating an ARMA error term, provided in Ahmed et al. (2010).

4.2.2 Multiobjective optimization

Optimization of system operating rules was carried out in a manner similar to Stagge (2012a), using SMS-EMOA (Emmerich et al. 2005; Beume et al. 2007), an Indicator-based Multiobjective Evolutionary Algorithm (MOEA), wrapped around the OASIS simulation model. SMS-EMOA is a steady-state Multi-Objective Evolutionary Algorithm designed to maximize the multi-dimensional hypervolume ($\mathcal{S}$-metric) dominated by a finite number

Table 4.1: *WMA operational characteristics.*

Reservoir	Manager	Total Storage 10^6 m^3	Available Storage 10^6 m^3	Watershed Area km^2	Upstream Distance km	Travel Time days
Jennings Randolph	CO-OP,USACE	109	51	681	320	9
Little Seneca	CO-OP	16	14	54	25	1
Savage	UPRC	24	23	272	320	9
Patuxent	WSSC	51	39	342	-	-
Occoquan	Fairfax	31	30	1,533	-	-

of points. Hypervolume metrics, developed by Zitzler and Thiele (1998) and Fleischer (2003), are invariant to objective scaling, tend to converge on the Pareto set, and assign a greater weight to regions with unique points or high curvature in the objective space.

As in Stagge (2012a), a version of SMS-EMOA based on the EMOA R package (Mersmann 2011) using simulated binary crossover (SBX) and polynomial mutation is used to optimize operational decision variables across multiple objectives. This optimization scheme has proven efficient and effective relative to other MOEAs in benchmark studies (Beume et al. 2007).

Six objective functions were developed in conjunction with water suppliers and the ICPRB and designed to cover the range of potential benefits within the Potomac River system. Target volumes and flows were often based on legal agreements, such as the Low Flow Allocation Agreement. Because the functional limit of current MOEAs has been shown to be approximately 10 objectives (Reed et al. 2012), this optimization model uses six objectives, which include:

1. **Shortage**, which minimizes delivery shortages to the water suppliers (volume)
2. **Storage**, which minimizes low storage volumes in any of the reservoirs (volume)
3. **Flowby**, which minimizes days when flow in the Potomac does not exceed low flow requirements (days of violation)
4. **Rec Season**, which minimizes days during the recreation season that Jennings Randolph levels fall below recreation facilities (days of violation)
5. **Whitewater**, which minimizes days when whitewater releases cannot be made due to low storage volume (days of violation)
6. **Env Flows**, which minimizes days when flow in the Potomac falls below recommended environmental levels for three consecutive days (days of violation)

These objectives are presented as a constrained multiobjective optimization problem, identical to that posed in Stagge (2012a):

$$\text{Minimize} \quad Z = Z_{\text{Short}}, Z_{\text{Stor}}, Z_{\text{Flowby}}, Z_{\text{Rec Season}}, Z_{\text{WW}}, Z_{\text{Env Flows}} \tag{4.1a}$$

$$Z_{\text{Short}} = \sum_i \sum_{t=0}^{n} \begin{cases} \frac{\text{Dem}_i(t) - \text{Del}_i(t)}{\text{Dem}_i(t)} & \text{if Dem}_i(t) > \text{Del}_i(t) \\ 0 & \text{otherwise} \end{cases} \tag{4.1b}$$

$$Z_{\text{Stor}} = \sum_j \sum_{t=0}^{n} \begin{cases} 100 - 6 \times \text{Stor}_j(t) & \text{if } 0 \leq \text{Stor}_j(t) < 10\% \\ 60 - 2 \times \text{Stor}_j(t) & \text{if } 10 \leq \text{Stor}_j(t) < 20\% \\ 40 - \text{Stor}_j(t) & \text{if } 20 \leq \text{Stor}_j(t) < 40\% \\ 0 & \text{if Stor}_j(t) \geq 40\% \end{cases} \tag{4.1c}$$

$$Z_{\text{Flowby}} = \sum_k \sum_{t=0}^{n} \left(\frac{Q_k(t) < Q_{\text{Flowby}}}{n} \right) \tag{4.1d}$$

$$Z_{\text{Rec Season}} = \sum_{t=0}^{n_{\text{Rec Season}}} \left(\left(\frac{\text{Elev}_{\text{JR}}(t) > \text{Elev}_{\text{Beach}}}{n_{\text{Rec Season}}} \right) + 2 \times \left(\frac{\text{Elev}_{\text{JR}}(t) > \text{Elev}_{\text{WV}}}{n_{\text{Rec Season}}} \right) + 5 \times \left(\frac{\text{Elev}_{\text{JR}}(t) > \text{Elev}_{\text{MD}}}{n_{\text{Rec Season}}} \right) \right) \tag{4.1e}$$

$$Z_{\text{WW}} = \sum_{t=0}^{n_{\text{WW}}} \left(\frac{Q_{\text{WW}}(t) = 0}{n_{\text{WW}}} \right) \tag{4.1f}$$

$$Z_{\text{Env Flows}} = \sum_{t=0}^{n} \left(\frac{(Q_{\text{LF}}(t) \text{ and } Q_{\text{LF}}(t-1) \text{ and } Q_{\text{LF}}(t-2)) < 200 \text{ MGD}}{n} \right) \tag{4.1g}$$

where each of the Z terms represent individual objective functions. For all objective functions, n represents the total number of days in the time series, i represents the 5 individual water suppliers, and j represents the 6 reservoir storage accounts: (1) Jennings Randolph Water Quality, (2) Jennings Randolph Water Supply, (3) Savage, (4) Patuxent, (5) Occoquan, and (6) Little Seneca. Z_{Short} (Equation 4.1b), sums the percent water delivery shortage at all supply points, including WSSC, Fairfax Water, the USACE, the city of Westernport, and the city of Rockville, where Dem_i refers to daily demand, Del_i refers to daily delivery. Z_{Stor} calculates a penalty when reservoir usable storage falls below 40% of the usable storage in the baseline year 2012. Penalties increase as storage approaches zero using a piecewise function which approximates the existing drought restriction set-

points (Metropolitan Washington Council of Governments 2000). Z_{Flowby}, which sums all days when the legally prescribed flowby, Q_{Flowby} is not satisfied by flow, Q_k, at each of the k locations. The pertinent flowbys are 60 MGD at Luke, 300 MGD at Great Falls and 100 MGD at Little Falls. $Z_{\text{Rec Season}}$ (Equation 4.1e), refers to the summer Recreation Season, which occurs each year between May 1 and Aug 31, represented in the function by $T_{\text{Rec Season}}$. During this period, water managers strive to maintain water levels in the Jennings Randolph Reservoir, represented as Elev_{JR}, above three recreation access points. These points, termed E_{Beach}, E_{WV}, and E_{MD}, are 1455 ft, 1445 ft, and 1420 ft, respectively. Z_{WW} (Equation 4.1f) calculates the ratio of days when whitewater releases, Q_{WW}, cannot be made due to low storage volume. Whitewater releases are set to occur on the 15^{th} and 30^{th} of April and May, whose set is represented as T_{WW}. $Z_{\text{Env Flows}}$ (Equation 4.1g), uses a measure to summarize water supply activity's effect on the ecological health of the Potomac River. While the legal flowby requirement below Little Falls is set at 200 MGD, the Potomac Basin Large River Environmental Flow Needs study stated that there "is strong concern that a continuous, multi-day period of flows at or very close to 100 MGD would be injurious to the biota" (Cummins et al. 2010). This function sums the number of occurrences when flow below Little Falls, Q_{LF}, remains below 200 MGD for 3 or more consecutive days.

4.2.3 Climate adjusted streamflow generation

The effect of climate change is simulated by stochastically generated daily climate-adjusted streamflow and precipitation time series. These daily time series were generated using the Markov Chain Model, described in detail in Stagge (2012b). In this method, GCM-scale climate indicators are related to discrete monthly climate states, extracted from the historical record for the study region. The transition probabilities between these climate states are then adjusted based on GCM climate projections. The parameters of a daily streamflow model, similar to Aksoy (2003) and Szilagyi et al. (2006), are controlled by the monthly climate state and used the generate climate-adjusted daily streamflow. Daily flow is generated based on a two-state (increasing/decreasing) Markov chain, with ris-

ing limb increments randomly sampled from a Weibull distribution and the falling limb modeled as exponential recession. Stagge (2012b) showed this model capable of both reproducing historical streamflow statistics at the daily, monthly and annual time step and of generating climate-adjusted streamflows that match the general findings of classical climate downscaling studies (Najjar et al. 2009; Milly et al. 2005; Hayhoe et al. 2007).

Daily streamflow was generated for USGS stream gauge 01646500, located on the Potomac River near the Little Falls pumping station in Washington, DC and spatially disaggregated to daily streamflow and precipitation values at the necessary upstream sites using the "Method of Fragments" (Srikanthan and McMahon 1982; Porter and Pink 1991), as in Stagge (2012a). Flows were bias-corrected using quantile-quantile mapping to remove residual model bias, particularly at the upstream sites.

4.3 Results

4.3.1 Projected Changes to WMA Water Supply Reliability

Three major processes are projected to affect the reliability of the WMA water supply system over the next century. These are demand change, reservoir sedimentation, and climate change. To identify the relative impact of these processes on the system, the system was simulated while adjusting each parameter in isolation.

Demand Change

Per the Low Flow Allocation Agreement, signed by all member states, the ICPRB provides a minimum 20 year forecast of demand change once every 5 years. The most recent projection, Ahmed et al. (2010), evaluates demand change through the year 2040. These predictions are based on recent water use information provided by the WMA water suppliers and demographic projections from the most recent MWCOG Round 7.2 Cooperative Forecast (Metropolitan Washington Council of Governments 2009). Demand change

Table 4.2: *Projected WMA population and demand change (2010-2040). Demand is presented as 10^3 m^3/d. Percent change from 2010 is presented in parentheses.*

	Population (in Millions)		*Water Demand*			
	2010	2040	2010	2020	2030	2040
Fairfax	1.54	2.03 (32.0%)	663	755 (13.8%)	826 (24.5%)	866 (30.7%)
WSSC	1.72	2.01 (16.6%)	651	707 (8.6%)	746 (14.7%)	771 (18.6%)
Aqueduct	0.98	1.23 (26.0%)	571	624 (9.2%)	652 (14.1%)	673 (17.8%)
Rockville	0.05	0.06 (37%)	18	20 (10.4%)	22 (20.8%)	24 (31.3%)
Total WMA	4.28	5.33 (24.5%)	1,903	2,106 (10.7%)	2,246 (18.0%)	2,335 (22.7%)

beyond 2040 is not considered in this study, as water demand forecasts tend to become unreliable beyond the 30 year horizon in this region (Ahmed et al. 2010), given the added uncertainty of population change and innovations in water efficiency.

The MWCOG Round 7.2 Cooperative Forecast (Metropolitan Washington Council of Governments 2009) predicts an increase in population of approximately 1 million (24.5%) between 2010 and 2040, which corresponds to a projected water demand increase of 432×10^3 m^3/d (22.7%) (Table 4.2). The greatest increase in population, and therefore water demand, is projected to occur within the Fairfax Water service area of Northern Virginia. Demand increase for Fairfax Water is projected to increase by 31% between 2010 and 2040, while the WSSC and Washington Aqueduct service areas are expected to increase demand by 19 and 18%, respectively (Ahmed et al. 2010). The City of Rockville, which maintains a separate water supply, is projected to have a relatively large increase in demand by percent (31.3%), but this remains a small portion of the total WMA water supply because of Rockville's small service area.

This projected increase in demand will produce a consistent increase in Recreation Season failures, $Z_{\text{Rec Season}}$, and Environmental Flow failures, $Z_{\text{Rec Season}}$ (Figure 4.2). By the year 2040, this increase in demand alone will result in an additional loss of approximately 0.5 days/year with access to the Beach (2.0% increase) and 0.9 days/year with access to the West Virginia boat ramp (58.3% increase). While this loss of recreation time may not appear significant, a 58.3% increase in the more severe WV boat ramp failures suggests that demand will drive a loss of recreation revenue. Additionally, recreation failures tend

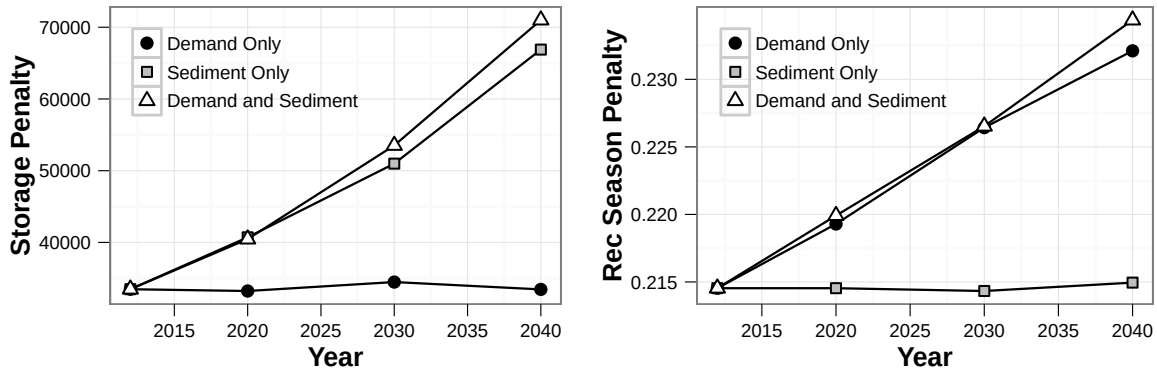

(a) *Storage* **(b)** *Recreation Season*

Figure 4.2: *Effect of demand increase and reservoir sedimentation on Storage and Recreation Season objectives.*

to occur in extended groups, rather than a single instance. In this way, the additional failures may significantly affect individual recreation seasons.

Increased demand does not significantly affect WMA storage as a whole (Figure 4.2), however, it is important to note that increased demand begins to adversely affect storage in the Little Seneca Reservoir by the 2030 demand year.

Sedimentation

Usable reservoir storage volume is expected to decrease with time due to the deposition of sediment carried by reservoir inflows. Sedimentation rates were analyzed in Ahmed et al. (2010) using the non-parametric Kendall-Theill Robust Line (Sen 1968; Thiel 1950), which determined that sedimentation rates ranged between 57×10^3 and 481×10^3 m^3/yr for the Little Seneca and Jennings Randolph reservoirs, respectively (Table 4.3). References for the bathymetric surveys are provided in Table 4.3.

Reservoirs in the WMA water supply system are projected to lose 7-15% of their usable storage volume due to sedimentation in the 30 years between 2010 and 2040. Based on the most recent survey, the sedimentation rates in the Jennings Randolph Reservoir is particularly high relative to the other reservoirs Table 4.3 , and significantly greater

Table 4.3: *Projected sedimentation and storage loss (2010-2040). All volumes are presented as 10^3 m^3. Percent change from 2010 is presented in parentheses.*

Reservoir	Usable Storage (10^6 m^3)		Sed Rate	Source
	2010	2040	(10^3 m^3/yr)	
Jennings Randolph	102,500	88,100 (-14.1%)	481	USACE (1997)
Little Seneca	13,800	12,100 (-12.3%)	57	Hagen (1999)
Occoquan	29,500	25,000 (-15.4%)	151	CDM (2002)
Patuxent	38,100	35,400 (-7.2%)	91	Ortt et al. (2007)
Savage	23,300	21,200 (-8.8%)	68	Ahmed et al. (2010)

than the original "design" sedimentation rate of 25×10^3 m^3/yr, which was based on upstream suspended sediment concentrations (Burns and MacArthur 1996). By 2040, the storage capacity loss in the Jennings Randolph Reservoir is projected to be 25% of the original storage volume (14.1% between 2010 and 2040). Despite these predictions of storage loss, sedimentation rates tend to change with time, as the sediment contribution of upstream watersheds change. Increased development tends to increase sediment load per area (Allmendinger et al. 2007), though this effect may be mitigated by improvements in non-point source runoff treatment. It is important to note that the Jennings Randolph watershed, historically home to coal mining, has seen a decrease in this industry and has been subject to increased oversight with respect to non-point source runoff.

As expected, reservoir sedimentation is expected to increase the frequency and severity of reservoir storage shortage, defined as usable storage $< 40\%$ by Z_{Stor} (Figure 4.2). This noted increase is due to storage failures in the Patuxent and Savage reservoirs. Interestingly, the Jennings Randolph and Little Seneca water supply reservoirs do not develop storage failures until the 2040 sedimentation level. This suggests that there may be opportunities for improving Z_{Stor} as storage is lost to sedimentation through changes in how load is allocated among the reservoirs. Because $Z_{\text{Rec Season}}$ is strongly tied to storage in the Jennings Randolph, it is not surprising that $Z_{\text{Rec Season}}$ is relatively unaffected by sedimentation losses (Figure 4.2). Further, sedimentation has little impact on the flow measures, Z_{Flowby} and $Z_{\text{Env Flows}}$.

Table 4.4: *Evaluated global climate models (IPCC - AR4).*

Model	Institution	Location	Reference
CCSM3	National Center for Atmospheric Research (NCAR)	USA	Collins et al. (2006)
CGM_3.1	Canadian Centre for Climate Modeling and Analysis	Canada	Flato (2005)
CSIRO_MK3	CSIRO Atmospheric Research	Australia	Gordon et al. (2002)
MIROC_3.2	Center for Climate System Research	Japan	Watanabe et al. (2011)
PCM1	National Center for Atmospheric Research (NCAR)	USA	Washington et al. (2000)

Climate Change

Output from five GCM simulations (Table 4.4) was used to generate streamflow and precipitation throughout the Potomac watershed at 30 year intervals (2010-2039, 2040-2069, 2070-2099) using the streamflow generation method presented in Stagge (2012b). These simulations predict a slight increase (1-7%) in mean annual flow over the next century, with the majority of this increase occuring during the winter and early spring. Conversely, mean summer flows are predicted to decrease, particularly during July and August, caused by a shift towards shorter, intense, but sporadic rain events. These general trends match well with similar simulations of climate change in the region (Najjar et al. 2009; Pyke et al. 2008; Hayhoe et al. 2008). An important factor with water management implications is the prediction that the date of the minimum annual flow in the Potomac River is predicted to shift 2-5 days earlier in the year, on average, by the 2070-2099 period (Stagge 2012b). As expected, the highest emission scenario, SRES A2, results in the most severe shifts in streamflow, while the low emission scenario, SRES B1, produces a more modest change.

The effect of climate change alone on water supply reliabilty in the WMA region is shown graphically in Figure 4.3. Simulation of climate change predicts an increase in nearly all objective functions over the next century. Results presented in Figure 4.3 account for model bias by correcting streamflows using quantile-quantile bias correction and then comparing each climate-adjusted scenario to a simulation of current climate

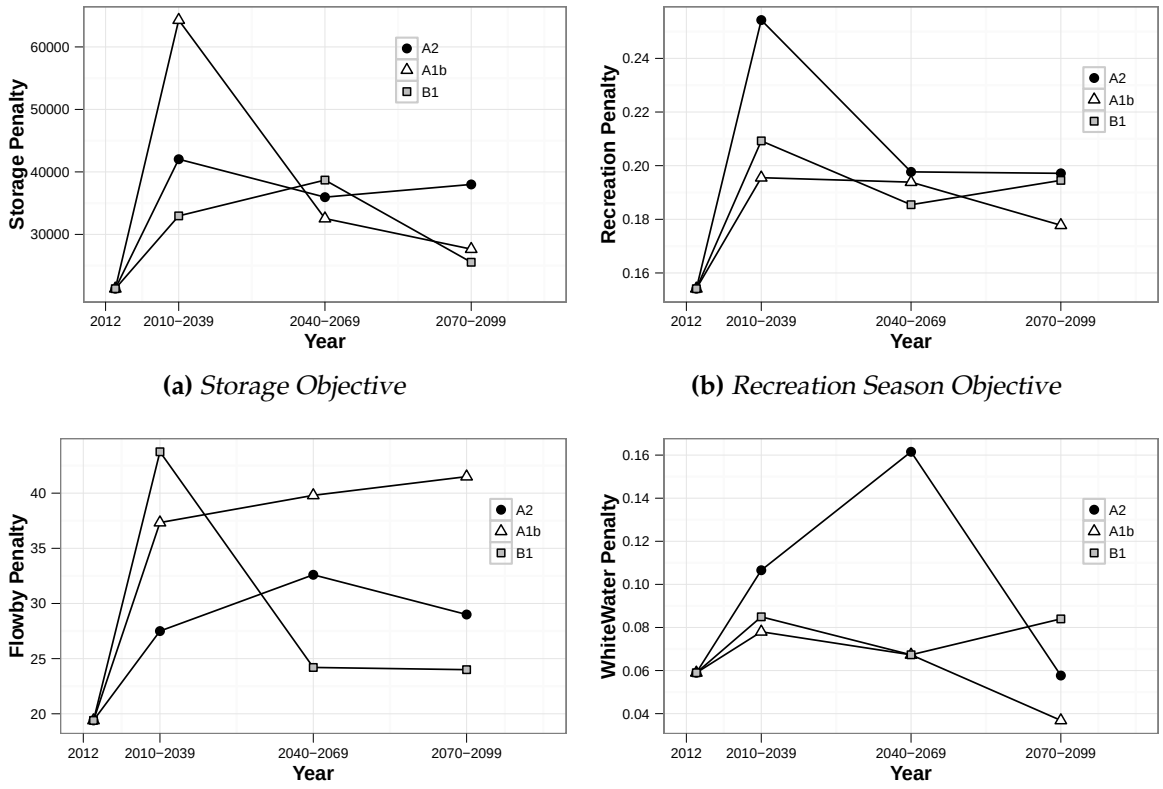

(a) *Storage Objective*

(b) *Recreation Season Objective*

(c) *Flowby Objective*

(d) *Whitewater Objective*

Figure 4.3: *Effect of climate change on system objectives. Lines represent the mean of 5 GCMs: CCSM, CGM, CSIRO, MIROC, and PCM1 for the A2, A1b, and B1 emission scenarios.*

conditions using an identical model. Interestingly, the greatest change in most objective functions occurs in the first part of the next centry (2010-2039), though streamflow trends continue relatively consistently throughout the century (Stagge 2012b). This trend may suggest that the current rules developed based on the historical streamflow record may not be robust to shifts in the timing and distribution of streamflow subject to climate change. This further stresses the importance of adaptation studies.

When examined in greater detail, the climate-adjusted streamflows result in an increase in Patuxent and Savage storage failures, though the severity of these failures actually tends to decrease throughout the century. This is presumably because load is shifted to other reservoirs such as the Little Seneca and Occoquan, which previously did not pro-

duce storage failures, but begin to once subjected to climate change streamflows. Though storage in the Jennings Randolph Reservoir is never low enough to be considered a storage failure, climate change conditions significantly decrease the number of days with access to the Jennings Randolph beach by 300-400 days, or 3.9-5.2 days/year. Access to the WV boat dock is decreased by an average of 0.4-1.3 days/year. Whitewater releases are predicted to be curtailed an additional 4-14 days over the simulation period, an increase of 18.3-41.2%.

4.3.2 Adaptation Strategies

Although simulations predict that the combined effect of demand increases, reservoir sedimentation and climate change will decrease the WMA's water supply effectiveness, there is potential to improve efficiency and decrease vulnerabilities by adapting operating rules to these changing conditions.

As in Stagge (2012a), five rule modifications were considered with regard to adaptation: the buffer equation, load shifting, demand restrictions, and reservoir rule curves for the Jennings Randolph and Patuxent reservoirs. Using the multiobjective evolutionary algorithm SMS-EMOA, parameters within these rules were adjusted to improve performance of the system. Adaptation rules were generated using both the historical record and the CSIRO A2 scenario (2070-2099), both subject to year 2040 levels of demand and sedimentation. The CSIRO output was chosen as representative of A2 conditions at the end of the next century. In verification tests, the CSIRO model consistently produced good statistical agreement with the historical record across daily, monthly and annual time steps.

As expected based on simulation, conditions in the 2070-2099 CSIRO climate change scenario are more challenging for the system than simulation with historical climate and 2040 future demand/sedimentation. This results in larger Storage, Flowby, Recreation Season, and Environmental Flow penalties, though the Whitewater penalty remains equiv-

Table 4.5: *Optimization results for 2040 demand/sedimentation conditions. All values represent the maximum % improvement over the existing operation rules.*

	Z_{Stor}	Z_{Flowby}	$Z_{\text{Rec Season}}$	Z_{WW}	$Z_{\text{Env Flows}}$
Buffer Eq	0.55	20.00	0.71	0	11.11
JR Rule Curve	0.19	26.67	0.12	83.33	4.94
Patux Rule Curve	6.12	6.67	0.24	0	6.17
Load Shifting	0.45	13.33	0.36	0	2.47
Demand Res	2.87	26.67	0.47	0	10.49

alent. No shortage failures were noted, because the existing operating rules prioritize satisfying daily demand. This remains consistent with water suppliers' expectations.

Buffer Equation

Within the WMA water supply operating rules, the buffer equation is designed to balance storage levels between the reservoirs on the main-stem Potomac, the upstream Jennings Randolph and downstream Little Seneca Reservoirs. Reservoir releases are calculated based on estimated demand; however, the buffer equation adjusts these releases based on the imbalance, in percent usable storage, between the Jennings Randolph Water Supply volume and Little Seneca storage. If the Water Supply volume in the Jennings Randolph is lower than storage in the Little Seneca Reservoir, the buffer is negative, reducing releases from the upstream Jennings Randolph under the assumption that the deficit will be satisfied through additional releases from the downstream Little Seneca Reservoir. Conversely, if levels in the Little Seneca Reservoir are lower than the Jennings Randolph Water Supply account, the buffer is positive, producing a release from the Jennings Randolph Reservoir that is larger than necessary, based on the assumption that Little Seneca releases will be curtailed to allow the reservoir to refill. Under the current policy, the slope of the Buffer Equation (Figure 4.4) is identical for both of these situations, adding or subtracting a maximum of 568×10^3 m^3/d. Stagge (2012a) found that Z_{Flowby} and $Z_{\text{Env Flow}}$ can be improved by adding an intermediate breakpoint to the buffer equation and increasing the equation slope. Conversely, Recreation Season storage can be improved by adding an

Table 4.6: *Optimization results for future conditions (CSIRO A2, 2070-2099 climate). All values represent the maximum % improvement over the existing operation rules.*

	Z_{Stor}	Z_{Flowby}	$Z_{\text{Rec Season}}$	Z_{WW}	$Z_{\text{Env Flows}}$
Buffer Eq	20.71	50	37.79	88	15.20
JR Rule Curve	1.27	16.67	9.24	98	15.20
Patux Rule Curve	6.39	4.17	0	0	2.34
Load Shifting	1.29	8.33	0	0	4.09
Demand Res	1.46	4.17	0.52	0	5.26

additional rule, which uses a much lower buffer when both reservoirs are nearly full ($>$ 90%).

Under future conditions, the Buffer Equation modification has a similar effect, reducing the frequency of missed flowby targets and the number of days with consecutive days with extreme low flows. Buffer equation adjustments are capable of mitigating the impact of climate change, reducing penalties in the 2070-2099 realization to levels comparable to 2040 simulations with demand and sedimentation only. However, no version of the Buffer Equation is capable of reducing system-wide penalty measures to current, 2012 levels.

As with current conditions, the Buffer Equation reduces flowby and environmental flow failures by increasing buffer flow on the left side of the equation, corresponding to the situation when usable Little Seneca storage (%) is lower than Jennings Randolph (Figure 4.4) . Using the optimized buffer equation, a significantly greater release is made from the Jennings Randolph in this situation, which in turn reduces load on the Little Seneca Reservoir and acts as a pulse in the Potomac River to prevent extreme low flows downstream of Little Falls. The shape of the Buffer Equation needed to improve Z_{Flowby} and $Z_{\text{Env Flow}}$ does not significantly change with time between current conditions Stagge (2012a) and 2070-2099 conditions.

A trend towards larger buffer flows over time exists among solutions that optimize $Z_{\text{Rec Season}}$. In particular, the slope of the right side of the Buffer Equation, which controls how Jennings Randolph releases are curtailed when Jennings Randolph storage falls below Little Seneca storage, is projected to increase with time (Figure 4.5). As stress on the system increases with time, it follows that Jennings Randolph releases must increasingly

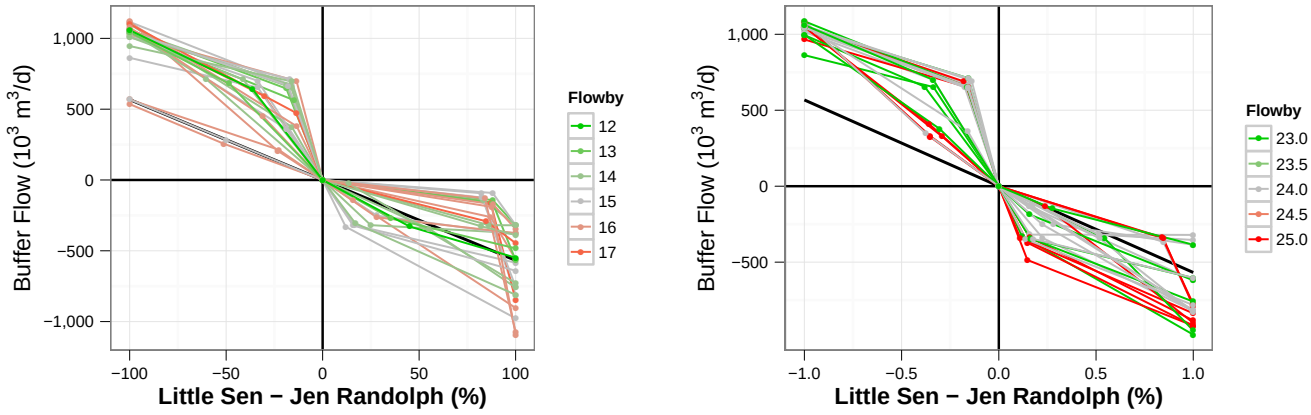

(a) *2040 Conditions* **(b)** *2070-2099 Conditions*

Figure 4.4: *Optimized buffer equation under future conditions with respect to Flowby. Current operating rules are shown by the bold, black line between 568×10^3 m^3/d and - 568×10^3 m^3/d. For each non-dominated solution, the color scale shows the improvement (green) or decrease (red) in objective function relative to current policy.*

be reduced to protect Recreation Season storage, particularly when Jennings Randolph storage is low relative to other reservoirs in the WMA system.

Load Shifting

While the Buffer Equation deals only with balancing releases between Jennings Randolph and Little Seneca, Load Shifting controls how daily demand is allocated to the offline reservoirs, the Patuxent and Occoquan. When predicted flow in the Potomac River is not sufficient to satisfy predicted demand, production at the Patuxent and Occoquant water treatment plants is temporarily increased above standard production levels. Following the load shifting event, production at the offline reservoirs is curtailed an equivalent amount, to replenish storage. Load shifting occurs only when storage in the Jennings Randolph, Little Seneca, Occoquan and Patuxent remains above trigger points, called Load Shift Storage Indices.

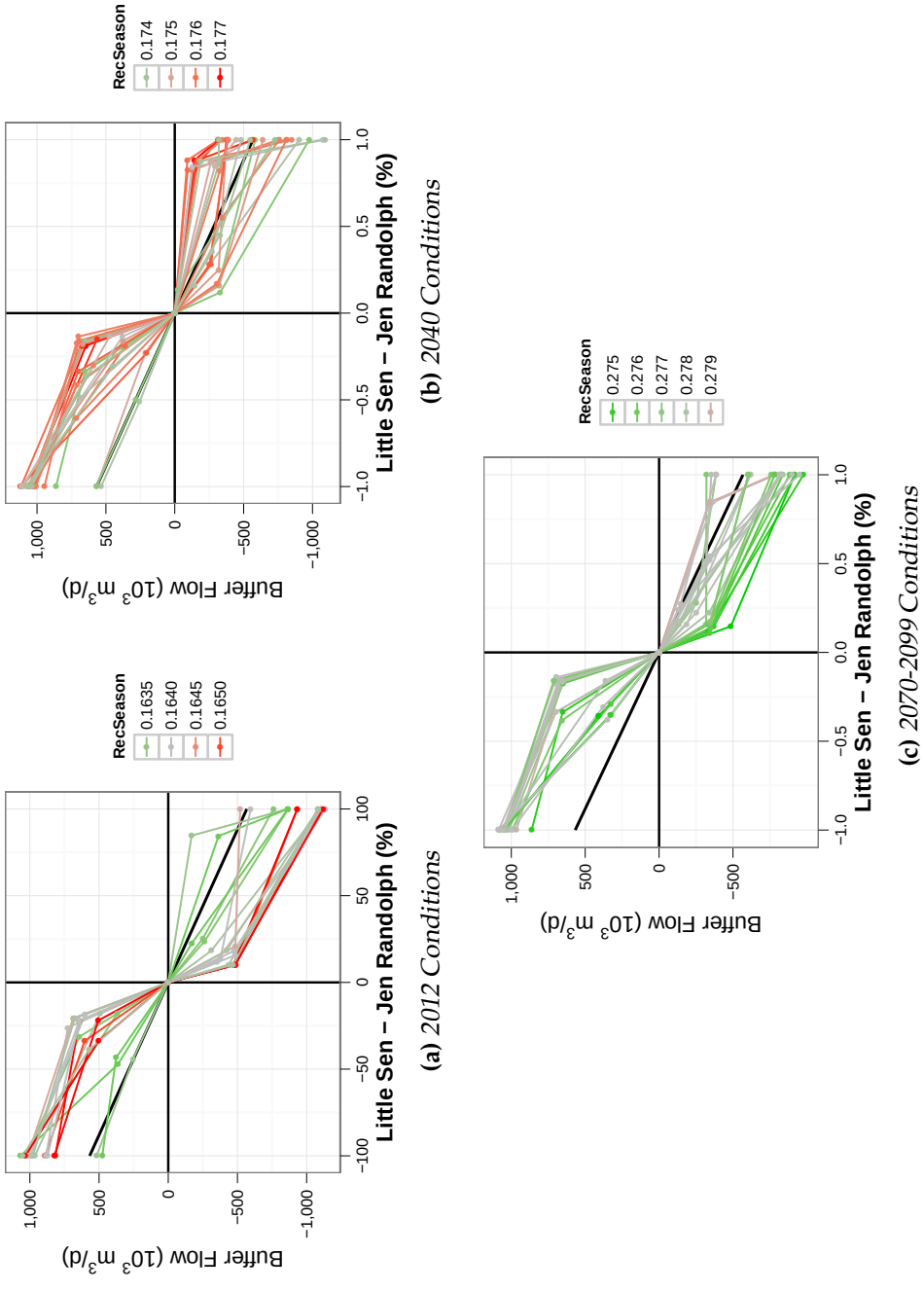

Figure 4.5: *Progression of optimal Buffer Equation with respect to the Recreation Season. Current operating rules are shown by the bold, black line between 568×10^3 m^3/d and - 568×10^3 m^3/d. For each non-dominated solution, the color scale shows the improvement (green) or decrease (red) in objective function relative to current policy.*

Modification of the Storage Indices and Load Shift equation has relatively little impact on the WMA system in simulations of future demand/sedimentation conditions (Table 4.5) and climate change (Table 4.6). While changes to load shifting generally results in better performance than the current policy, this improvement cannot completely mitigate the effects of climate change or of demand and sedimentation change.

No trends exist over time time among the optimized load shifting parameters, suggesting that the effectiveness of load shifting has been maximized and that no further improvements will be realized with time. Adjustments to the load shift equation were relatively successful under current conditions because the Occoquan Reservoir had unused storage which could be used to reduce load on the already stressed Patuxent Reservoir. However, as future conditions constrain and stress the entire WMA system, this additional Occoquan storage is not as readily available, as shown by increases in Occoquan storage penalties (storage < 40 %).

Additionally, benefits were realized under current conditions by increasing the Load Shift Storage Indices. Increasing these rule parameters shifts load from the Patuxent and Occoquan reservoirs to the Little Seneca Reservoir sooner in drought conditions. Similar to findings for the Load Shift equation, this adjustment improves overall system effectiveness under future conditions, but is limited by increased demands on the Little Seneca Reservoir.

Monthly Rule Curves

All reservoirs in the WMA water supply system operate, at least during a portion of the year, according to zone-based rule curves, except for Little Seneca which maintains a full storage volume throughout the year. To determine adaptation potential, operating rule curves for the Jennings Randolph and Patuxent Reservoirs were evaluated using multiobjective optimization. The Jennings Randolph Reservoir was chosen for evaluation because it is the primary water supply reservoir on the Potomac River, while the Patuxent Reservoir was most vulnerable to storage failures.

Jennings Randolph water quality storage is managed by the Baltimore District of the U.S. Army Corps of Engineers and uses 3 zone-based rule curves (high, medium, and low) to guide water quality releases during the non-Recreation Season months (September through April). These releases are designed to approximate the natural contribution of the Potomac River's impounded North Branch, while refilling the reservoir prior to the summer recreation season. Recreation releases are handled by a separate set of stepped rules, designed to maintain recreational storage targets, conditional on current storage.

The multiobjective evolutionary algorithm, SMS-EMOA was used to adjust the medium and low rule curves for the Jennings Randolph Reservoir. Similar to findings in Stagge (2012a), modifications of the Jennings Randolph rule curves primarily improved objectives related to Jennings Randolph storage, reducing $Z_{\text{Rec Season}}$ by 0.1-9.2% and Z_{WW} by 83.3-98%.

The seasonal distribution of flows in the Potomac River is predicted to shift due to climate change towards higher flows during the winter and spring, followed by lower flows in the summer and early fall (Stagge 2012b). This seasonal trend is mirrored by a shift in the optimized Jennings Randolph Reservoir rule curves, increasing the middle and low rule curves between March and May, immediately prior to the recreation season. A similar trend was noted while optimizing the system with regard to current conditions; however, the trend is more pronounced given future conditions. These newly adjusted rules force the Jennings Randolph to operate more conservatively, making smaller releases during this time. In this way, the climate-induced increase in spring flows is used to increase the available storage buffer prior to a summer flow regime characterized by a greater proportion of low flows.

Modification of the Patuxent rule curve is designed to maintain adequate storage in the highly stressed Patuxent Reservoir while providing additional water supply for the WSSC. Simulations suggest that the Patuxent Reservoir is vulnerable during future droughts, typically entering low storage ($< 40\%$) conditions prior to the remaining WMA reservoirs and thereby contributing to the Z_{Stor} penalty. For both evaluated cases (2040

demand/sedimentation, CSIRO 2070-2099), adjusting the Patuxent rule curves improves Z_{Stor} by 6.1-6.4 %.

The Patuxent Reservoir operates based on 2 rule curves which control daily water treatment withdrawals based on storage zone. This improvement is attributed to an increase of approximately 1,000-1,500$\times 10^3$ m^3 in both the upper and lower rule curves between the months of September and February. This modification allows the Patuxent Reservoir to refill more effectively if storage is low during the fall and winter by decreasing water treatment rates and shifting load back to the Potomac River. While this shift is similar in both the climate change simulation and the sediment and demand change simulation, the optimal rule curves deviate in mid-summer. Most likely because of the predicted increase in summer droughts due to climate change, the upper and lower Patuxent rule curves tend to be approximately 300$\times 10^3$ m^3 higher through the months of July and August. This allows the Patuxent Reservoir to conserve storage and shifts load to other sources during severe summer droughts.

Demand Restrictions

The Metropolitan Washington Council of Governments has standardized the implementation of water use restrictions by setting three demand restriction levels: voluntary, mandatory and emergency, each with a unique storage trigger (Metropolitan Washington Council of Governments 2000). As part of the MWCOG agreement, all regional governments have agreed to abide by these triggers, declaring restrictions simultaneously. Voluntary restrictions are triggered when combined storage in the Jennings Randolph and Little Seneca reservoirs falls below 60%. Trigger points for mandatory and emergency restrictions are set at 25 and 5% of either Jennings Randolph or Little Seneca storage, respectively (Table 4.7). This is a simplification of the actual MWCOG demand restriction rules to improve computational time, but matches actual operation very well. Percent demand restriction, shown in Table 4.8, is based on water use reductions during the drought of 1999 and other historical restrictions. Reduction in water use is typically achieved by

Table 4.7: *Optimized demand restriction triggers, in % usable storage. Current demand restriction triggers (Metropolitan Washington Council of Governments 2009) are presented as a single value, termed "MWCOG", while optimized results for the 2040 Demand and Sedimentation case "2040" and the CSIRO A2 2070-2099 case, "2070", are presented as a range across all non-dominated solutions.*

	Jennings Randolph			Little Seneca		
	MWCOG	2040	2070 A2	MWCOG	2040	2070 A2
Voluntary	60	74-85	74-83	60	73-82	72-83
Mandatory	25	17-25	18-25	25	24-53	26-59
Emergency	5	11-17	11-15	5	4-15	3-14

banning lawn watering, filling of swimming pools, operation of ornamental fountains, and other similar activities.

In a review of the WMA under current conditions, Stagge (2012a) found that the existing MWCOG demand restriction triggers would not be implemented during a repeat of the historical streamflow record and current demand levels. Using an identical multiobjective optimization scheme, new trigger points were evaluated and proven to improve system operation, greatly decreasing Flowby and Environmental Flow penalties. Reservoir storage was improved, though to a lesser extent.

As stress on the WMA water supply increases due to the factors discussed earlier, the likelihood of demand restrictions increases, highlighting the importance of an effective demand restriction policy. Under the existing MWCOG policy and 2040 demand and sedimentation levels, the WMA service area would undergo 3 years with Voluntary restrictions based on simulations using 79 years of historical climate data. Simulations based on the CSIRO 2070-2099 A2 climate scenario increase the number of years with Voluntary restrictions to 4, 3 of which eventually required mandatory restrictions. Optimization of the demand restriction triggers and the corresponding demand reduction produced improvements in all objective functions as discussed further below.

Similar to findings for current conditions, system performance is improved by increasing the Voluntary trigger from 60% of Jennings Randolph and Little Seneca storage to 74-85%. Another finding is that the operations improved when the Mandatory restriction

Table 4.8: *Optimized demand restriction water use reduction (%). Current demand restriction policy (Metropolitan Washington Council of Governments 2009) is presented as a single value, termed "MWCOG", while optimized results for the 2040 Demand and Sedimentation case "2040" and the CSIRO A2 2070-2099 case, "2070", are presented as a range across all non-dominated solutions. Optimized values for Emergency restrictions are not presented, as these restrictions are not imposed.*

	June-Sep			Remainder of Year		
	MWCOG	2040	2070 A2	MWCOG	2040	2070 A2
Voluntary	5	4.1-6.2	2.2-5.3	3	8.6-11.8	4.4-8.0
Mandatory	9.2	8.6-11.8	4.4-8.0	5	3.6-8.4	8.6-11.5
Emergency	13.3-18.6	13.9-19.7		15 12.5-19.5	13.3-18.5	

trigger point was decreased from 25% to 17-25% for Jennings Randolph storage but increased from 25% to 24-59% for Little Seneca storage (Table 4.7). This difference occurs because Little Seneca storage is prioritized within the reservoir release rules. Because Little Seneca storage is utilized only during extreme drought events, its storage typically remains higher than the Jennings Randolph Reservoir. Additionally, because of its small size, slow refill rate, and small travel time, it is vital to protect storage in the Little Seneca Reservoir during drought events.

These updated drought restriction rules improve Z_{Flowby} by 4.2-26.7%, $Z_{\text{Env Flows}}$ by 5.3-10.5%, and greatly reduce the frequency and severity of low reservoir storage penalties. These changes particularly improve Patuxent and Occoquan storage, given the 2070-2099 climate scenario. These improvements are tempered by an increase in demand restrictions, though the change is likely within an acceptable range, increasing the number of Voluntary restrictions from 4 to 8 years over a 79 year period.

4.4 Conclusions

The effects of climate change are increasingly being considered in conjunction with population/demand change and reservoir sedimentation in forecasts of water supply vulnerability. A case study was presented, based on the Washington DC Metropolitan Area water supply, where the relative effects of these factors are first evaluated using system

simulation and then addressed using multiobjective optimization to develop modified operational rules. These rules form the basis for a system adaptation strategy to optimize efficient management in the system without the need for physical improvements. All simulations and optimization were evaluated with respect to 6 objectives: demand shortage, reservoir storage, minimum flowby requirements, recreation days, whitewater releases, and consecutive days with extremely low flows, termed environmental flow days.

A system-wide increase in demand of 22.7% by the year 2040 is projected to decrease available storage in the Jennings Randolph Reservoir, decreasing the number of Recreation days, measured above lake access points. Increased demand is also projected to increase load on downstream reservoirs, resulting in an increase in consecutive low flow days.

WMA reservoirs are projected to lose 7-15% of their usable storage volume due to sedimentation between 2010 and 2040, causing an increase in storage failures (defined as volume $< 40\%$), predominantly in the Patuxent and Savage Reservoirs. By 2040, the effects of sedimentation alone will begin to cause occasional storage failures in the Jennings Randolph and Little Seneca Reservoirs as well.

Climate change is also projected to increase water supply vulnerability in the WMA. Climatic trends in the region are towards higher flows in the winter and early spring, followed by lower flows in the summer, with more sporadic but intense storm events (Stagge 2012b). Simulations of 5 GCMs predict an increase in storage failures within the system, with Savage Reservoir failures projected to increase 36% by 2070-2099. By the end of the century, storage failures begin to occur in the Little Seneca and Occoquan reservoirs, where historically they did not occur. An increase in storage penalties is accompanied by a decrease in whitewater releases and a doubling of Recreation Season failures.

Using the multiobjective evolutionary algorithm, SMS-EMOA, linked to a hydrologic simulation/reservoir decision model, OASIS, 5 potential modifications to existing operating rules were evaluated. These include a buffer equation, which balances load between upstream and downstream reservoirs, a load shifting equation, which balances load between Potomac and off-line reservoirs, water use restrictions, and zone-based rule curves

for the Jennings Randolph and Patuxent Reservoirs. Use of a multiobjective evolutionary algorithm to optimize the operation rules proved to be efficient and functional, as it allowed for *a posteriori* decisions regarding the relative importance of the objectives. None of the optimized operating rules were able to completely mitigate the combined effects of demand change, sedimentation and climate changes. However, some, such as the buffer equation, were able to mitigate the effect of climate, with respect to the objectives.

Flowby and environmental flow penalties were decreased by modifying the buffer equation to allow separate equations for upstream and and downstream imbalances. Results for the load shift equation remain very similar to the optimized load shift equation found for current conditions (Stagge 2012a). This suggests that the effectiveness of this rule is maximized. Optimization of the zone-based rule curves suggests that Jennings Randolph storage should be managed more conservatively during March, April and May in the future, while storage in the Patuxent could be improved by managing the reservoir more conservatively in the refill period (September - February). The Patuxent rule curve shows a distinct trend towards more conservative refill operation with the increasing effects of climate change. Evaluation of demand restriction triggers suggests that system-wide operation could be improved by increasing the reservoir storage triggers for the minor, voluntary restriction. For the more severe, mandatory restriction, the optimized rules suggest a decrease in the Jennings Randolph trigger and an increase in the Little Seneca trigger. In this latter case, the increase in the Little Seneca trigger is due to its relatively small size and long refill rate.

Using a combination of synthetic streamflow generation, water resources decision modeling and multiobjective optimization, the potential vulnerabilities of the WMA water supply system have been evaluated. Further, this work provides a framework for developing and comparing strategies to mitigate the effects of demand and climate change.

4.5 Acknowledgments

James Stagge is a Via Doctoral Fellow and gratefully acknowledges support from the Via program and the Institute for Critical Technology and Applied Science (ICTAS). The authors would also like to thank the Interstate Commission on the Potomac River Basin (ICPRB) and Hydrologics, Inc. for providing data access and research support.

Bibliography

Ahmed, S. N., K. R. Bencala, and C. L. Schultz (2010). 2010 Washington Metropolitan Area water supply reliability study; part 1: Demand and resource availability forecast for the year 2040. Technical Report ICPRB 10-01, Interstate Commission on the Potomac River Basin.

Aksoy, H. (2003). Markov chain-based modeling techniques for stochastic generation of daily intermittent streamflows. *Advances in Water Resources 26*(6), 663–671.

Allmendinger, N. E., J. E. Pizzuto, G. E. Moglen, and M. Lewicki (2007). A sediment budget for an urbanizing watershed, 1951-1996, Montgomery County, Maryland, U.S.A. *Journal of the American Water Resources Association 43*, 14831498.

Beume, N., B. Naujoks, and M. Emmerich (2007). SMS-EMOA: Multiobjective selection based on dominated hypervolume. *European Journal of Operational Research 181*, 1653–1669.

Burns, M. and R. MacArthur (1996). Sediment deposition in Jennings Randolph reservoir, Maryland and West Virginia. In *Proceedings of the Sixth Federal Interagency Sedimentation Conference.*, Las Vegas, Nevada.

CDM (2002). Water supply master planning: Identification of future FCWA water supply needs. Technical report.

Collins, W. D., C. M. Bitz, M. L. Blackmon, G. B. Bonan, C. S. Bretherton, J. A. Carton, P. Chang, S. C. Doney, J. J. Hack, T. B. Henderson, J. T. Kiehl, W. G. Large, D. S. McKenna, B. D. Santer, and R. D. Smith (2006). The Community Climate System Model Version 3 (CCSM3). *Journal of Climate 19*, 2122–2143.

Cummins, J., C. Buchanan, C. Haywood, H. Moltz, A. Griggs, R. C. Jones, R. Kraus, N. Hitt, and R. V. Bumgardner (2010). Potomac basin large river environmental flow needs. Technical report, Interstate Commission on the Potomac River Basin.

Emmerich, M., N. Beume, and B. Naujoks (2005). An EMO algorithm using the hypervolume measure as selection criterion. Volume 3410 of *Lecture Notes in Computer Science*, pp. 62–76. Springer.

Flato, G. (2005). The Third Generation Coupled Global Climate Model (CGCM3).

Fleischer, M. (2003). The measure of Pareto Optima: Applications to multi-objective metaheuristics. In *Evolutionary Multi-Criterion Optimization. Second International Conference, EMO 2003*, pp. 519–533. Springer.

Gordon, H. B., L. D. Rotstayn, J. L. McGregor, M. R. Dix, E. A. Kowalczyk, S. P. O'Farrell, L. J. Waterman, A. C. Hirst, S. G. Wilson, M. A. Collier, I. G. Watterson, and T. I. Elliott (2002). The CSIRO Mk3 climate system model. Technical Report 60, CSIRO Atmospheric Research Technical Paper.

Hagen, E. R. and R. C. Steiner (1999). Little Seneca Reservoir "natural" daily inflow development. Technical Report 99-3, Interstate Commission on the Potomac River Basin.

Hayhoe, K., C. Wake, B. Anderson, X.-Z. Liang, E. Maurer, J. Zhu, J. Bradbury, A. DeGaetano, A. Stoner, and D. Wuebbles (2008). Regional climate change projections for the Northeast USA. *Mitigation and Adaptation Strategies for Global Change 13*, 425–436.

Hayhoe, K., C. Wake, B. Anderson, X.-Z. Liang, E. Maurer, J. Zhu, J. Bradbury, A. DeGaetano, A. M. Stoner, and D. Wuebbles (2007). Regional climate change projections for the Northeast USA. *Mitigation and Adaptation Strategies for Global Change 13*(5-6), 425–436.

Meehl, G. A., T. F. Stocker, W. D. Collins, P. Friedlingstein, A. T. Gaye, J. M. Gregory, A. Kitoh, R. Knutti, J. M. Murphy, A. Noda, and et al. (2007). Global climate projections: Climate Change 2007: The physical science basis (Chapter 10) (the fourth assessment report). *Cambridge University Press New York*, 747–845.

Mersmann, M. (2011). *emoa: Evolutionary Multiobjective Optimization Algorithms*. R package version 0.4-8.

Metropolitan Washington Council of Governments (2000). Metropolitan Washington water supply and drought awareness response plan: Potomac River system. Technical Report 20703, Washington DC.

Metropolitan Washington Council of Governments (2009). Round 7.2 cooperative forecasting: Employment, population, and household forecasts to 2030 by traffic analysis zone. Technical report, Washington DC.

Milly, P. C. D., K. A. Dunne, and A. V. Vecchia (2005). Global pattern of trends in streamflow and water availability in a changing climate. *Nature 438*(7066), 347–350.

Najjar, R., L. Patterson, and S. Graham (2009). Climate simulations of major estuarine watersheds in the Mid-Atlantic region of the US. *Climatic Change 95*, 139–168.

Ortt, R. A., S. VanRyswick, and D. Wells (2007). Bathymetry and sediment accumulation of Tridelphia and Rocky Gorge reservoirs. Technical Report 07-03, Maryland Department of Natural Resources, Maryland Geological Survey, Coastal and Estuarine Geology.

Porter, J. W. and B. J. Pink (1991). A method of synthetic fragments for disaggregation in stochastic data generation. In *Hydrology and Water Resources Symposium*, Institution of Engineers, Australia, pp. 187–191.

Pyke, C. R., R. G. Najjar, M. B. Adams, D. Breitburg, M. Kemp, C. Hershner, R. Howarth, M. Mulholland, M. Paolisso, D. Secor, and et al. (2008). Climate change and the Chesapeake Bay: State-of-the-science review and recommendations. *Order: A Journal On The Theory Of Ordered Sets And Its Applications 7415*(9), 1–6.

Reed, P. M., J. D. Herman, J. R. Kasprzyk, and J. B. Kollat (2012). Evolutionary multiobjective optimization in water resources: The past, present, and future. *Advances in Water Resources*.

Sen, P. K. (1968). Estimates of the regression coefficient based on Kendall's tau. *Journal of the American Statistical Association 63*(324), 1379–1389.

Srikanthan, R. and T. A. McMahon (1982). Stochastic generation of monthly streamflows. *Journal of the Hydraulics Division-ASCE 108*(3), 419–441.

Stagge, J. H. (2012a). Genetic algorithm optimization of a multi-reservoir system with long lag times. In *Optimization of Multi-Reservoir Management Rules Subject to Climate and Demand Change in the Potomac River Basin, Ph.D. Dissertation, Chapter 3*. Blacksburg, VA: Virginia Tech.

Stagge, J. H. (2012b). Markov chain model for generation of daily climate-adjusted streamflows. In *Optimization of Multi-Reservoir Management Rules Subject to Climate and Demand Change in the Potomac River Basin, Ph.D. Dissertation, Chapter 2*. Blacksburg, VA: Virginia Tech.

Szilagyi, J., G. Balint, and A. Csik (2006). Hybrid, Markov chain-based model for daily streamflow generation at multiple catchment sites. *Journal of Hydrologic Engineering 11*(3), 245.

Thiel, H. (1950). A rank-invariant method of linear and polynomial regression analysis (parts 1-3). *Proceedings of the Koninalijke Nederlandse Akademie van Weinenschatpen 53*, 1397–1412.

USACE (1997). Metropolitan Washington water supply and drought awareness response plan: Potomac River system. Technical report, U.S. Army Corps of Engineers.

Washington, W. M., J. W. Weatherly, G. A. Meehl, A. J. J. Semtner, T. W. Bettge, A. P. Craig, W. G. J. Strand, J. Arblaster, V. B. Wayland, R. James, and Y. Zhang (2000). Parallel climate model (PCM) control and transient simulations. *Climate Dynamics 16*, 755–774.

Watanabe, S., T. Hajima, K. Sudo, T. Nagashima, T. Takemura, H. Okajima, T. Nozawa, H. Kawase, M. Abe, T. Yokohata, T. Ise, H. Sato, E. Kato, K. Takata, S. Emori, and M. Kawamiya (2011). MIROC-ESM: model description and basic results of CMIP5-20c3m experiments. *Geoscientic Model Development Discussions 4*, 1063–1128.

Zitzler, E. and L. Thiele (1998). Multiobjective optimization using evolutionary algorithms - a comparative case study. In *Conference on Parallel Problem Solving from Nature (PPSN V)*, Amsterdam, pp. 292–301.

Chapter 5

Conclusions

In order to develop a more sustainable, resilient water supply, water planners and engineers must consider a range of non-stationary factors, including demand change, reservoir sedimentation and climate change. These factors are projected to increase stress on the Washington DC metropolitan area (WMA) water supply over the next century. A comprehensive analysis of these issues, with a focus on the WMA water supply, was presented in this study, focused on three distinct aspects of the problem:

Manuscript 1 outlined the development and application of a novel method for the generation of daily, climate-adjusted streamflow timeseries. This method relates GCM-scale climate indicators to discrete climate states in a Markov chain climate model, which in turn controls the parameters of a daily flow model. This method is extensible and capable of generating long sequences of feasible, synthetic daily flows that reproduce streamflow statistics at the daily, monthly and annual time scales. Mean annual streamflow in the Potomac River is projected to increase by 1-7% by 2100, with the majority of this increase occurring during the winter and early spring. Conversely, summer flows are projected to decrease, particularly during July and August, caused by a decrease in large, sustained storm flows. This change in summer flow is projected to increase the severity of extreme low flows slightly and to shift the date of the annual minimum flow, which historically occurs in mid-September, 2-5 days earlier by the 2070-2099 time period.

Manuscript 2 examined the existing water management strategies of the WMA, given current demand and climate. The unique layout of the WMA system creates a 9-10 day lag between reservoir releases and their subsequent capture close to Washington DC. This delay remains beyond the forecast horizon of accurate weather predictions, introducing added uncertainty to the water management decision making process. Five potential modifications to existing operating rules were evaluated by pairing a multiobjective evolutionary algorithm solver with a daily hydrologic simulation and decision model. Modifying the Load Shift Index, which prevents load being shifted to the Patuxent and Occoquan reservoirs during times of low storage, reduced storage penalties by 2.4% and flowby penalties by 7.1%. Additionally, the existing trigger points for water use restrictions were found to be set lower than necessary. By increasing these trigger points, flowby and environmental flows were improved by 14.3 and 18.9%, respectively.

Manuscript 3 evaluated the potential impacts of demand, sedimentation, and climate change on the WMA water supply system, identifying changes in system vulnerability over the next century. Population and demand growth are predicted to decrease reservoir storage and increase the number of consecutive low flow days downstream of Little Falls, Washington DC. Reservoir sedimentation is projected to greatly affect reservoir storage, increasing the severity of low reservoir storage events by 114%, predominantly in the Patuxent and Savage Reservoirs. Climate change is predicted to increase stress on the WMA water supply, lowering reservoir storage and decreasing water availability for recreation and whitewater releases. Adaptation strategies are developed using the optimization scheme developed in Manuscript 2. Several mitigation opportunities are identified, including better balancing between the Jennings Randolph and downstream reservoirs, more conservative rule curves for the Patuxent and Jennings Randolph reservoirs, and more balanced triggers for implementing water use restrictions. The modified Patuxent rule curve improves storage in the system by 6.1-6.4%, while adjustment to the water use restrictions improves flowby by 4.2-26.7% and greatly reduces the frequency and severity of low reservoir storage.

Specific results regarding climate and demand change on streamflows in the Potomac watershed and the use of evolutionary algorithms to develop adaptation strategies are vitally useful within the Washington, DC region. But the methods developed in this study are also generally applicable to a wide range of water supply and vulnerability studies. There is great potential for continued exploration and research based on improving the climate-adjusted streamflow generation model. Climate variables with longer periodicity, such as ENSO measures, or more complex models of surface-groundwater interaction could be included in the streamflow generation model. There is also potential to expand the scope of rule forms considered in the optimization model. These rules could potentially include conditional forecasts of streamflow. Finally, there is potential to use new, auto-adaptive evolutionary algorithms, which are more robust with regard to initial parameter selection.